# Members without transverse reinforcement

# Systematic Fracture Mechanics Study of Shear Failure in Beams under Distributed Load

## Rupture par cisaillement de poutres sous charge répartie

## Bruchmechanische Studie des Schubbruches von Bauteilen unter Gleichlast

**Johan BLAAUWENDRAAD**
Professor
Delft Univ. of Technol.
Delft, The Netherlands

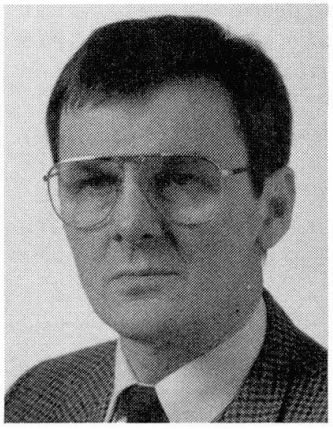

Johan Blaauwendraad, born 1940, obtained his civil engineering degree in 1962 at Delft University. He joined TNO for research, moved to Rijkswaterstaat, obtained his doctor's degree in 1973. Is now professor of Civil Engineering in Delft since 1979.

**Q. B. WANG**
Doctoral student
Delft Univ. of Technol.
Delft, The Netherlands

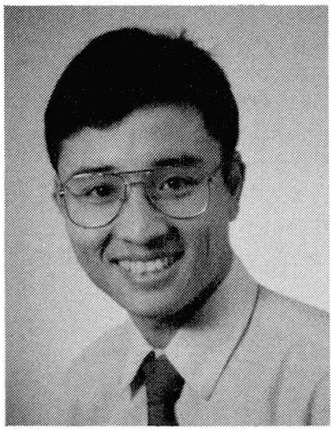

Qing Biao Wang, born 1962, received his civil engineering degree in 1988 at Delft University. He has been carrying out research investigating the shear strength of reinforced concrete beams using the finite element method.

**SUMMARY**

Shear failure is studied computationally in a systematic way for beams under distributed load with only longitudinal reinforcement. The shear capacity relies mainly on tensile tractions in the governing crack, aggregate interlock and dowel-action being neglectable. Scale effects are simulated correctly. Parameters are slenderness, brittleness, reinforcement ratio and the influence of a simultaneously acting normal compressive force.

**RÉSUMÉ**

A l'aide de l'ordinateur, la rupture par cisaillement est étudiée systématiquement pour des poutres sous charge répartie ne comprenant qu'une armature longitudinale. La résistance au cisaillement dépend essentiellement des contraintes de traction dans le système de fissuration principal, l'adhérence de la pâte de ciment aux aggrégats et l'effet de goujon des barres d'armature ne jouant qu'un rôle négligeable. Les effets d'échelle sont correctement pris en compte, tandis que les paramètres étudiés sont l'élancement, la fragilité, le pourcentage d'armature et l'action simultanée d'une force de compression axiale.

**ZUSAMMENFASSUNG**

Schubversagen wird auf numerische Weise systematisch für Träger ausschliesslich verteilter Belastung mit Biegebewehrung untersucht. Die Schubkapazität hängt vornehmlich ab von Zugspannungen in dem bestimmenden Riss. «Aggregate interlock» und «dowel» action können nicht nennenswert beitragen. Massstabeffekte werden gut simuliert. Die untersuchten Parameter sind die Schlankheit, Sprödigkeit, Bewehrungsmass und der Einfluss einer gleichzeitig aktiven Druckkraft.

## 1. PROBLEM STATEMENT

This study originates from the construction of tunnels of rectangular cross-section crossing rivers and canals.
Rijkswaterstaat (Dutch State Public Works) commissioned the research organisation TNO to execute a number of tests on beams under distributed loading. In these tests 2 parameters have been varied [1]. One is the ratio of the positive mid-span moment and the end-of-span negative moment. So this parameter controls the amount of 'clamping-in'. The other parameter is the ratio of length-of-span and depth. This parameter controls the slenderness of the beams.
In figure 1 five different ratios are shown for the mid-span moment and the end-of-span moment (for a fixed value of the slenderness parameter), together with the crack pattern which occurs. The fat-drawn crack is due to shear failure. In all 5 cases the maximum shear force occurs at the beam end, but the shear failure does not always occur at that place. In stead the failure crack sometimes moves inwards the beam-span. This phenomenon is rather confusing for a designer, who is used to analyzing his diagrams for moments and shear forces and after that considers his structure on a section-by-section basis. In fact he is accustomed to checking the sections in which maximum moments and shear forces occur and to specify reinforcement demand at those positions. This approach appears to be meaningless in the case of a beam under distributed loading, at least for the prediction of the shear capacity.
The aim of the present study is to complete the experimental findings by computational investigations. It is hoped to better understand the available experimental results, but also to find new results for load cases and structures which have not been included in the experiments. In fact, the paper refers strongly to Hillerborgs publication [2].

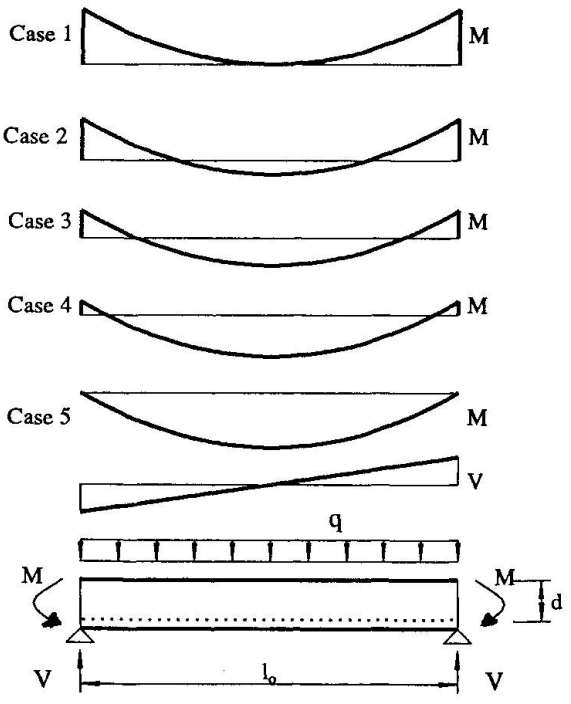


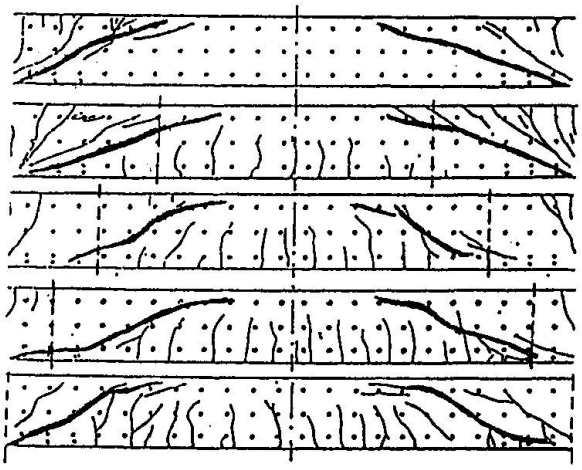

Fig.1
Five different moment lines (5 different moment parameters) and the respective crack patterns of the beams. All beams have the slenderness parameter $l_o/d = 4.5$ and d = 150 mm

## 2. ANALYSIS METHOD

The study has been started from the view-point of the predictor-corrector method, as proposed by Rots [3]. The program DIANA is used for all analyses.
In a discrete crack three different force transfer mechanisms can be taken into account:
- tensile traction (model Hillerborg)
- aggregate interlock (model Walraven)
- dowel action (results Fenwich)

For the tensile tractions normal to the crack faces a linear softening branch is adopted in the $\sigma$-w diagram for the stress $\sigma$ and crack opening w. The tangent should be close to the value at tensile strength in the real curvilinear softening branch.
The aggregate interlock model of Walraven has been adopted, as reported in [4], which defines the tangential shear stress and the normal compression in a rough crack as nonlinear functions of the crack opening w, the crack-sliding $\Delta$ and the concrete compressive strength $f_c$.
For dowel-action a nonlinear spring has been programmed, whose stiffness is obtained from simulation of the dowel-experiments of Fenwich [5].
From a series of analyses it has been concluded that aggregate interlock and dowel-action do not contribute noticeable to the shear capacity. If the discrete crack is chosen properly (according to what is found in experiments), the crack faces are only loaded by tensile tractions (mode I). Only in the cover layer of concrete a crack-sliding $\Delta$ of some importance can occur, but not sufficient to mobilize an important contribution of aggregate interlock and dowel-action to the shear capacity. At peak load these contributions are negligible. They first start to grow after peak load has been reached, but at that time the contribution of the tensile tractions drops down rapidly. The conclusion is that the shear capacity must be fully provided by the tensile softening stresses.

## 3. PARAMETER STUDY FOR DISTRIBUTED LOAD

From preliminary calculations a number of lessons have been learned. To find a correct failure load the following applies:
- the smeared crack approach correctly simulates the beam stiffness, but is very time-consuming and does not converge properly for all analyses
- the analyses using one single discrete crack do not simulate the stiffness correctly, but predict the ultimate peak load well in short run time
- the crack tip does not reach the compressive zone for the cases studied, and the inclination of cracks is important.
- in a correct crack path no aggregate interlock can develop
- dowel action can only develop after passing of the peak load and can therefor be excluded
- scale effects are due to tensile softening in the crack and to the fact that bond does not follow scaling. Good performance of the model is found if a constant bond-interface is used equal to the beam width.

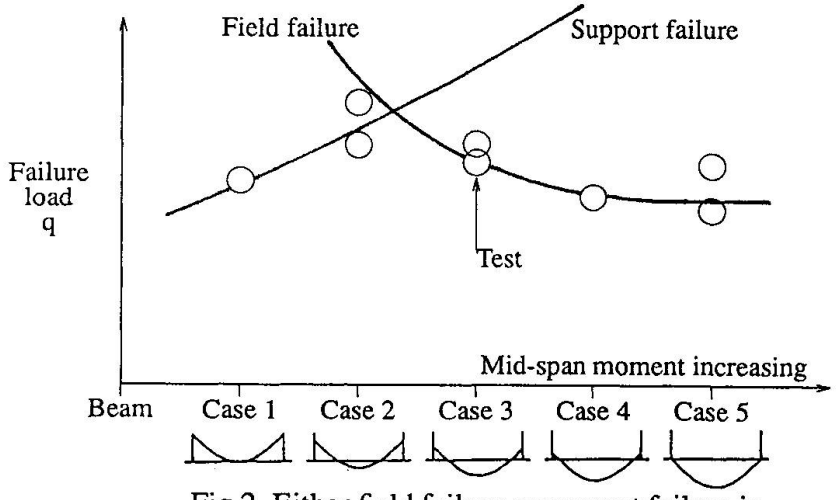


Fig.2. Either field failure or support failure is determining, depending on the moment parameter (the amount of clamping-in)

Starting from these findings a parameter study has been started for beams under distributed loading on basis of the predefined crack approach. When we closely inspect the crack patters in figure 1, it is noticed that two different failure mechanisms can occur, depending on the moment parameter (ratio of end-span moment and mid-span moment). In figure 2 is expressed the expectation that the two different failure types, field failure and support failure, can be studied separately and that for each moment parameter must be determined which one determines the lowest capacity and consequently failure. Test results support this expectation.
In this paper only the field failure is subject of examination. From here the length of the shear span is called *l (the distance between two counter-flexure points)*, the depth of the beam is d, the material property $l_{ch}$ is a characteristic length defined by

$$l_{ch} = \frac{EG_f}{f^2_{ct}}$$

In this expression E is the elasticity modulus, $G_f$ the fracture energy release and $f_{ct}$ the concrete tensile strength. The reinforcement ratio for the longitudinal bottom reinforcement is $\rho$. The bond is determined by an elasto-plastic $\tau$-$\Delta$ diagram. The stiffness in the diagram D and the maximum value of the bond stress $\tau_{max}$ are kept constant in all analyses. The width b of the beam is used for the total bond-interface. A normal force N can occur, which yields an additional constant compressive stress $\sigma_N$. The following parameters are studied:

(1) Slenderness
$$\frac{l}{d} = 6,9,12$$

(2) Brittleness number
$$\frac{d}{l_{ch}} = \frac{3}{4}, \frac{3}{2}, 3, 6$$

(3) Reinforcement ratio
$$\rho = \frac{1}{2}, 1, 2$$

(4) Axial compression
$$\frac{\sigma_n}{f_{ct}} = 0, 1, 2$$

The computations are all done using a constant reference depth d=1.0 m and width b=1.0 m.

A major decision is the choice of the shape and the position of the predefined crack. The inclination is chosen according to the elastic principle stresses in the centerline of the beam when no axial force is present. This appears to be in close agreement with experiments. A small vertical part is chosen near the longitudinal reinforcement. The length of this part is d/15.
From experiments the position of the cracks can be chosen very convincingly. There is no need to run many smeared crack analyses to produce the same results.
It is not necessary to draw the complete half beam into the computations. A beam part is chosen which roughly extends over a length d to the right and left from the beginning of the crack, and this part is loaded in accordance with the elastic cross-section stresses. A mesh of triangular 3-noded elements is applied in the surroundings of the crack path.
A series of results has been got. In figure 3 the influence of the slenderness l/d, the reinforcement ratio $\rho$ and the brittleness number $d/l_{ch}$ on the shear capacity $q/q_{ref}$ is shown in one diagram. The reference load $q_{ref}$ is the maximum load for the combination

$$\frac{l}{d} = 9, \qquad \frac{d}{l_{ch}} = 6 \qquad \text{and } \rho = 1\%$$

The influence of the reinforcement is moderate (about 5% between $\rho$ = 1% and $\rho$ = 2%). Doubling the slenderness from 6 to 12 increases the capacity by about a factor 3. Increase of the brittleness number by a factor 8 from 0.75 to 6 does drop down the shear capacity roughly by 30%. So the most important parameters are the slenderness and the brittleness number.
Figure 4 plots the shear strength against the slenderness l/d for $\rho$=1% and different $d/l_{ch}$. It appears that $d/l_{ch}$ does not interfere much with the effect of l/d. Similar observation is obtained for $\rho$=2%.
Figure 5 has been made to investigate the influence of the reinforcement ratio $\rho$ in a larger domain. The ratio $\rho$ has been varied from 0 to 3 for a beam with

$\frac{l}{d} = 9$, $\frac{d}{l_{ch}} = 3$. Again $q_{ref}$ refers to the combination $\frac{l}{d} = 9$, $\frac{d}{l_{ch}} = 3$ and, $\rho$ = 1%.

Hereby $\Sigma C$ is chosen to be equal to b for practical reason. For smaller $\rho$ it is a reasonable assumption to reduce $\Sigma C$ linearly with $\rho$ and for larger $\rho$ the limit value of b is used. In the same diagram is shown the curve according to Zutty and the rule of the Eurocode.
Figure 6 shows the influence of normal compressive stress. It is seen that the influence may modeled with a linear function.

Meanwhile continuing effort is made to conclude on an engineering model, such that designers can understand and use either the model or rules derived from it.

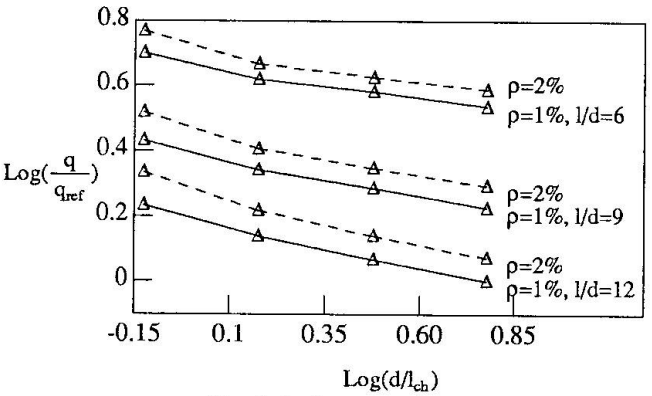


Fig.3. Influence of $d/l_{ch}$, $\rho$ and l/d
(For $q_{ref}$: l/d = 12, $d/l_{ch}$ = 6.0, $\rho$ = 1%)

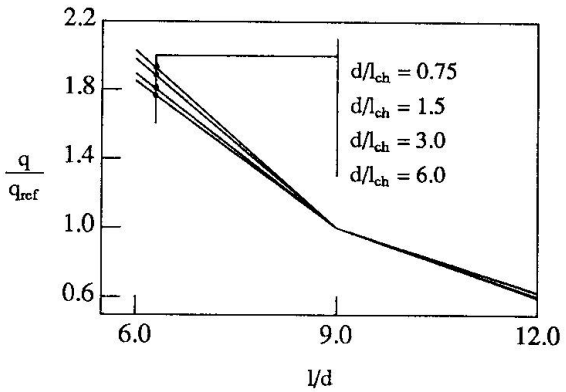


Fig.4. Influence of slenderness l/d
($\rho$ = 1%, for $q_{ref}$: l/d = 9)

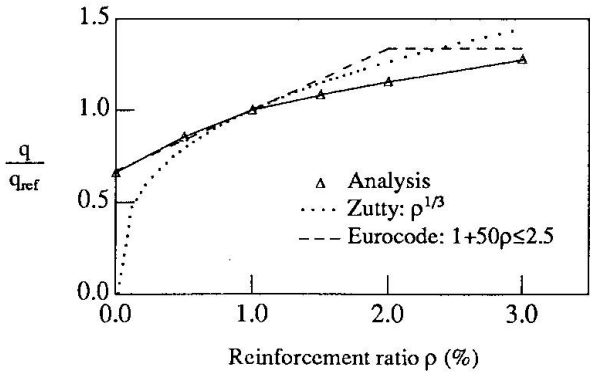


Fig.5. Influence of reinforcement ratio $\rho$
(l/d=9, $d/l_{ch}$=3.0, for $q_{ref}$: $\rho$ = 1%)

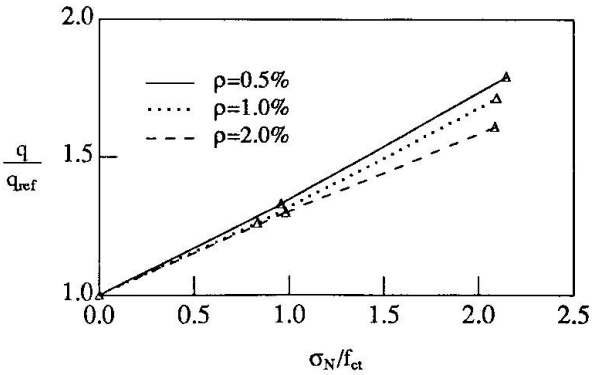


Fig.6. Influence of axial compressive stress
(l/d=9, $d/l_{ch}$=3.0, for $q_{ref}$: $\sigma_N$ = 0)

## 4. CONCLUSIONS

1. Beams under distributed load and clamped-in conditions can fail in shear in two modes, here called support failure and field failure. The field failure can be modeled as a diagonal cracking failure. The field failures occur at positions which are supprizing to designers. Their convential section by section approach can not be applied in judging the shear capacity of beams.
2. The predictor-corrector method in which a smeared crack approach and a predefined discrete crack path are used sequentially, appears to be a necessary and successful way to predict the diagonal cracking shear failures.
3. The inclination of the predefined crack path must be chosen carefully. Shear failure occurs when the crack is so inclined that it cannot provide sufficient resistance.
4. The effect of dowel-action and aggregate interlock is negligible in the well-chosen crack path. Bond and tension-softening are important factors for shear capacity of diagonal cracking.
5. Size effect can be modelled correctly. The tension softening is most important. Bond has an additional effect.
6. The parameter study for field failure so far has revealed that the brittleness number and the slenderness have significant importance. Doubling the longitudinal reinforcement ratio does not have much effect. In the practical range the order of 10%
7. From continued research it is hoped to derive design rules or engineering models to be applied by designers.

## 5. ACKNOWLEDGEMENT

The support of prof. R. de Borst and dr. J.G. Rots in this project is highly appreciated.

## 6. REFERENCES

1. Gijsbers, F.B.J., Monnier, Th.: Analysis of the shear capacity of slabs and beams with a rectangular cross-section.
   Report TNO-IBBC nr. B-78-76/62.3.4003, 1978 (in Dutch).
2. Hillerborg, A.: "Reliance upon concrete tensile strength", Introductory report, proc. of IABSE colloquium on "structural concrete", Stuttgart, 1991.
3. Rots, J.G.: "Computational modeling of concrete fracture", Dissertation, Delft University of Technology, 1989
4. Walraven, J.C.: "Mechanisms of shear transfer in cracks in concrete", Report A26/79-02, Delft University of Technology, Nov. 1978.
5. Fenwich R.C. and Paulay, T.: "Mechanisms of shear resistance of concrete beams", J. of Structural Division, ASCE, Oct. 1968, pp. 2325-1339.
6. Blaauwendraad, J. and Wang, Q.B.: Overview of systematic study for shear failure in reinforced concrete beams and slabs without shear reinforcement under distributed load. Report Delft University of Technology, reportnr. 25.2-90-2-18

# Model for Structural Concrete Members without Transverse Reinforcement

## Modélisation d'un élément en béton dépourvu d'armatures transversales

## Modell für Konstruktionsbauteile ohne Stegbewehrung

**Karl-Heinz REINECK**
Dr. Eng.
University of Stuttgart
Stuttgart, Germany

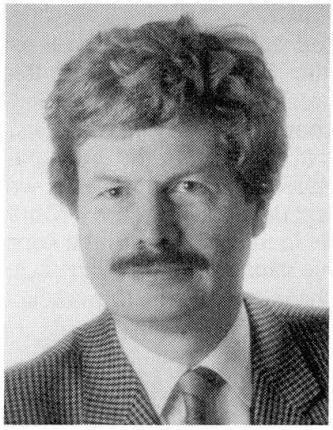

Karl-Heinz Reineck received his degrees at the University of Stuttgart. His research covers theoretical work and several experiment projects on the shear behaviour of structural members as well as large-scale tests on reinforced concrete-shells for offshore platforms. He is a member of the CEB-Commission «Member Design».

**SUMMARY**

The presented mechanical model for structural concrete members without transverse reinforcement explains the structural behaviour from cracking until failure. The loads are transferred by an inclined biaxial tension-compression field between the cracks and this can be visualized by a simple truss. For calculating the failure load the discrete cracks must be examined and the load is mainly transferred in the tension zone of the member by friction of the crack-faces and by the dowel force of the longitudinal reinforcement. An explicit equation for the ultimate shear force is derived following clear mechanical principles. The theory explains the size effect on «shear»-failures as well as the influence of axial compression or prestress and of axial tension or restraints, and it also yields satisfactory results for lightweight concrete members.

**RÉSUMÉ**

Ce modèle présente le comportement d'une telle structure de la fissuration à la rupture. L'effort tranchant se transmet entre les fissures par une traction et une compression que l'on modélise par un treillis. Le calcul de la résistance doit tenir compte des fissures elles-mêmes et des effets fondamentaux de l'effort tranchant par rapport à la friction des surfaces des fissures ainsi que l'effet de goujon des barres d'armature. L'équation explicitant la résistance ultime au cisaillement est dérivée suivant des principes de mécanique clairs. La théorie explique l'influence de la taille de l'élément en béton sur la rupture par cisaillement. L'influence négative on positive sur la charge ultime des forces de compression ou de traction axiales, ainsi que de la précontrainte peut donc être décrite. L'utilisation de relations constitutives appropriées montre que le modèle examiné donne des résultats satisfaisants dans le cas d'éléments légers en béton.

**ZUSAMMENFASSUNG**

Das vorgestellte mechanische Modell für Konstruktionsbetonbauteile ohne Stegbewehrung erfasst das Tragverhalten von der Rissbildung bis zum Bruch. Die Querkraft wird durch ein zweiachsiges Zug-Druck-Spannungsfeld zwischen den Rissen übertragen und kann vereinfachend durch ein Fachwerk veranschaulicht werden. Zur Berechnung der Traglast müssen die diskreten Risse und die wesentlichen Querkrafttragwirkungen betrachtet werden: die Rissreibung und die Dübelwirkung der Längsbewehrung. Es wird eine explizite Beziehung für die Bruchquerkraft nach klaren mechanischen Prinzipien abgeleitet. Die Theorie erklärt den Massstabeinfluss bei «Schub»-brüchen, den Einfluss von Längsdruckkräften, der Vorspannung und von Längszugkräften oder Zwangsbehinderungen und sie liefert auch befriedigende Ergebnisse für Leichtbetonbauteile.

## 1. INTRODUCTION

In present codes members without transverse reinforcement like slabs are still designed with respect to resist shear forces with purely empirically derived formulae. Since such formulae are limited to the past experimental evidence (which often is not clearly described) they do not cover all "shear problems" like that of fully cracked members in silos or foundations with large depths and very low reinforcement ratios. Therefore a clear theory based on a model for the structural behaviour is needed so that practising engineers can solve the future tasks. Such a model for members without transverse reinforcement is also a prerequisite for a consistent design concept for structural concrete since these members form the link between members with transverse reinforcement and unreinforced concrete members. Since the latter obviously require the concrete tensile strength, a consistency in modelling strutural concrete can only be reached if its use is clearly acknowledged.

The only load transfer of a point load on a member without using the concrete tensile strength (apart from the anchorage) are direct struts from the load to the supports tied together by the non-staggered tension chord. This model complies with the lower bound theorem of the theory of plasticity. It yields the full bending capacity at midspan, but this is contradicted by many tests, as e.g. Kani /1/, Leonhardt/ Walther /2/ and Bresler/Scordelis /3/. The reason is obvious from the crack pattern: the assumed compression strut is very flat and crosses the widely opening failure crack. The model is wrongly applied and the theory of plasticity is not valid for this case, as was again recently confirmed by Muttoni /4/. The direct transfer of the total load by inclined struts is only possible if the load is so near to the supports, that the struts are situated over the cracks. This also means, that the shear force cannot only be transferred in the compression zone as pretended e.g. by Kotsovos /5/, but that there is a shear transfer in the cracked tension zone of members without transverse reinforcement.

## 2. MODEL

### 2.1 Assumptions

The failure of members without transverse reinforcement is characterized by a single crack propagating into the compression zone and therefore the pattern of the discrete cracks is modelled as shown in Fig. 1 for the well-known test beam with a point load. The B-region with shear force then consists of the solid concrete "teeth" between the cracks as established by the works of Kani /1/, Fenwick /6/ and Taylor /7/. In each tooth the decrease $\Delta T$ of the force in the tension chord is equilibrated by an equivalent force in the compression chord and the following shear carrying actions:

- dowel force $V_d$ of longitudinal reinforcement.
- friction along the cracks with the vertical component $V_f$; the term friction is used instead of "aggregate interlock" since it applies to all concrete types.

Both actions are combined with a shear force component in the compression zone, but this does not indicate an inclined compression chord. All assumptions are further explained in /9/, where the model is derived and justified and the results are compared with tests.

### 2.2 Equilibrium

The load is transferred by all the shear carrying actions (Fig.1a):

$$V = V_c + V_f + V_d \tag{1}$$

From the equilibrium of moments of a tooth (Fig.1b) as well as of the isolated compression zone alone, the following equation may be derived for the shear force component in the compression chord (notation see Fig.1):

$$V_c = \frac{2}{3}\,\frac{c}{z}\,V \tag{2}$$

From that follows that only a small proportion of the total shear force is transferred in the compression chord. Consequently the load is mainly carried in the cracked tension zone. With Eq.(2) the term $V_c$ can be replaced in Eq.(1) and with $z = d - c/3$ the vertical equilibrium is given by:

$$V = \frac{z}{d-c}\left(V_f + V_d\right) \tag{3}$$

The moment equilibrium of the free-body diagram in Fig.1a yields an equation for the force in the longitudinal steel depending on the moment and the shear carrying actions. With Eq.(3) the force $V_f$ may be replaced and the following equation for the strain in the longitudinal steel be derived:

$$\epsilon_s = \frac{1}{E_s A_s z}\left[V\,(x + \Delta x) + N\,z_c - V_d \frac{z}{ta}\right] \qquad \text{with : } \Delta x = \frac{d-c}{ta}\left(1 + \frac{2}{3}\frac{c}{z}\right) \quad ; \; ta = \tan\beta_r \tag{4}$$

Similarily the force and the strain in the compression chord may be determined.

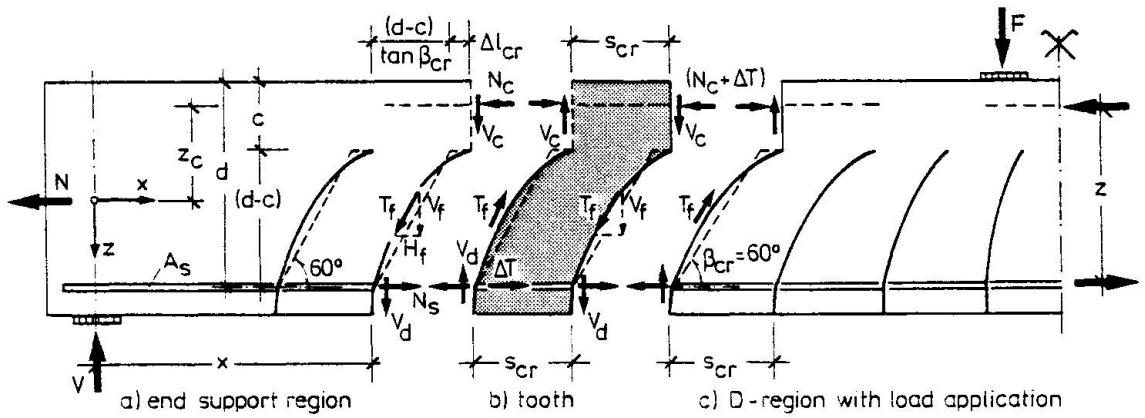


Fig.1: Member with tooth-elements and its forces

## 2.3 Stress Fields in the Tension Zone

The distribution of the friction stresses along the crack depends on the crack shape as well as on the proportion between the shear carrying actions, whereby both parameters are interrelated with each other. Instead of iteratively determining an "exact" distribution for a defined crack shape, a simple assumption is made for a statically admissable stress field in the tension zone.

The distribution of the friction stresses $\tau_f$ is made up by a constant part $\tau_{f1}$ (Fig.2a) and a parobolic distribution $\tau_{f2}$ (Fig.2b). The latter considers that the dowel action reduces the slip in the lower part of the crack and therefore its value is related to the dowel force. The equilibrium of the shear stresses along the neutral axis (Fig.2b) yields the condition:

$$\tau_{f2} = 2 \cdot v_{n,d} \qquad \text{with } v_{n,d} = V_d / b_w (d-c) \tag{5}$$

With the given $\tau_f$-distribution the shear force $V_f$ in Eq.(3) may be expressed by the representative shear stress $\tau_f$ at the mid-height of the crack:

$$V = b_w \cdot z \cdot \tau_f + \frac{3}{4} \frac{z}{d-c} V_d \tag{6}$$

The shear force may now be determined for any load stage after cracking if constitutive laws are formulated for the resistances $\tau_f$ and $V_d$ as done in /9/.

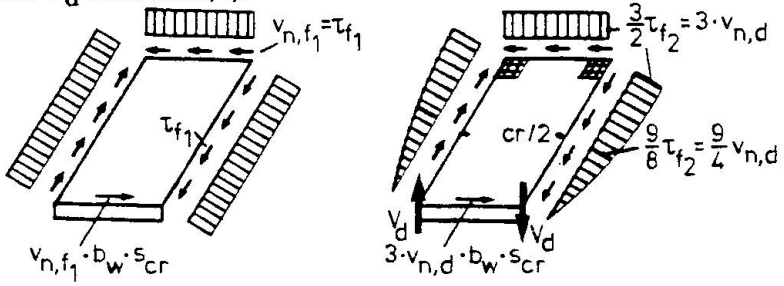


Fig.2: Distribution of friction and shear stresses in tension zone of tooth /9/

However, the model is not complete if not also the stress field in the tooth between the cracks is known so that "the structural action may be visualized" (Breen /8/). Since the stresses involved are small the linear elastic theory may be applied. The constant friction stresses $\tau_{f1}$ result in an inclined biaxial compression tension field (Fig.3a). The stress field for the dowel action with the combined friction stresses $\tau_{f2}$ is not elementary and therefore a strut-and-tie model is derived (Fig.3b). The concentrated tension tie for the dowel force spreads out and is equilibrated by the biaxial compression-tension field in the concrete resulting from the friction stresses.

## 2.4 Truss Model

The stress field between the cracks is mainly characterized by the inclined biaxial tension-compression field, which was first proposed in /10/. It is therefore obvious, that the simple truss shown in Fig.4 represents well the main feature of the structural action of members without transverse reinforcement. With that the concept of strut-and-tie models can also be extended to members or parts of members which are unreinforced. It must, however, be pointed out that the failure cannot be assumed by simply limiting the capacity of the tensile struts to the axial tensile strength of the concrete, but that the discrete crack and the shear carrying mechanisms must be looked at.

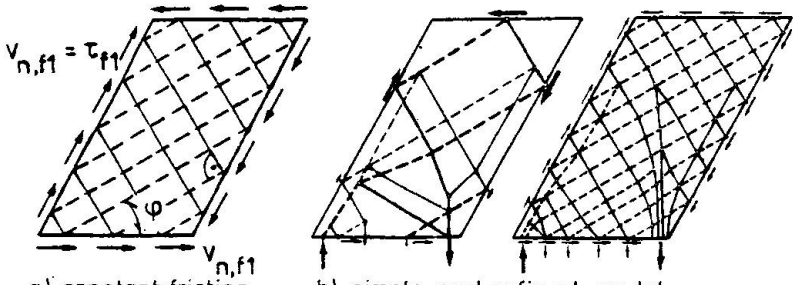


Fig.3: Stress fields between cracks

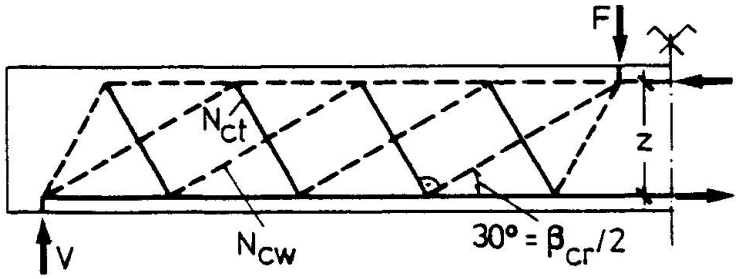


Fig.4: Truss model for members without transverse reinforcement

## 3. CONSTITUTIVE RELATIONS

For the steel and the concrete in compression bi-linear stress-strain relations can be assumed. The axial tensile strength of the concrete of

$$f_{ct} = 0,246 \cdot f_c^{2/3} \tag{7}$$

is an average value determined from the relative few tests where the tensile strength was actually determined with control specimens. With that the ultimate dowel force of the longitudinal reinforcement can be determined according to the proposal by Baumann /11/ or Vintzeleou and Tassios /12/.

The transfer of forces in cracks depends not only on the tensile strength of the concrete, but also on the roughness as well as on the crack width$\Delta n$ and the slip$\Delta s$ increase as clearly described by Walraven /13/. It was assumed that the limiting friction stress is that transferrable without normal stress on the crack surface:

$$\tau_{fu} = 0,45 \cdot f_{ct} \left(1 - \frac{\Delta n}{\Delta n_u}\right) \quad \text{with} \quad \Delta n_u = 0,9 \text{ mm} \tag{8a}$$

With this value a critical slip of the crack faces is reached:

$$\Delta s_u = 0,336 \ \Delta n + 0,01 \ [\text{mm}] \tag{8b}$$

## 4. ULTIMATE CAPACITY

After the limiting friction stress $\tau_{fu}$ and the critical slip $\Delta s_u$ acc. to Eq.(8) are reached, the tooth rotates and separates from the compression zone. The crack width at the mid-height of the crack can be derived from the horizontal crack opening $\Delta u$ due to the elongation of the longitudinal steel and the slip (Fig. 5) giving the failure criterion:

$$\Delta n = 0,71 \cdot \varepsilon_s \cdot s_{cr} \tag{9}$$

With that the friction stress $\tau_{fu}$ acc. to Eq.(8a) is known and may be inserted in Eq.(6) for the total shear force. If then the Eq.(4) is used to replace the steel strain the following explicit equation for the ultimate load may be derived in the critical section with $x_u$=(a-1,5d):

$$V_u = \frac{b_w \ d \ 0,4 f_{ct} - 0,16 \frac{f_{ct}}{f_c} \lambda \frac{z_c}{d} N + V_{du}}{\left[1 + 0,16 \frac{f_{ct}}{f_c} \lambda \left(\frac{a}{d} - 1\right)\right]} \tag{10}$$

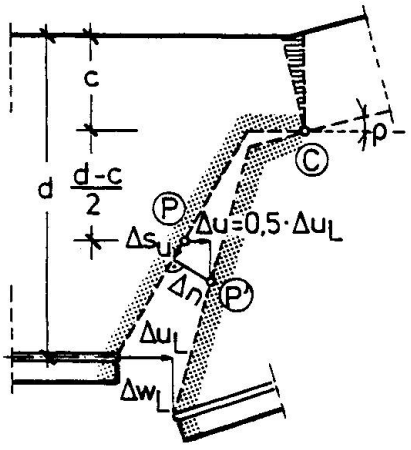


Fig.5: Kinematic consideration for crack width

Thereby the parameter $\lambda$ is a dimension-free value for the crack width:

$$\lambda = \frac{\varepsilon_{sy} \cdot d}{\omega \cdot \Delta n_u} = \frac{f_c}{E_s \cdot \rho} \cdot \frac{d}{\Delta n_u} \quad \text{with} \quad \omega = \rho \frac{f_y}{f_c} \tag{11}$$

It comprises the well-known influence of the longitudinal reinforcement ratio as well as that of the depth of the member. With that a simple dimensioning diagram for the dimension-free ultimate shear force can be presented (Fig.6).

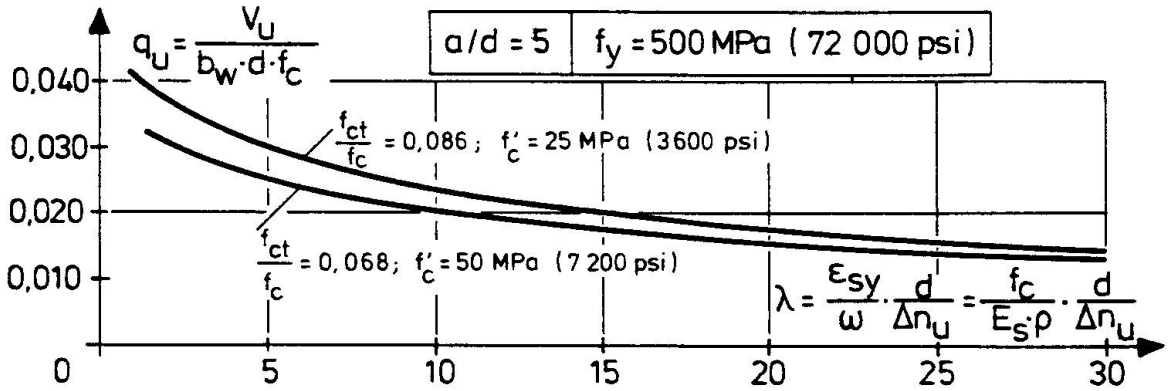


Fig.6: Dimensioning diagram for the ultimate shear force or load

## 5. DISCUSSION

### 5.1 Size Effect

The influence of the absolute depth of the member on the ultimate shear force is now obvious: the crack width increases proportionally with the crack height or the depth of the member (Fig.5), and consequently acc. to Eq.(8) the friction stress as the dominant shear carrying capacity is reduced. A further smaller size effect is also due to the dowel action /9/.

The proposed model is conservative if the crack width is very small as for thin members. Then the total length of the crack may be within the fracture zone near the crack-tip and small tensile stresses can be transferred up to a maximum crack width of about 0,15mm (Hillerborg and König /8/). This is shown in Fig.7 where the distributions of these tensile stresses along the crack are plotted for different test beams from Walraven /14/: the crack width increases with increasing depths and the extent of the fracture zone decreases. Since the model already relies on these tensile stresses within the curved part of the crack near its top (see Fig.3 and /9/), only the shaded area in Fig.7 remains for an additional contribution to the capacity of the member. For all members with larger depths the vertical component of the resultant $T_{ct}$ is small and contributes only 5 to 7 % to the ultimate dimension-free shear force; only in case of the beam A1 it increases to 20 % since the crack widths remain very small. However, such members with small depths normally fail in "bending" (like this beam A1), unless they are extremely heavily reinforced.

A further size effect is on the cracking moment and thereby on the steel strain due to the tension stiffening effect of the concrete between cracks. However, this is only worth considering for members with extremely high values $\lambda$, like e.g. foundation slabs with 2m depth and very low reinforcing ratios /9/.

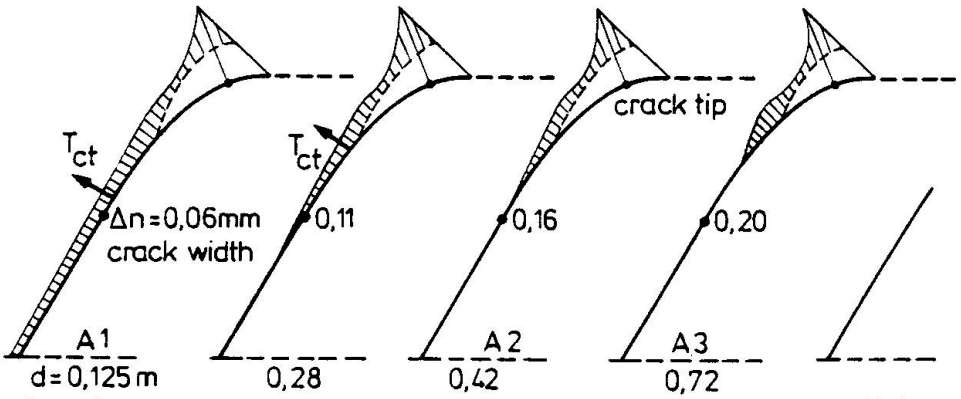


Fig.7: Distribution of tensile stresses in the fracture zone for some test beams with increasing depth

## 5.2 Axial Forces and Prestress

Axial forces were considered in the equilibrium equation for determining the force in the tension chord leading to Eq.(6), and Fig.8 gives an examples of its influence on the ultimate shear force. Axial compressive forces increase and tensile forces decrease the capacity as qualitatively already known. This is the more pronounced the higher the depth of the member is, since then the crack width is larger and more sensitive towards changes in the steel strain.

The proposed model and theory can also consistently be extended to fully cracked members due to high axial tension (Fig.8) or even restraints /9/. In such a case the shear force can only be transferred by friction along the crack and by the dowel forces of both reinforcement layers. Thereby the amount of the top-reinforcement, as expressed by the parameter $\eta$ in Fig.8, is of course decisive for the crack width and consequently the possible frictional resistance.

The structural model for a prestressed member is the same as given in Fig.4, apart that the inclinations of the compression struts may be slightly flatter due to the flatter crack inclinations. The influence of prestress on the ultimate load is best explained by looking at the stiffness of the tension chord (which is a prestressed tie), since its strain governs the width of the failure crack. The tension chord of a p.c.-member with the same mechanical reinforcing ratio is different in comparison to a r.c.-member:

- the strain will normally be smaller, but can also be larger if almost the yield strength is reached;
- the dowel force is smaller, because less steel area is needed and smaller diameters are used.

This is reflected in the comparison of ultimate capacities in Fig.9. The p.c.-member exhibits larger failure loads for large depths than the corresponding r.c.-member, but for small depths there is almost no difference.

## 5.3 Lightweight Concrete

The proposed model is also valid for lightweight concrete (LC) and only the constitutive relations must be adapted. The concrete tensile strength is lower than for normal concrete and a reduction to 66 % can be assumed /9/. The friction capacity acc. to Eq.(8a) is also reduced due to the lower tensile strength, but furthermore higher values for the critical slip occur than given in Eq.(8b):

$$\Delta s_u = 0{,}38 \cdot \Delta n + 0{,}01 \quad [\text{mm}] \tag{12}$$

With these minor modifications the proposed theory gives quite satisfactory results in comparison with an empirical formulae by Walraven /14/ as shown in Fig. 10.

## REFERENCES


1. Kani, G.N.J.: The riddle of shear failure and its solution. ACI-Jour.61 (1964), April, 441-467
2. Leonhardt, F.; Walther, R.: Schubversuche an einfeldrigen Stahlbetonbalken mit und ohne Schubbewehrung. DAfStb H.151, Berlin, 1962
3. Bresler, B.; Scordelis, A.C.: Shear strength of reinforced concrete beams. ACI-Jour. 60 (1963), 51-74
4. Muttoni, A.: Applicability of the theory of plasticity for dimensioning reinforcing concrete (in German). Dr.-thesis, ETH Zürich, 1989, 1-180
5. Kotsovos, M.D.: Compressive force path concept: basis for reinforced concrete ultimate limit state design. ACI Struct. Journal V.85, Jan.-Feb. 1988, 68-75
6. Fenwick, R.C.; Paulay, T.: Mechanisms of shear resistance of concrete beams. ASCE-Journal Struct. Div. V.94, 1968, ST 10, Oct., 2325-2350
7. Taylor, H.P.J.: The fundamental behaviour of reinforced concrete beams in bending and shear. In: ACI-SP 42, 43-77, Detroit, 1974
8. IABSE Colloquium "Structural Concrete". Introd. Reports. Stuttgart 1991
9. Reineck, K.-H.: A mechanical model for the behaviour of reinforced concrete members in shear (in German), Dr.-thesis., Univ. Stuttgart, 1990, 1-273
10. Reineck, K.-H.: Models for the design of reinforced and prestressed concre members. CEB-Bull.146, 43-96, Paris, 1982
11. Baumann, Th.: Tests on the dowel-action of the longitudinal reinforcement of r.c.-beam (in German). DAfStb 210, W. Ernst u. Sohn, Berlin, 1970, 42-83
12. Vintzeleou, E.N.; Tassios, T.P.. Mathematical models for dowel action under monotonic conditions. Mag. of Concrete Research 38 (1986), 13-22
13. Walraven, J.C.: Aggregate interlock: a theorectical and experimental analysis. Dr.-thesis, Delft Univ., 1980, 1-197
14. Walraven, J.C.: The influence of depth on the shear strength of lightweight concrete beams without shear reinforcement. Report S-78-4, Stevin Laboratory, Delft University, Dept. of Civil Eng.
15. Kirmair, M.: Das Schubtragverhalten schlanker Stahlbetonbalken - theoretische und experimentelle Untersuchungen für Leicht- und Normalbeton. DAfStb 385, Berlin, 1987

# Full-Scale Shear Tests on two Bridges

## Essais de cisaillement in situ sur deux ponts

## Querkraftversuche in voller Skala auf zwei Brücken

**Mario PLOS**
Res. Assist.
Chalmers Univ. Technol.
Göteborg, Sweden

**Kent GYLLTOFT**
Prof. Dr.
Chalmers Univ. Technol.
Göteborg, Sweden

**Krister CEDERWALL**
Prof.
Chalmers Univ. Technol.
Göteborg, Sweden

**SUMMARY**

Full-scale shear tests were performed on two concrete highway bridges constructed in 1980. The test results reveal short-comings in the design models when a combination of shear and moment actions leads to failure. The results show the need for better design models based on a clear physical understanding of failure. Fracture mechanics can be used together with the finite element method to obtain a better understanding of the failure process.

**RÉSUMÉ**

Les tests de cisaillement concernent deux ouvrages construits en 1980, les essais ayant été menés sur les ponts eux-mêmes. Les résultats montrent des défauts dans les modèles d'étude existants lorsque la rupture est due à l'action combinée des moments et de l'effort tranchant. Il s'agit donc d'établir de meilleurs modèles basés sur une compréhension physique claire du phénomène de rupture. La mécanique de la rupture utilisée conjointenement à la méthode des éléments finis permet d'obtenir une meilleure compréhension dans ce domaine.

**ZUSAMMENFASSUNG**

Grossversuche zur Schubtragfähigkeit von zwei 1980 erbauten Betonstrassenbrücken wurden durchgeführt. Die Versuche zeigen Mängel am Berechnungsmodell auf, wenn eine Kombination von Querkraft und Biegemoment zum Bruch führt. Die Ergebnisse beweisen die Notwendigkeit von besseren Berechnungsmodellen basierend auf physikalischem Verständnis des wirklichen Bruches. Bruchmechanik wird zusammen mit der Finite Element Methode verwendet, um ein besseres Verständnis des Bruchverhaltens gewinnen.

## 1. INTRODUCTION

The design rules for shear capacity set out in the European concrete codes is mainly based on laboratory tests on a comparatively small scale. In two full-scale tests we had the possibility to investigate the shear capacity for considerably larger structures than is normal in laboratories. The full-scale tests were performed on two concrete highway bridges, constructed in 1980. Both bridges were loaded close to one of the supports in order to cause shear failure.

The purpose of the tests was to improve knowledge by examine the bearing capacity of the bridges, and to study how these big and complex structures act under shear load leading to failure. The test results were compared with the design model in the Swedish concrete code. The results indicate that the design models are able to predict the shear capacity in cases where typical shear failures are achieved. In more complex cases, however, when a combination of shear and moment actions leads to failure, clear shortcomings were found in the design models of the code.

The tests are also intended to be used to improve methods of analysis. Finite element models of the bridges intended for fracture mechanics analysis are now under evaluation.

## 2. FULL SCALE SHEAR TESTS

### 2.1 The bridges

Full scale shear tests were performed on two concrete portal frame bridges. One of the bridges was a non-prestressed slab frame bridge with a free span of 21 m (fig 1 and 2).

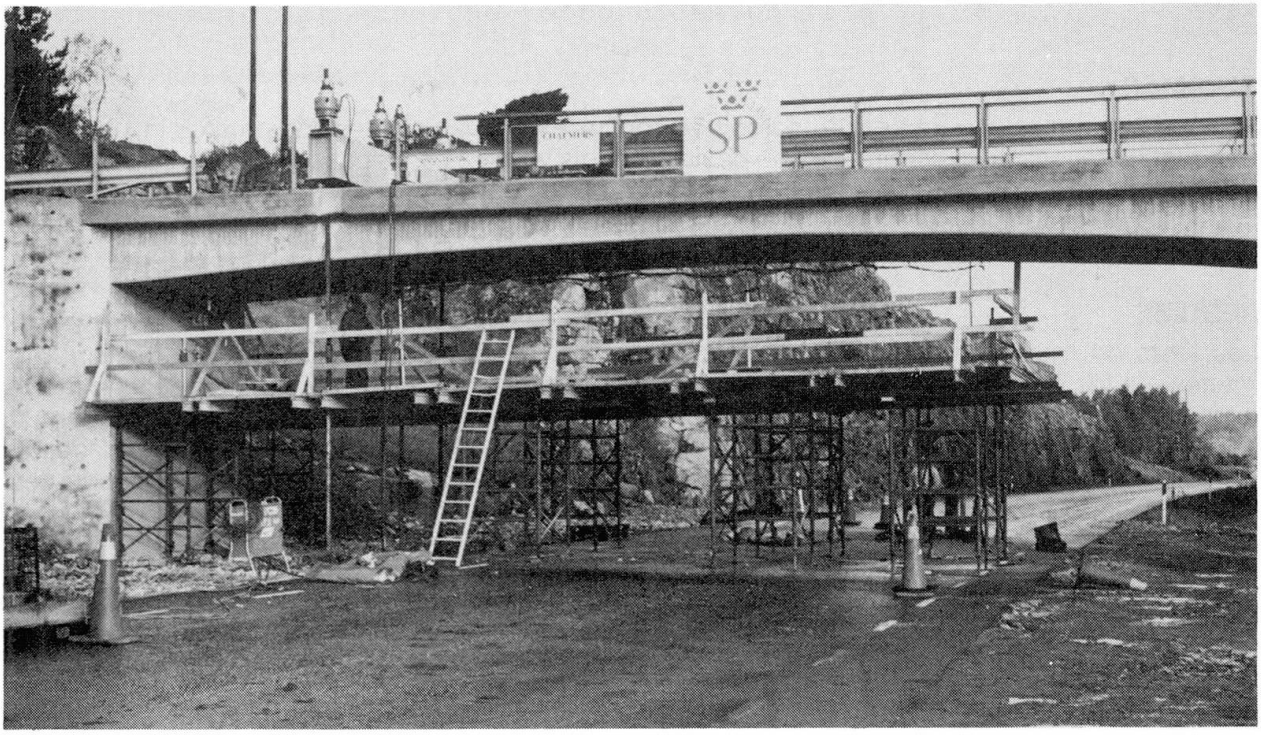


Fig. 1 Non-prestressed bridge during test preparation.

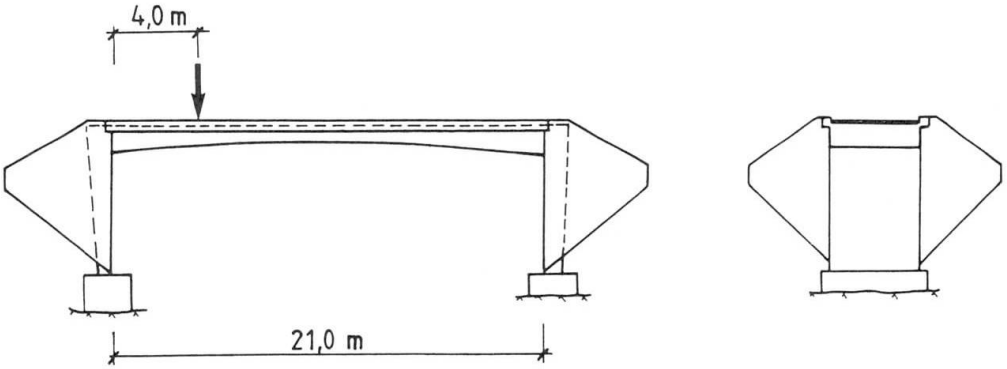


Fig. 2 Non-prestressed bridge

The other bridge was prestressed and had a free span of 31 m (fig 3 and 4). The span consisted of two post-tensioned beams connected by a bridge deck slab. The beams and the slab were connected with the front walls at the supports, forming a frame.

## 2.2 Test arrangements

The loads were applied through steel bars anchored to the rock under the bridges and transferred to the bridges by hydraulic jacks (fig 5). Loads, deflections and strains were measured during the tests, and crack growth was registered. The concrete strength was tested on cylinders drilled out of the bridges.

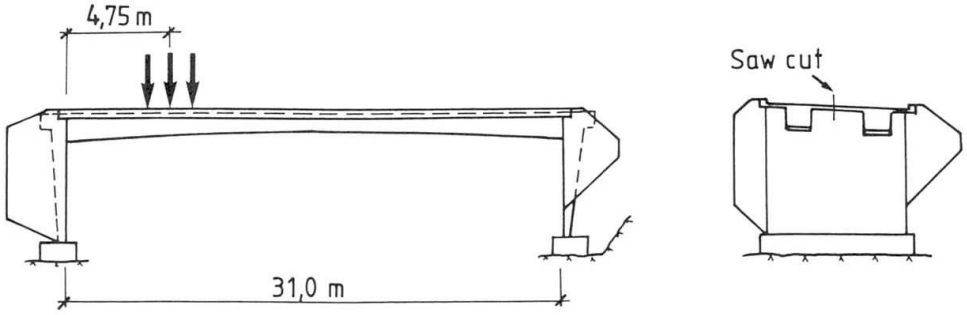


Fig. 3 Prestressed bridge

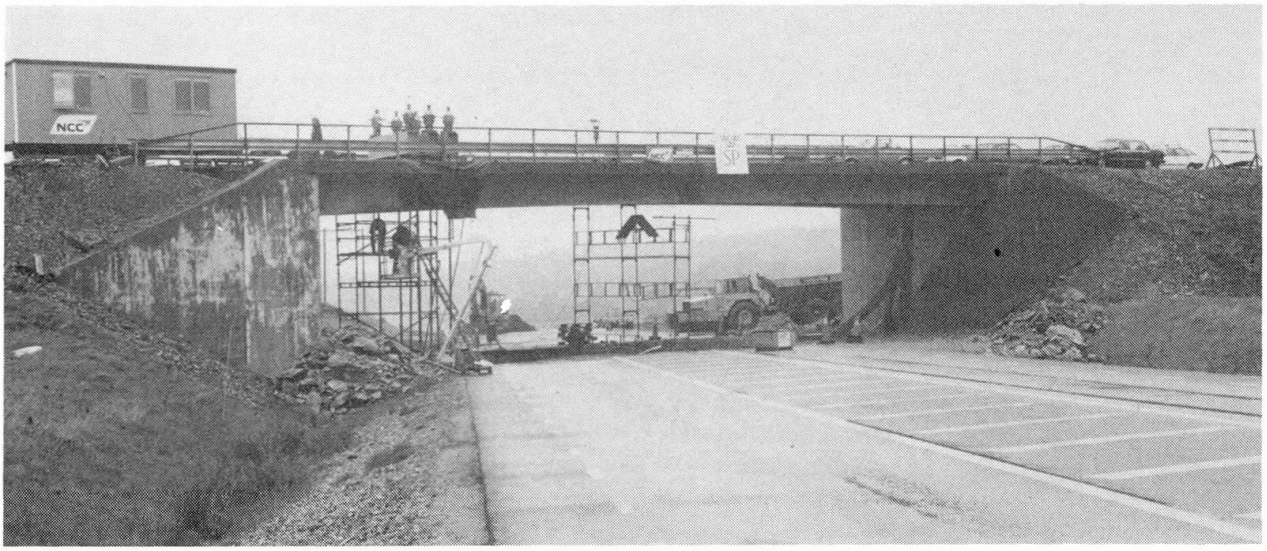


Fig. 4 View of the prestressed bridge

## 2.3 Test performance

The non-prestressed bridge was loaded 4,00 m from one of the supports and failed at a load of 4,5 MN due to a sudden diagonal shear crack (fig 6). The bridge was substantially cracked due to bending, and some shear-bending cracks were observed close to the loading section before the failure occurred.

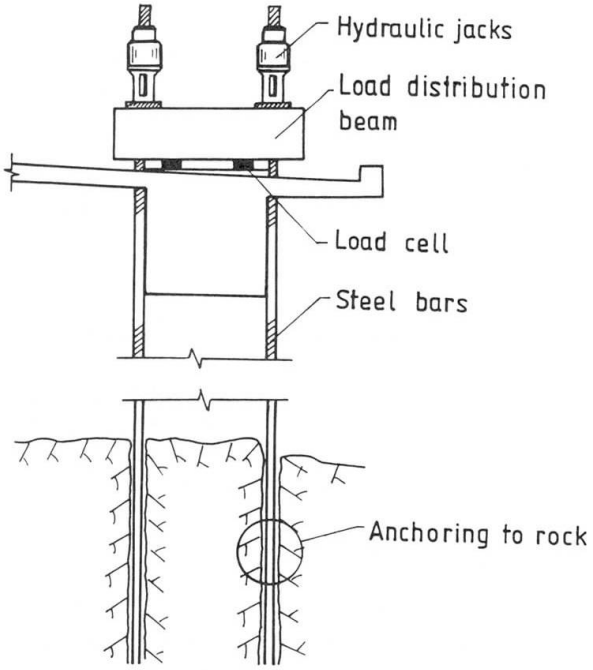


Fig. 5 Loading arrangement

The failure of the prestressed bridge was more complicated. Before the test this bridge was cut longitudinally between the two main beams and one of the beams was loaded about 4,75 m from one of the supports. After extensive cracking due to bending, together with a few shear-bending cracks, the support closest to the load unexpectedly failed at a load of 8,5 MN. The support failure lead to a redistribution of the moment, with increasing moment in the loading section.

When the support failed, the load decreased to 6,0 MN. Further loading with the jacks lead to large deformations and several inclined cracks in the shear span. The final failure occurred at a load of 6,3 MN, when the concrete at the upper edge of the loading section crushed due to compression (fig 7).

Fig. 6 Shear failure in the non-prestressed bridge

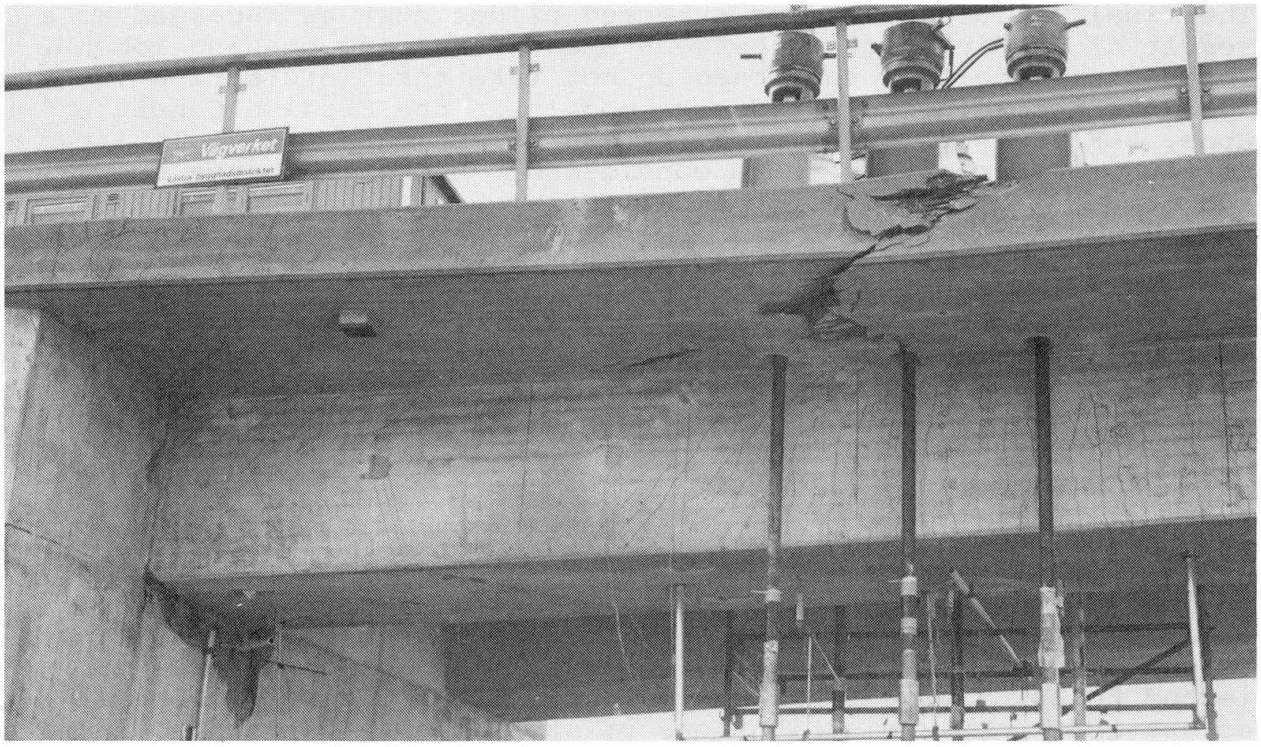

Fig. 7 Failure in the prestressed bridge. Cracking, support failure and concrete compression failure at the top of the loading section can be seen.

## 3. EVALUATION

The main purpose of the evaluation was to compare the bridges' real shear force at failure with their shear capacities according to the design model in the Swedish Concrete Code, BBK 79 /1/. Both the real shear force along the bridges and their shear capacities are dependent on the stiffness of the bridges and the degree of restraint at the supports. Due to cracking of the concrete and, for the prestressed bridge, failure in the support, stiffnesses and restraint conditions changed during loading.

To determine the stiffnesses and the degrees of restraint, computer programmes based on the finite element method were used. The stiffnesses were approximately calculated from the crack formation registered during the tests. By adjusting the calculated stiffnesses and varying the degree of restraints in the finite element model so that the calculated deflections were the same as the measured deflections of the bridges, proper models of the bridges were created. By analysing the obtained models the bridges moment and shear force distribution were determined. The shear capacities according to codes were then calculated and compared with these shear forces present in the bridges at failure.

## 4. RESULTS

In the non-prestressed bridge a typical shear failure occurred. The moment and shear distribution of this bridge are under evaluation, but preliminary results indicate good agreement between the capacity according to the model in the code and test results.

The final failure in the prestressed bridge must be regarded as a result of the interaction between shear force and bending moment. The design models in the codes do not take this interaction into account. According to the design models in the Swedish Concrete Code, BBK 79, both shear capacity and moment capacity, calculated as separate capacities, were considerably higher than the shear and moment in the bridge at final failure.

It should however be observed that the final failure was achieved at a load level lower than the maximal. The difference between calculated shear capacity and shear force in the bridge was much smaller at maximum load level than at the final failure. The moment in the loading section, however, increased considerably from maximum load level until final failure occurred. The effect of moment must therefore have a decisive influence on the failure.

## 5. CONCLUSIONS

To sum up, the design models used in the codes for calculation of shear capacity seems to work well for structures subjected mainly to pure shear action. In more complex cases, for structures subjected to both large shear and moment actions, where prestress occurs and where redistributions of stesses have taken place, the design models are unable to predict capacity. It is therefore not sufficient to modify the design models used today. Instead research should be intensified to find models that better describe what happens when structures are subjected to loading until failure, so that the design can be based on a clear physical understanding of the failure.

Fracture mechanics together with the finite element method will be used to analyse these bridges to obtain a better understanding of the failure process, but also to further develop fracture mechanics as a tool in the analysis.

## 6. ACKNOWLEGEMENT

The tests have been performed in cooperation with The Swedish National Testing and Research Institute (SP), the Swedish Road Administration and Luleå University of Technology.

## REFERENCES

1. Statens betongkommitte', Bestämmelser för betongkonstruktioner, BBK 79, Utgåva 2 (Regulations for concrete structures, second edition), AB Svensk Byggtjänst, 1988 (in Swedish).

2. KJELLGREN L. and BERGSTRÖM G., Skjuvförsök på spännarmerad rambro (Shear test on prestressed concrete frame bridge), Div. of Concrete Structures, Chalmers University of Technology, Diploma thesis 90:1, Göteborg, February 1990 (in Swedish).

3. VO MINH H. and PLOS M., "Skarvning av armering i ramhörn (Splicing of reinforcement in frame corners)", Div. of Concrete Structures, Chalmers University of Technology, Diploma thesis 88:2, Göteborg, April 1988 (in Swedish).

# Stirrups or Fibers

## Etriers ou fibres

## Bügeln oder Fasern

**Fernand MORTELMANS**
Professor
Cath. Univ. of Leuven
Leuven, Belgium

Fernand Mortelmans, born 1926, received his engineering degree and Ph.D. at the State University of Ghent. Currently he is carrying out research on reinforced concrete beams subjected to combined action of bending moment and shear force, cracks, steel fibers and detailing of reinforcement. He has designed several important structures in Belgium.

**Lucie VANDEWALLE**
Senior Assistant
Cath. Univ. of Leuven
Leuven, Belgium

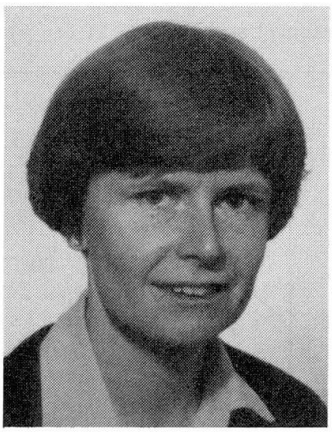

Lucie Vandewalle, born 1958, received her engineering degree and Ph.D. at the Catholic University of Leuven. Her field of research mainly concerns reinforced concrete and bond between steel and concrete.

**SUMMARY**

It is usual that the longitudinal reinforcement of a beam is calculated by means of the bending moment and the transverse reinforcement by means of the shear force. From extensive research carried out at the K.U. Leuven it was shown that in the compression zone of a beam a great part of the shear force is taken up. Consequently, more shear force can be taken up by the extension of the compression zone, i.e. by the provision of more longitudinal reinforcement. In this contribution an attempt is made to show that the global detailing of reinforcement may be determined by the interaction of bending moment, longitudinal and shear force.

**RÉSUMÉ**

Il est d'usage de déterminer l'armature longitudinale et transversale en considérant respectivement le moment fléchissant et l'effort tranchant dans une poutre. Une recherche étendue à la K.U. Leuven a démontré qu'une partie importante de l'effort tranchant est reprise dans la zone comprimée. Il est donc possible de reprendre un effort tranchant plus élevé en augmentant la zone comprimée, c.à.d. en renforçant l'armature de traction. Dans la présente communication on tente à démontrer que le dispositif complet et détaillé de l'armature peut être déterminé à partir de l'ensemble du moment fléchissant et de la force longitudinale et transversale.

**ZUSAMMENFASSUNG**

Es ist üblich, dass die Längsbewehrung eines Balkens aus dem Biegemoment, und die Querbewehrung aus der Querkraft berechnet wird. Aus einer umfassenden, an der K.U. Leuven durchgeführten Untersuchung hat sich ergeben, dass in der Druckzone eines Balkens ein grosser Teil der Querkraft aufgenommen wird. Es kann folglich mehr Querkraft durch Ausdehnung der Druckzone, d.h. durch Zulegen von Längsbewehrung aufgenommen werden. In diesem Beitrag wird versucht nachzuweisen, dass die gesamte Bewehrungsdetaillierung durch die Zusammenwirkung von Biegemoment, Längs- und Querkraft bestimmt werden kann.

## 1. INTRODUCTION

During the design of concrete structures, the determination of concrete dimensions and the detailing of reinforcement are of major concern. It is usual to calculate the longitudinal reinforcement and the transverse reinforcement independently of each other. The longitudinal reinforcement results from the bending moment and the normal force, the other reinforcement is necessary for the shear force.
This of course is a rough approach : internal forces are invented by engineers but fysically they do not exist.

## 2. INTERACTION BENDING MOMENT/SHEAR FORCE FOR A GIVEN CROSS SECTION

About twelve years ago, the so-called M-N-V- (bending moment (M), normal force (N) and shear force (V)) research program was started at the K.U.Leuven. From this investigation a **mathematical model** for the ultimate limit design has been developed, which permits taking into account :

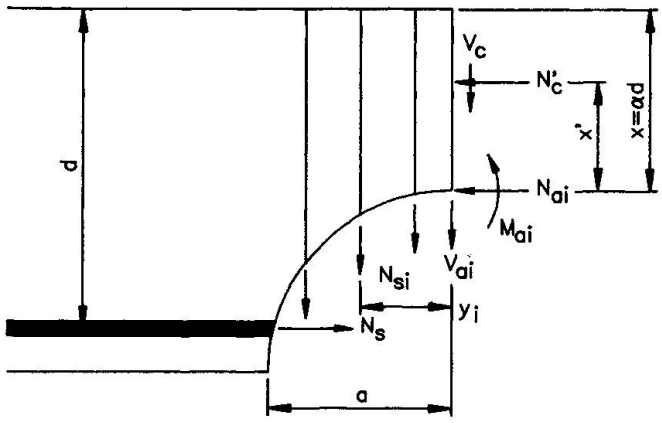


Fig. 1

- the normal force in the compression zone ($N'_c$)
- the absorbable shear force in the compression zone ($V_c$)
- the forces in the stirrups ($N_{si}$)
- the force in the tension reinforcement ($N_s$)
- the aggregate interlock ($M_a$,$V_a$,$N_a$)
- the shape of the crack.

The section is subjected to combined bending, compression and shear (M, N, V).
The normal force ($N_c$) and its situation (x') in the compressed zone can be calculated from the stress-strain diagram, proposed by CEB : [1]

$$\sigma_c = f_c \frac{\varepsilon_c}{2} \left(2 - \frac{\varepsilon_c}{2}\right) \qquad \text{for } 0 < \varepsilon_c \leq 2\ ‰ \qquad (1)$$

$$= f_c \qquad \text{for } 2 < \varepsilon_c \leq 3.5\ ‰$$

If also shear stresses act in addition to longitudinal stresses, several failure criteria can be used.
In our case (normal stress + shear stress) the simplest relation $\sigma_I/\sigma_{II}$ is a lineair function. It seems to be also a safe one.
From this relation the absorbable shear stress can be calculated

$$\tau_c = \sqrt{\frac{1}{4}\left[\left(\frac{1-K}{1+K}\right)^2 - 1\right]\sigma_c^2 + \frac{(1-K)K}{(1+K)^2}\sigma_c + \left(\frac{K}{1+K}\right)^2} \quad \text{with } K = \frac{f_{ct}}{f_c} \qquad (2),(3)$$

This elliptic criterion is shown in figure 2.

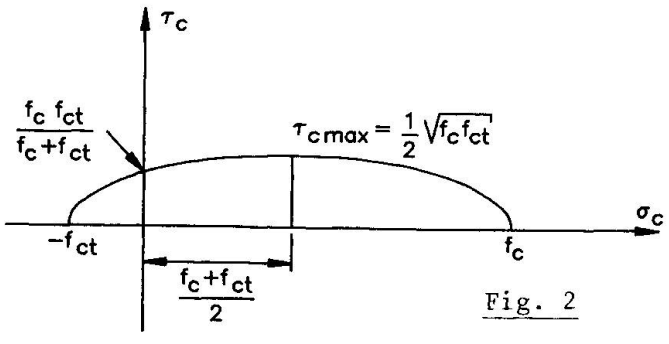


Fig. 2

From the shear stress-diagram the shear force $V_c$ can be calculated [2][3]. $V_c$ as well as $N_c$ are parameter functions of the deformation $\varepsilon_{cu}$ of the concrete on the upper side.
It is then possible to draw a diagram $n_c/v_c$ with

$$n_c = \frac{N_c}{\alpha\ b\ h\ f_c}$$

$$v_c = \frac{V_c}{\alpha\ b\ h\ f_c},$$

valid for a rectangular cross section (see Fig.3).

This relation $n_c/v_c$ has been confirmed by test results (see x in Fig. 3)[2,3,4]

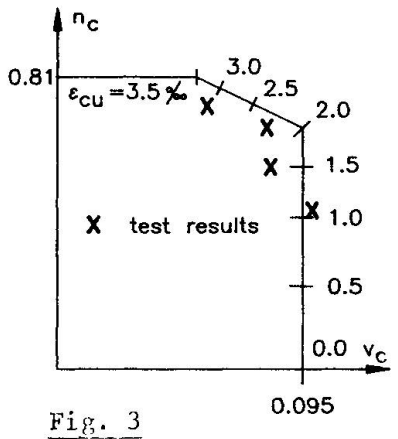


Fig. 3

Finally the horizontal projection of the crack has also been formulated by experiment for rectangular as well as for T shaped sections [6,7].
The influence of the aggregate interlock has been translated by the formulas, proposed by Prof. Walraven [5]. The shape of the crack has been determined in an experimental way [6].
The force in the reinforcement depends of course on the $\sigma_s/\varepsilon_s$-diagram of the steel.
The relation crack width/steel stress is based on the $\tau/\delta$ relation mentioned in [8].
Expressing the equilibrium of the section, we find an interaction diagram N/V for a given longitudinal force and given dimensions of the cross-section :

$$\begin{cases} N_c + N_{ai} - N_s = N & (4) \\ V_c + V_{ai} + \Sigma N_{si} = V & (5) \\ N_c x' + M_{ai} + \Sigma N_{si}\ y_i + N_s(d-v) = M & (6) \end{cases}$$

Since the interaction between the different forces does not follow a lineair course, the calculation can only be carried out step by step by means of a computer.
Given for example

$b = 300$ mm
$d = 650$ mm
$f_{ck} = 27$ N/mm$^2$
$A_s = 4$ ⌀ 20 BE 400
$3$ ⌀ 20 BE 400
$2$ ⌀ 20 BE 400
$N_c = 0$

the interaction bending moment/shear force can be computed.
In Fig. 4 the interaction

$$m = \frac{M}{\alpha\ b\ h^2\ f_{cd}} \quad (7)$$

$$v = \frac{V}{\alpha\ b\ h\ f_{cd}} \quad (8)$$

is plotted for several values of $A_s$ (4 ⌀ 20, 3 ⌀ 20 and 2 ⌀ 20) and several values of stirrup percentages ($\bar{\omega}_b$ = 0 - 0,1 - 0,2).

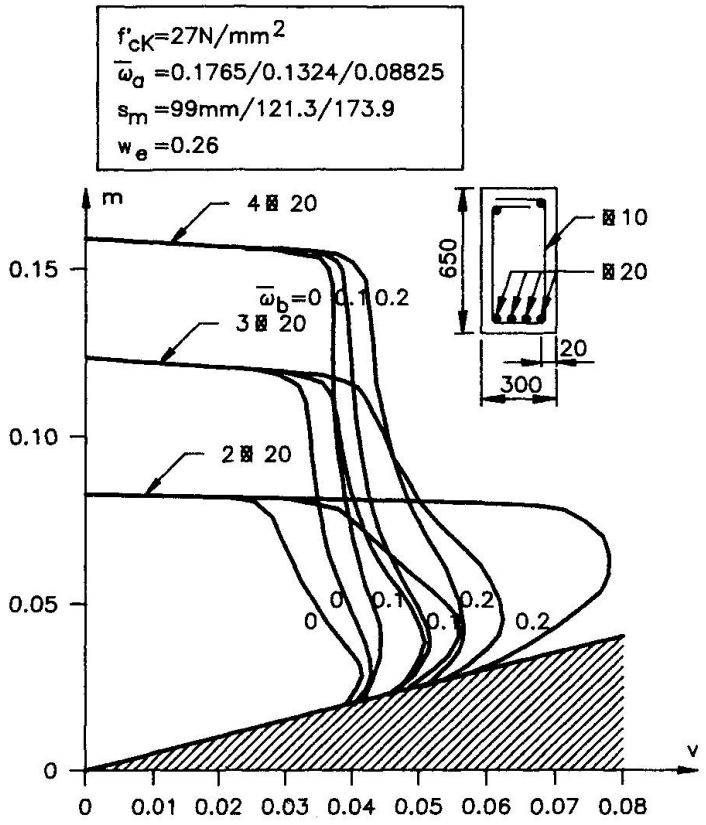


Fig. 4

## 3. INFLUENCE OF STIRRUPS

From the investigation as explained in 2 some important conclusions can be drawn.

1. The compression zone takes up a considerable part of the shear force.
2. The contribution of the stirrups is rather restricted.
3. The influence of the stirrups diminishes when the tension reinforcement increases.
4. The aggregate interlock decreases when the tension reinforcement is reduced.

It may be stated that when the area of the tension reinforcement increases - as a result of which the size of the compression zone expands - more shear force can be taken up by the concrete. The stirrups may then become unnecessary. So, more shear force can be taken up by increasing the tension reinforcement or by applying a (limited) prestressing.

The mathematical model is applicable both for reinforced concrete, for prestressed concrete and for partially prestressed concrete.

At the moment, an attempt is being made to incorporate the mathematical model in a calculation method, which is easy to handle in practice.

When the aggregate interlock is not taken into account - which means an additional safety - the calculation already becomes a good deal more simple.

## 4. RELATION BENDING MOMENT/SHEAR FORCE FOR A GIVEN LOAD

Let us consider a beam on two supports (length $\ell$) with a uniformally distributed load (p). The longitudinal force is zero. The bending moment M and the shear force V at a distance x from the left support can be formulated as ($t = x/\ell$) :

$$M = \frac{p\ell^2}{2}(1 - t)t$$

$$V = \frac{p\ell}{2}(1 - 2t) \qquad (9)$$

Eliminating t between M and V and introducing the notations $m_p$, $v_p$ and $\lambda$

$$m_p = \frac{M}{b\ h^2\ f_{cd}} \qquad (10)$$

$$v_p = \frac{V}{b\ h\ f_{cd}} \qquad (11)$$

$$\lambda = \frac{p\ell^2}{8\ b\ h^2\ f_{cd}} \qquad (12)$$

we find an interaction $m_p/v_p$

$$m_p = \lambda\ [1 - (\frac{v_p}{\lambda})^2\ (\frac{\ell}{h})^2] \ . \qquad (13)$$

This interaction $m_p/v_p$ due to the load p is to be secured by the interaction diagram $m_o/v_o$ that the section is capable to bear ($m_o = \alpha$ m, $\alpha_o = \alpha$ v).
In the figure 5 both interactions are drawn schematically.
Full lines represent the load relation, dotted lines concern the "bearing capacity" of the chosen section for stirrup percentages $\bar{\omega}$ = 0 - 0,1 and 0,2.
For the case drawn in figure 5 it is clear that for a slender beam ($h/\ell$ = 0,05 and even $h/\ell$ = 0,10) no stirrups are required.
When $h/\ell$ increases - for example $h/\ell$ = 0,15 - stirrups become necessary from the point A to the point B.
So it is clear that a lot of beams can be designed without stirrups. On the other hand less slender beams may need some stirrups near to the support. At the addition of steel fibers in the concrete mix the interaction lines $m_o/v_o$ move to the right. This has been proved by dr.ir. L. Van de Loock [9] in his doctor's thesis.

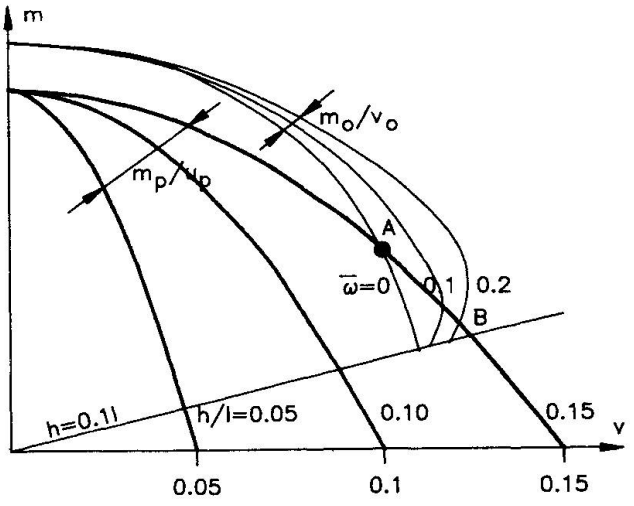


Fig. 5

## 5. DETAILING OF THE REINFORCEMENT

Even if no stirrups are necessary, it seems to us that it is advisable to add a limited quantity of fibers in the concrete in order to secure a minimum tensile strength and an adequate post cracking behaviour.
Of course, not all the beams can be considered for reinforcing without stirrups. We think that a scientific dosage of longitudinal reinforcement, steel fibers (15 to 20 $kg/m^3$) and stirrups makes it possible to design more economically most of the common beams. Besides, it is known that cracks often start at the location of the stirrups.

## REFERENCES

1. CEB. Modelcode 1978

2. MORTELMANS F., "Interaction diagram bending moment/shear force considering the absorbable forces in the cracked and the non cracked concrete", internal paper 20-ST-13 of 18-10-1984, Leuven.

3. MORTELMANS F., "Relatie tussen buiging en dwarskracht" (relation between bending moment and shear force), Cement nr. 10, 1985.

4. MORTELMANS F., VANDEWALLE L., "A new criterion for concrete in compression", Rilem Workshop on applications of fracture mechanics to concrete structures, Abisko (Zweden), 28-30 June 1989, (will be published by Chapman and Hall).

5. WALRAVEN J.C., "Aggregate Interlock : A theoretical and experimental analysis", University Press, Delft 1980.

6. VANDEWALLE L., CARNOY D., "Scheurpatroon van balken in gewapend beton", Afstudeerwerk K.U.Leuven, 1981.

7. HEMMATY Y., "Crack Pattern of T-section. Beams in reinforced concrete", Masters Degree 1986.

8. VOS E., REINHARDT L., "Bond resistance of deformed bars, plain bars and strands under impact loading", report 5-80-6, Delft.

9. VAN DE LOOCK L., "M-D model voor betonnen balken met rechthoekige sectie voorzien van langswapening en staalvezels" (M-V model for concrete beams with rectangular cross section with longitudinal reinforcement and steel fibers), Ph. D., K.U.Leuven 1989.

# Detailing for Shear with the Compressive Force Path Concept

## Cisaillement et concept de champ de forces de compression

**Atallah S. KUTTAB**
Assistant Professor
Birzeit University
Birzeit

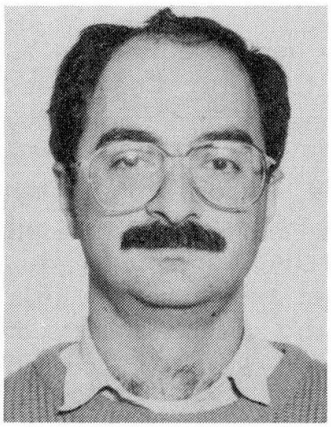

Atallah Kuttab is a member of CEB Task Force Group GTG 24 «Practical Design Utilising Multiaxial States of Stress», and member of CEB Permanent Commission PC 4 «Members Design».

**David HALDANE**
Senior Lecturer
Heriot-Watt Univ.
Edinburgh, Scotland

David Haldane is actively involved in the numerical modelling and the experimental validation of the behaviour of structural concrete members particularly in the fields of deep beams and impact loading.

**SUMMARY**

The paper presents the results from tests on simple beams which were reinforced in compliance with the compressive force path concept using stirrups that did not extend the full depth of the beam. The test specimens when compared with conventionally reinforced ones showed higher strength and ductility. Furthermore, it is shown that the classification of beams according to their shear span to effective depth ratio is not only confusing but unnecessary.

**RÉSUMÉ**

Ce rapport présente les résultats de tests effectués sur des poutres simples en béton, armées sur la base du concept de champ de forces de compression et possédant des étriers courts ne s'étendant pas sur toute le hauteur de la poutre. Les échantillons expérimentaux se sont montrés plus résistants et ductiles que les échantillons armés de façon conventionnelle. De plus, il est démontrée que la classification des poutres en function du rapport «a/d» dans ce cas porte non seulement à confusion mais n'est pas nécessaire.

**ZUSAMMENFASSUNG**

Im vorliegenden Artikel werden die Versuchsergebnisse von einfachen Stahlbetonträgern, die nach dem «compressive force path concept» mit nicht über die ganze Höhe des Trägers reichenden Bügeln bewehrt wurden. Die Versuche zeigten im Vergleich zu konventionell verstärkten Trägern erhöhte Festigkeit und Duktilität. Darüber hinaus wurde deutlich, dass die Klassifikation von Trägern in Bezug auf das «a/d» Verhältnis nicht nur verwirrend, sondern unnötig ist.

## 1. INTRODUCTION

The practice of detailing reinforced concrete members is somewhat irrationally dependent to a large extent on its structural function. As an example, the provision of transverse reinforcement in a column implies that compressive zones in general require the presence of such reinforcement; while on the other hand, the introduction of transverse reinforcement to a simple beam is largely dependent on whether or not shear stresses are present. This apparent inconsistency in present day practice appears to have originated from the adoption of design principles based on an uniaxial state of stress. In addition, the design of structural concrete for some cases, for example shear design, follows physical models which do not represent the true behaviour.

In this context, MacGregor (1) described the ACI(2) shear design equations as "empirical mubo-jumbo". The tendency in present Code Drafting Committees (2,3,4,5) is to move towards procedures comparable in rationality and generality to the plane sections approach for flexure and axial load. The objective of the design procedures for shear is to try to assess the amount of shear reinforcement required to carry that portion of the shear forces in excess of that which can be sustained by the concrete alone. In order to achieve this aim various approaches based on concepts such as the latest truss models (6), the compression field theory (7), the lower and upper-bound of the theory of plasticity (8), etc are being adopted. Essentially, the element which is common to these models is the assumption that the diagonally cracked concrete forms the strut through which the load is transferred from the point of application to the support. This has necessitated extensive research in order to determine the characteristics of diagonally cracked concrete (7) and the impact of size effects related to concrete in tension (9). This approach has resulted in semi-empirical relationships which have required continuous modification to "fit" the results which were available from experimental investigations. The complexity of the approach lies in the modelling of physically unstable media, due to the continuous cracking of concrete, in the analysis which poses problems in satisfying both equilibrium and compatibility of strains in the idealised structure.

In fact, research over the past three decades which was aimed at resolving the riddle of shear, most notably the work by Kani (10), has resulted in models based either on the behavioural characteristics of the concrete cantilevers which form between adjacent flexural cracks, or the development of arch action in the beams as the ultimate loads were approached. Kotsovos (11) has more recently used the compressive force path concept to explain the behaviour of simple beams in shear. It was concluded that the concrete below the neutral axis did not contribute significantly to the shear capacity of the beam. This was in direct agreement with the findings of the investigations carried out by Kani (10) in which the approach based on the strength of the concrete cantilevers and the one based on the presence of arch action were totally dependent on the strength of the concrete in the compression zone. The indications from published research work are that for concrete beams unreinforced for shear, the concrete in the compression zone is almost entirely responsible for the ability of the section to resist the applied shear loadings.

It is advocated here, based on the behaviour of unreinforced concrete in shear, that the shear capacity of a beam could be enhanced and thus increasing its

overall strength by confining the concrete in the compression zone. This is normal practice in the case of either disturbed regions or axial members (12). The adoption of such an approach would therefore transform the complexity of the flexure-shear interaction to one of designing a compression member. A series of tests has been undertaken on simple beams reinforced with stirrups which did not extend down over the full depth of the beam thus locally confining the concrete in the enclosed compression zone. In addition to observing the strength variations between the individual beams comparisons have been made with the behaviour of beams which were conventionally reinforced.

## 2. RESEARCH SIGNIFICANCE

This investigation forms part of a research programme whose principal objective is the development of a set of design procedures for structural concrete members which are compatible with their true behaviour. It is believed that the adoption of concepts based on observed failure modes will result in simpler and more realistic approaches to the analysis and design of such structural concrete members.

## 3. TEST SPECIMENS AND EXPERIMENTAL RESULTS

The test beam specimens, which were all under-reinforced, are described in Figure 1. Typical failure modes and load-deflection relationships for the various specimens are illustrated in Figures 2 and 3 respectively.

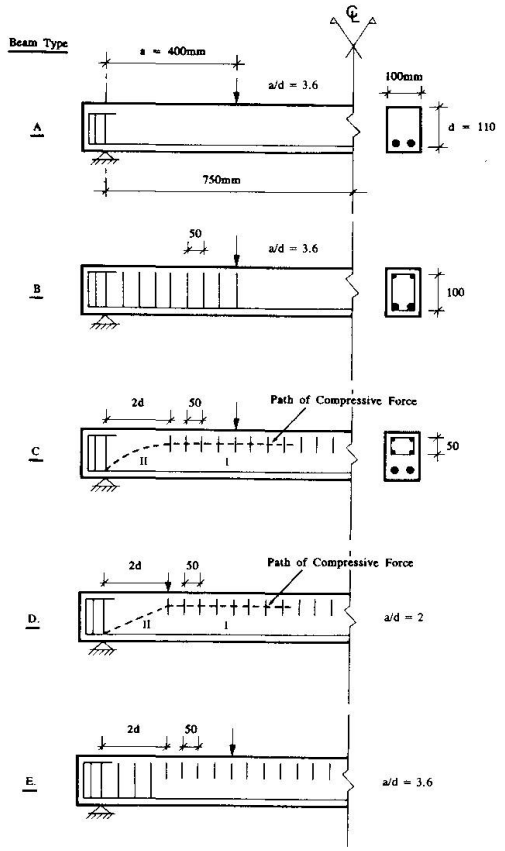


FIGURE 1. TEST SPECIMENS.

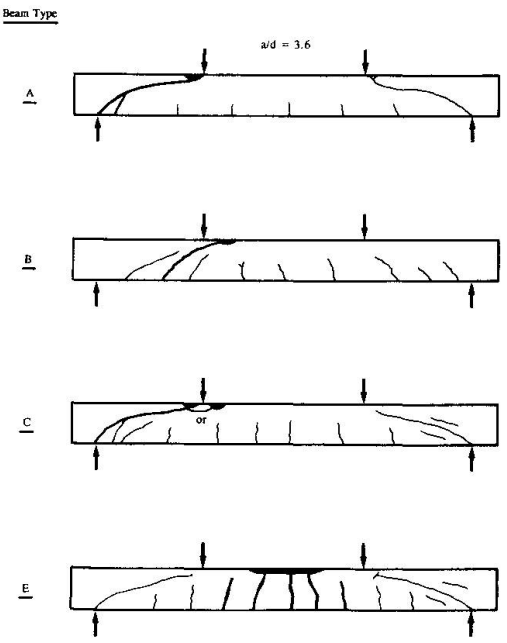


FIGURE 2. MODES OF FAILURE.

Notes:

1. Concrete strength is 28MPa (28 days).
2. Diameter and strength of main steel reinforcement is 12mm and 410MPa respectively.
3. Diameter and strength of transverse steel reinforcement is 6mm and 280MPa respectively.

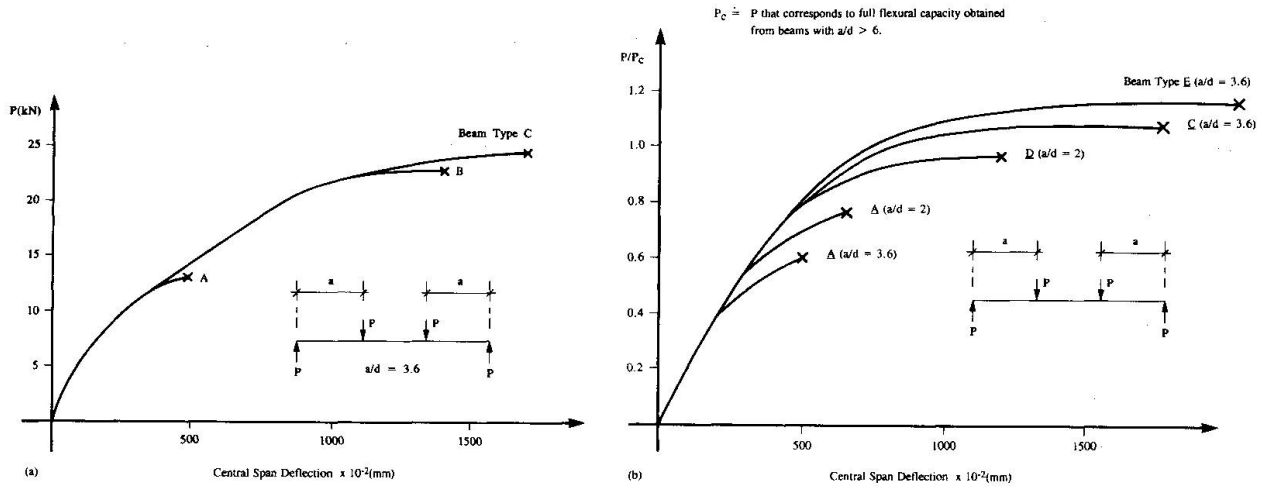


FIGURE 3 (a & b). LOAD DEFLECTION RESULTS.

## 4. DISCUSSION OF RESULTS

### 4.1 Modes of Failure

The resulting modes of failure of the beams without stirrups (type A beam in Figure 2) and those reinforced in compliance with Code provisions (type B beam in Figure 2) were as expected. In the case of the type C beams shown in Figure 2, the failure mode cannot be explained in terms of current theories. It was expected, and in accordance with the current theories of beam behaviour, that the failures of the type A and the type C beams would be similarly controlled by their shear capacity since both were unreinforced for shear. However, the type C beams were able to attain their full flexural capacity. The crack patterns present in the type C beams were comparable to those obtained in the type B beams in terms of extensiveness, but characteristically similar to those present in the type A beams. The type C beams contained a major diagonal crack, similar to the one found in the type A beams, which was prevented from splitting the compression zone by the presence of the transverse reinforcement. This allowed the type C beams to develop their full flexural capacity and thus behave in a characteristically ductile manner.

### 4.2 Load Capacity and Ductility

The type C beams, in which only the compression zone was reinforced with stirrups, and in accordance with the latest truss models or compression field theory, were expected to have the same load carrying capacity as those without stirrups i.e. type A beams. From Figure 3(a) it was found that their load carrying capacity exceeded that of the type A beams by about 90%. In the case of the type C beams, the shear load could not have been carried by a truss structure as generally assumed in present Codes of Practice. The type C beams were found to have a 7% higher load carrying capacity and an approximately 20% higher ductility than the type B beams despite the fact that the type of stirrups normally forming the ties in the truss structure were not present in this case. The increased ductility exhibited by the type C beams could be explained by considering the forces to which the compression zone is

subjected to when the concrete becomes an unstable media due to continuous cracking. In the type B beams, the forces carried by the concrete after cracking are transferred to the stirrups which are anchored in the compression zone. It can be argued that this sudden transfer of stresses will produce impact loading on the compression zone which in turn would initiate a premature failure due to local crushing of the compression zone. This will therefore result in a reduction in the ductility of the beam. Alternatively, for the case of the type C beams the equilibrium of stresses at a section is solely controlled by the characteristics of the concrete in the beam. The provision of passive confinement by the introduction of stirrups in the compression zone creates a multiaxial state of stress in that region which would be able to satisfy equilibrium and compatibility conditions. The degree of ductility exhibited by the beams will depend to a large extent on the level of confinement provided in the compression zone.

### 4.3 Dependence on "a/d" value

Based on the compressive force path concept, the provision of the necessary transverse reinforcement in the beams, such that they will attain their full flexural capacity, would follow the same procedure regardless of the value of their shear span to effective depth ratio, a/d (13). For example, the compressive zone denoted by I in Figure 2 (type C and type D beams), requires confinement (by the provision of stirrups) regardless of the value of a/d and irrespective of whether or not it is subjected to shear forces. The region denoted by II in Figure 2 (type C and type D beams) follows traditional deep beam behaviour and therefore does not prevent the beam attaining its full flexural capacity. In fact, the type C and D beams were reinforced accordingly. The normalised results together with those of type A beams are shown in Figure 3(b) for comparative purposes. Both types of beams attained the full flexural capacity with higher ductilities than the type A beams. However, the provision of conventional stirrups in the deep beam region as in type E beams (refer to Figure 1) improved both ductility and strength as shown in Figure 3(b).

## 5. SUMMARY AND CONCLUSIONS

a) The load carrying capacities and ductilities of beams (Figure 3) were enhanced when the compression zone was passively confined with stirrups which did not extend down the full depth of the beam (Figure 1).

b) The special detailing approach adopted in the case of the type C beams (Figure 1) has recognised and attempted to conform to the true flow of stresses in the beam. The approach was essentially based on the compressive force path concept which accepts that the concrete below the neutral axis does not make a significant contribution to the load capacity of the beam. The acceptance and subsequent validation of such an approach will, for example, lead to the removal of the requirement for further investigations into the constitutive relationships for cracked concrete and the significance of the associated size effects in this context.

c) The complex problem of flexure-shear interaction could potentially be reduced to one of the design of axial members. Therefore, the work done on axial loaded concrete members (12) is expected to be directly applicable to this subject area.

d) When the analysis and design of structural concrete members is based on observed modes of behaviour it is anticipated that more rational procedures will be evolved. For example the existing classification of procedures for beam design which are normally dependent on the a/d ratio will become redundant and will lead to the removal of the lack of rationality which presently exists.

## ACKNOWLEDGEMENT

The specimens were tested by the students Ziyad Abu Hassanein and Hasheim Skeik from Birzeit University in partial fulfillment of their graduation requirements. Their assistance is gratefully acknowledged.

## REFERENCES

1. MACGREGOR, J.G., Challenges and Changes in the Design of Concrete Structures, Concrete International: Design and Construction, Vol. 6, No. 2, February 1984, pp. 48-52.
2. ACI COMMITTEE 318, Building Code Requirements for Reinforced Concrete, ACI 318-89) American Concrete Institute, Detroit, 1989.
3. Design of Concrete Structures for Buildings, (CAN3-A23.3-M84) Canadian Standards Association, Rexdale, 1984, 281pp.
4. Code of Practice for Design and Construction, (BS8110) British Standards Institution, London, 1985, Part 1, 154pp.
5. CEB-FIP Model Code for Concrete Structures, Comite Euro-Internationale du Beton and Federation Internationale de la Preconstrainte, English Edition, Paris, 1978, 156pp.
6. SCHLAICH, J., SCHAFER, K., and JENNEWEIN, M., Toward a Consistent Design of Structural Concrete, PCI Journal, May/June 1987.
7. COLLINS, P.C., and MITCHELL, D., A Rational Approach to Shear Design - The 1984 Canadian Code Provisions, ACI Journal, Vol. 83, November/ December 1986, pp. 925-933.
8. NIELSON, M.P., BRAESTRUP, M.W., JENSEN, B.C., and BACH, F., Concrete Plasticity, Special Publication, Danish Society for Structural Science and Engineering. Lyngby/Copenhagen, October 1978, 129pp.
9. BAZANT, Z.P., and OH, B.H., Crack Band Theory for Fracture of Concrete, Materials and Structures, Vol. 16, No. 93, May/June 1983, pp. 155-177.
10. KANI, G.N.J., The Riddle of Shear Failure and Its Solution, ACI Journal, Vol. 61, No. 4, April 1964, pp. 441-467.
11. KOTSOVOS, M.D., Compressive Force Path Concept: Basis for Reinforced Concrete Ultimate State Design, ACI Structural Journal, Vol. 85, No. 1, January/February 1988, pp. 68-75.
12. KUTTAB, A.S. and DOUGILL, J.W., Grouted and Dowelled Jointed Precast Concrete Columns: Behavior in Combined Bending and Compression, Magazine of Concrete Research (London), Vol. 40, No. 144, September 1988, pp. 131-142.
13. KUTTAB, A.S., Assessment of Concrete Structures Utilising Multiaxial Properties, Proceedings of the International Symposium on "Re-Evaluation of Concrete Structures" organised by the Danish Concrete Institute (DABI), Copenhagen/Lyngby, June 1988.

# Shear in Structural Concrete: a Reappraisal of Current Concepts

## Cisaillement du béton armé: nécessité de reconsidérer les concepts courants

## Schubtragfähigkeit: Fragwürdige Bemessungsgrundlagen

**Michael D. KOTSOVOS**
Dr. Eng.
Imperial College
London, UK

Michael D. Kotsovos obtained his Ph.D. in 1974 and his D.Sc. in 1981. Twice he has been awarded Henry Adams diplomas by the Institution of Structural Engineers, London. His research interests cover most aspects of structural concrete behaviour under static and dynamic loading conditions.

**SUMMARY**

Evidence is presented which demonstrates that current design concepts are incompatible with the ultimate limit state of reinforced concrete beams. It is found that shear capacity is associated with the strength of the compressive zone and not, as widely considered, the portion of the beam below the neutral axis. The mechanism of shear resistance and the causes of failure are identified and it is shown that modelling a reinforced concrete beam as a frame with inclined legs tied by the tension reinforcement can lead to reliable design solutions which are both more economical and safer than those resulting from current design models. It is suggested that any skeletal structural form can be considered as an assemblage of elements formed between consecutive points of inflection with the elements being described by the proposed model.

**RÉSUMÉ**

La preuve est établie que les concepts courants de dimensionnement sont incompatibles avec l'état de limite ultime des poutres en béton armé. La résistance au cisaillement est en réalité associée à la résistance de la zone comprimée et non pas à la zone située au-dessous de l'axe neutre, comme couramment considéré. On décrit ainsi le mode de résistance au cisaillement, de même que les causes de rupture; une poutre en béton armé modélisée par un cadre aux bords inclinés et reliés par l'armature de traction peut mener à des solutions de dimensionnement fiables qui sont bien plus sûres et économiques que celles résultant des modèles de conception courants. On suggère donc de considérer toute forme d'ossature comme un assemblage d'éléments décrits précédemment se formant entre deux points d'inflexion consécutifs.

**ZUSAMMENFASSUNG**

Versuchsergebnisse über die mangelhafte Beschreibung des Stahlbetonverhaltens mittels derzeitiger Bemessungsgrundlagen werden vorgetragen. Es wird gezeigt, dass die Schubtragfähigkeit nicht, wie üblich angenommen, dem unterhalb der Nullinie liegenden Balkenanteil zugeordnet ist, sondern der Tragfähigkeit der Betondruckzone. Der Mechanismus des Querkraftwiderstands und die Fehlerursache werden ermittelt. Es wird anschaulich vorgeführt, dass die Abbildung des Stahlbetonbalkens durch einen Rahmen mit schrägliegenden Beinen und Zugband zu zuverlässigen Bemessungslösungen führen, die nicht nur wirtschaftlicher, sondern auch sicherer als die Lösungen mittels derzeitiger Bemessungsgrundlagen wie Fachwerkträger und Druckstab mit Zugband sind. Es wird vorgeschlagen, das Stahlbetonskelett als Zusammenstellung solcher Elemente zwischen den aufeinanderfolgenden Momentennullpunkten zu betrachten.

## 1. INTRODUCTION

Current methods used for shear design often yield poor predictions of shear capacity. Fig. 1 provides an indication of such predictions and demonstrates the possibility for current Code provisions [1-5] to yield predictions which can be over-conservative in certain cases and unsafe in others. Clearly, the cause for such predictions should be attributed to the underlying concepts, common to all current shear design methods, rather than the various formulations used by particular methods for the implementation of the concepts in design.

In view of the above, it is considered that a reappraisal of the current design concepts should be a prerequisite for any future Code revision. Such a reappraisal, which is essential not only for improving existing design models but also, if necessary, for developing new ones, has formed the subject of recent work which has been aimed at identifying the fundamental causes of the observed behaviour of structural concrete members. The paper summarizes the main results of the work and describes a first attempt to implement them in design.

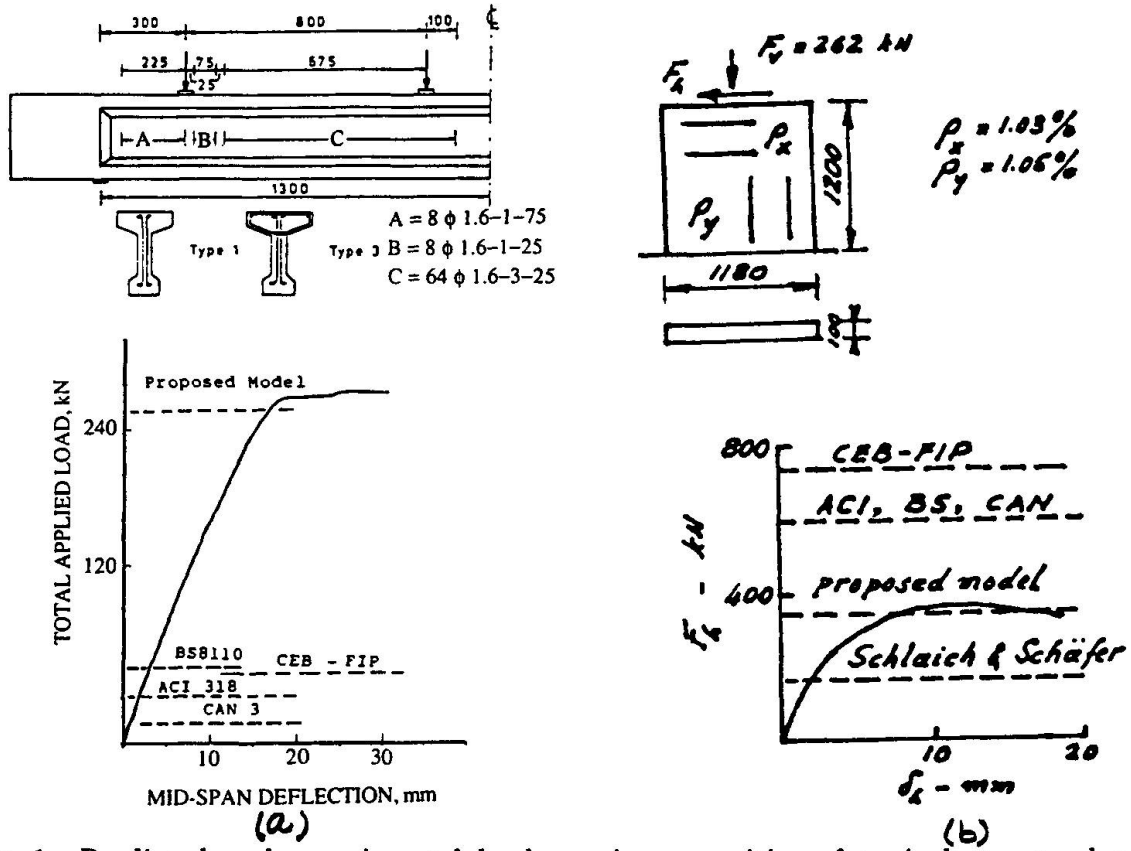


Fig. 1 Predicted and experimental load-carrying capacities of typical structural concrete members tested by (a) Kotsovos & Lefas [11] and (b) Maier & Thurlimann [12].

## 2. CONCEPTS UNDERLYING SHEAR DESIGN

Current methods for the design of structural concrete members are invariably based on the view that shear resistance is mainly provided by the portion of the member outside the compressive zone. In the absence of transverse reinforcement, such resistance is provided by concrete with main contributor the aggregate interlock which is effected by the shearing movement of the surfaces of inclined cracks. Shear failure is considered to occur when the shear capacity of a critical section is attained and, in order to prevent it, transverse reinforcement is provided to carry the portion of the shear force that cannot be sustained by concrete alone. Such reinforcement is designed on the basis of the assumption that the interaction between concrete and reinforcement can be described by a suitable strut and tie or truss model the strength of which may or may not rely on the contribution of aggregate interlock. In the former case, the model struts are considered to intersect the inclined cracks - and, hence, aggregate interlock is essential for the load-carrying capacity of the struts -

whereas in the latter, a strut is considered to be formed by concrete between consecutive inclined cracks.

## 3. TEST OF VALIDITY OF CONCEPTS

A test of the validity of the above concepts has been based on an investigation of the behaviour of RC beams, with various arrangements of transverse reinforcement (see Fig. 2a), subjected to two-point loading with various shear span to depth ratios ($a_v/d$) [6]. The main results of this programme are also given in Fig. 2a in the form of load-deflection curves for the beams tested.

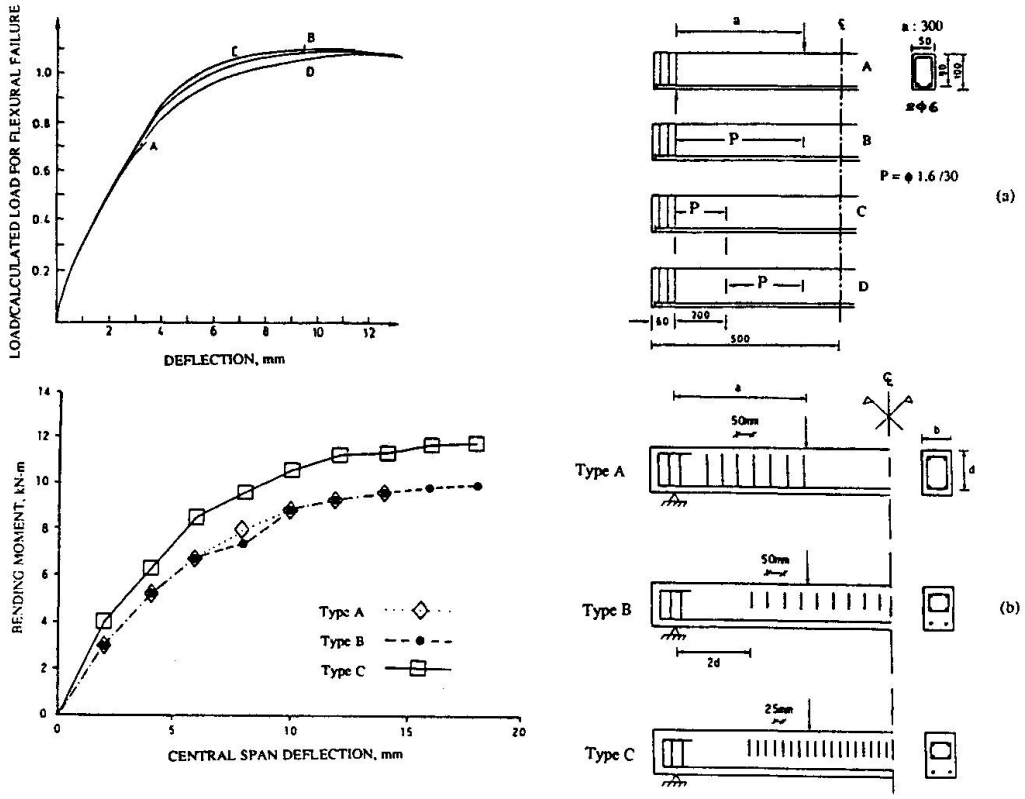


Fig. 2 Typical load-deflection relationships for beams with various stirrup arrangements tested by (a) Kotsovos [6] and (b) Kuttab [8].

On the basis of the concept of shear capacity of critical sections all beams with their shear span without transverse reinforcement, either throughout or over a large portion of its length, should have a similar load-carrying capacity. And yet, beams C and D were found to have a load-carrying capacity significantly higher than that of beams A. In fact, beams C and D exhibited ductile behaviour - a characteristic of under-reinforced concrete beams exhibiting a flexural mode of failure - and their load-carrying capacity was double that of beams A. These results clearly indicate that such behaviour cannot be explained in terms of the concept of shear capacity of critical sections.

The evidence presented in Fig. 2a also contrasts the view that aggregate interlock makes a significant contribution to shear resistance. This is because the large deflections exhibited by beams C and D led to a large increase of the inclined crack width and thus considerably reduced, if not eliminated, aggregate interlock. In fact, near the peak load, the inclined crack had a width in excess of 2 mm which is by an order of magnitude larger than that found by Fenwick and Paulay [7] to reduce aggregate interlock by more than half. It can only be concluded, therefore, that, in the absence of transverse reinforcement, the main contributor to the shear resistance of an RC beam at its ultimate limit state is the compressive zone, with the region of the beam below the neutral axis making an insignificant, if any,

contribution.

As for the concepts discussed so far, the test results are also in conflict with the truss or strut and tie concepts. A large portion of the shear span of beams C and D cannot behave as the models imply, since neither the absence of transverse reinforcement allows the formation of ties nor the presence of a wide inclined crack permits the formation of a strut. And yet, the beams sustained loads significantly larger than those widely expected. Such behaviour indicates that, in contrast with widely held views, truss or strut and tie behaviour is not a necessary condition for the beams to attain their flexural capacity once their "shear capacity" is exceeded.

The validity of the conclusions drawn from the results discussed above is supported by the results (see Fig. 2b) obtained in a more recent experimental work [8] which involved the testing of the RC beams also shown in Fig. 2b. The figures indicate not only that restricting the transverse reinforcement within the compressive zone does not reduce the load-carrying capacity of the beams, but also that designing such reinforcement so as to provide a more effective confinement to the compressive zone improves significantly both strength and ductility. It would appear, therefore, that, in contrast with current views, it is the compressive zone, and not the portion of a structural concrete member outside this zone, that provides shear resistance to the member.

## 4. MECHANISMS OF SHEAR RESISTANCE AND FAILURE

The underlying causes of shear resistance of the compressive zone have been investigated by testing RC T-beams with a web width significantly smaller than that considered, in compliance with current thinking, to provide adequate shear resistance [9]. Design details of a typical beam with a 2.6 m span tested under six-point loading are shown in Fig. 3 which also shows a typical mode of failure. The tests indicated that the load-carrying capacity of the beams was up to three times higher than that predicted on the basis of the currently accepted concepts. It was also found that failure usually occurred in regions not regarded by current Code provisions as the most critical. As the web width of these beams was inadequate to provide shear resistance, the above results support the view that the region of the beam above the neutral axis - the flange in the present case - is the main, if not the sole, contributor to shear resistance.

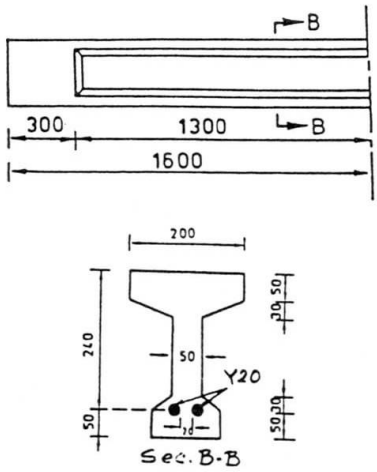


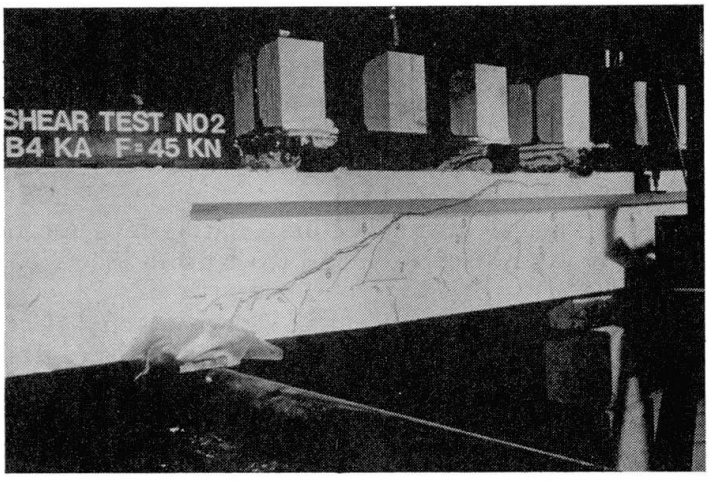


Fig. 3 RC T-beams under six-point loading. Design details and mode of failure [6].

It is also interesting to note in Fig. 3 that the inclined crack, which eventually caused failure, penetrated very deeply into the compressive zone. In fact, it locally reduced the depth of the neutral axis to less than 5% of the beam depth. In view of such a small depth of the compressive zone, it may be argued that concrete is unlikely to be able to sustain the high tensile stresses caused by the presence of the shear force. Such an argument is usually based on the erroneous assumption that concrete behaviour within the compressive zone of a beam at its ultimate limit state is realistically described by using uniaxial stress-strain characteristics. This assumption is in conflict with recent experimental information which has demonstrated quite conclusively that the stress conditions within the compressive zone

of an RC beam at its ultimate limit state are triaxial [6,10]; in fact, concrete in the region of a section through the tip of a deep flexural or inclined crack is subjected to a wholly compressive state of stress which represents the restraining effect of the adjacent concrete [10]. It is considered that a part of the vertical and horizontal components of this compressive state of stress counteracts the tensile stresses developing in the presence of the shear force. Hence, in spite of the presence of such a force, the state of stress remains compressive and this causes a significant enhancement of the local strength; a schematic representation of the mechanism providing shear resistance is shown in Fig. 4. However, eventually the shear force increases beyond a critical level and results in the development of tensile stresses sufficiently large to eliminate the restraining effect of the adjacent concrete thus creating a compression/tension stress field which reduces abruptly the local strength and causes failure.

## 5. IMPLEMENTATION IN DESIGN

A recent attempt to summarize the experimental information discussed in the preceding sections and present it in a unified and rational form has led to the formulation of the concept of the compressive force path [6]. On the basis of this concept, the load-carrying capacity of a structural concrete member is associated with the strength of concrete in the region of paths along which compressive forces are transmitted to the supports. The path of the compressive force may be visualized as a "flow" of compressive stresses with varying section perpendicular to the path direction and with the compressive force representing the stress resultant at each section (see Fig. 5). Failure has been shown to relate with the presence of tensile stresses in the region of the path and such stresses may develop due to a number of causes, the main ones being associated with changes in the path direction, the varying intensity of the compressive stress field along the path, bond failure at the level of the tension reinforcement between two consecutive flexural or inclined cracks, etc.

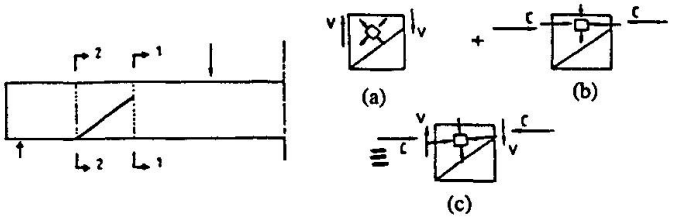


Fig. 4 Mechanism providing shear resistance.

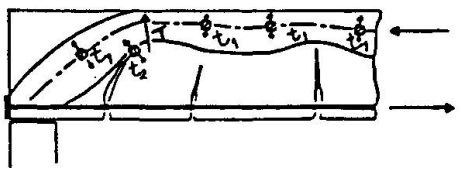

Fig. 5 Compressive force path.

The above concept has been implemented in design by modelling an RC beam as a frame with inclined legs tied by the tension reinforcement (see Fig. 6) with the frame providing a simplified representation of the compressive force path. In compliance with the proposed concept, failure of the model should occur due to failure of either the horizontal or inclined members of the frame or the joint of these members. A full description of the model together with design examples and experimental verification forms the subject of other publications [eg. 11] where it is shown that the resulting design solutions are not only more economical but also safer than those obtained by using the methods recommended by current Codes of practice. A typical example of the application of the above model in design is given in Fig. 1a which shows the design details of a simply supported beam subjected to four-point loading together with the load-deflection curve established by experiment. The Figure also includes the values predicted for load-carrying capacity by current Codes as well as that predicted by the proposed model and it is interesting to note that while the beam strength is closely predicted by the proposed model, it is between approximately 5 and 20 times larger than the Code predicted values. It is also important to note that the above model can form the basis for the design of more complex skeletal structural forms such as, for example, continuous beams, frames, etc. In such cases, the model shown in Fig. 6 represents an element of a skeletal structural form between two consecutive points of zero bending moment, as indicated in Fig. 7, with the transverse reinforcement at the point of zero moment being designed so as to represent an internal support forming between two

consecutive beam elements.

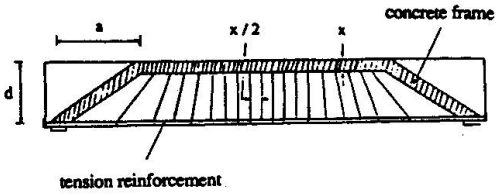


Fig. 6 Model for simply-supported beams.

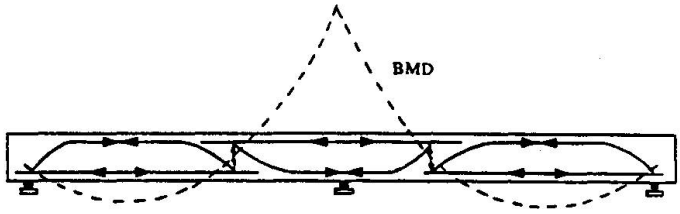


Fig. 7 Model for a continuous beam.

## 6. CONCLUSIONS

1. The concepts underlying shear design methods are found to be incompatible with the observed behaviour of RC beams. Shear capacity is shown to be provided by the compressive zone and not, as widely believed, the portion of the beam below the neutral axis.

2. Shear resistance is associated with the development of a triaxial compressive state of stress in the region of the tip of deep inclined cracks and failure eventually occurs due to the development of transverse tensile tensile stresses within the compressive zone.

3. Modelling an RC beam as a frame with inclined legs tied by the tension reinforcement is shown to lead to design solutions which are both safer and significantly more economical that those currently obtained. Such a model may be considered to represent the portion forming between consecutive points of inflection of any skeletal structural concrete configuration.

## 7. REFERENCES

1. American Concrete Institute. Building Code Requirements for Reinforced Concrete, ACI 318-83 (1983).

2. British Standards Institution. Code of Practice for Design and Construction, BS8110, 1 (1985).

3. Canadian Standards Association. Design of Concrete Structures for Buildings, CAN3-A23.3-M84 (1984).

4. CEB-FIP Model Code for Concrete Structures. Bulletin d' Information 124-125 (1978).

5. Schlaich J. and Schafer K. Konstruieren im Stahlbeton, Beton-Kalender 1984, Wilhem Ernst und Sohn, Berlin, 87-1004.

6. Kotsovos, M. D. Compressive force path: Basis for ultimate limit state reinforced concrete design. ACI Journal, 85 (1988), 68-75.

7. Fenwick, R. C. and Paulay, T. Mechanisms of shear resistance of concrete beams. Journal of the Structural Division, ASCE, 94 (1968), 2325-2350.

8. Kuttab A. Beam Tests. Presented at meeting of CEB Task Group 24 held in Dubrovnik (1988).

9. Kotsovos, M. D. , Bobrowski, J., and Eibl, J. Behaviour of RC T-beams in shear. The Structural Engineer, 65B (1987), 1-10.

10. Kotsovos, M. D. Consideration of Triaxial Stress Conditions in Design: A Necessity. ACI Journal, 84 (1987), 266-273.

11. Kotsovos, M. D. and Lefas, I. D. Behaviour of reinforced concrete beams designed in compliance with the compressive force path. ACI Structural Journal, 87 (1990), 127-139.

12. Maier J. and Thurlimann B. (1985) Bruchversuche an Stahlbetonscheiben. Bericht No. 8003-1, Institut für Baustatik und Konstruktion, ETH Zurich.

# Shear Strength of Beams at Very Low Temperatures

## Résistance à l'effort tranchant de poutres à très basses températures

## Schubtragfähigkeit von Stahlbetonbalken im Tieftemperaturbereich

**Luc TAERWE**
Lecturer
Univ. of Ghent
Ghent, Belgium

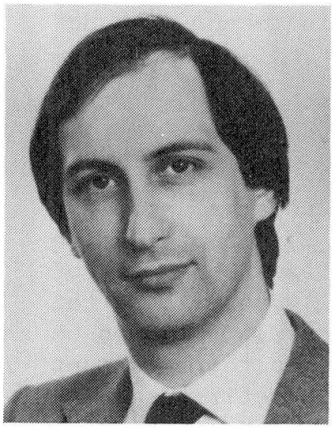

Luc Taerwe graduated as Civil Engineer at the University of Ghent in 1975 where he also obtained his Doctor's degree. At the Magnel Laboratory he is involved in research on nonlinear behaviour of concrete structures, high strength concrete, quality assurance and stochastic modelling. He is the recipient of several scientific awards.

**Hendrik LAMBOTTE**
Prof. Emeritus
Univ. of Ghent
Ghent, Belgium

Hendrik Lambotte was Director of the Magnel Laboratory for Reinforced Concrete from 1983 to 1990 and Full Professor involved in teaching and research on reinforced and prestressed concrete. He is chairman of the Belgian Standardization Committee on Concrete, member of the Advisory Committee of CEB and of the Editorial Group of EC 2.

**SUMMARY**

Loading tests on 14 reinforced concrete beams were performed both at ambient temperature and at −165°C. Most beams failed in shear. From the results, it follows that under cryogenic conditions shear strength increases considerably. This effect is mainly due to the increase of concrete tensile strength at low temperatures. Also restrained thermal shortening of the reinforcing steel has a beneficial effect.

**RÉSUMÉ**

Une série de 14 poutres en béton armé a été soumise à un essai de mise en charge et ceci à températures ambiantes et à −165°C. La plupart des poutres présentent une rupture à l'effort tranchant. Les résultats des essais montrent que la résistance à l'effort tranchant augmente considérablement en environnement cryogénique. Ce phénomène peut être attribué principalement à l'augmentation de la résistance à la traction du béton à basses températures. La contraction thermique empêchée de l'acier à également un effet favorable.

**ZUSAMMENFASSUNG**

An einer Reihe von insgesamt 14 Stahlbetonbalken wurden Schubversuche durchgeführt, sowohl bei Umgebungstemperatur als auch bei −165°C. Die meisten Balken erwiesen einen Schubbruch. Aus den Versuchsergebnissen folgt, dass die Schubtragfähigkeit erheblich zunimmt im Tieftemperaturbereich, was hauptsächlich am günstigen Einfluss der niedrigen Temperaturen auf die Betonzugfestigkeit zugeschrieben werden kann. Auch die verhinderte thermische Dehnung des Betonstahls hat einen günstigen Einfluss.

## 1. INTRODUCTION

Knowledge of the structural behaviour of concrete members at very low temperatures is particularly important for the design of storage tanks for liquefied natural gas (LNG). In the case of LNG tanks with elevated base slab (e.g. at Zeebrugge, Belgium) the area around the supporting columns has to be checked for punching shear not only under regular but also under accidental loading conditions involving cooling of the slab from above due to spill from the inner steel container. Also the wall to base connection is an area subjected to important shear forces. Hence the need to investigate the influence of very low temperatures on shear resistance of reinforced concrete beams and slabs. In this paper, the results of loading tests on beams are discussed by addressing the influence of low temperatures on material properties and by considering the action effects caused by internal restraints. As pointed out by Breen [1], particular types of loading and restraints are among the technical challenges that remain to be explored. Moreover, shear strength is one of the typical fields where reliance on concrete tensile strength is taken into account, as indicated by Hillerborg in [2].

## 2. TEST PROGRAM

Loading tests were performed on 14 reinforced concrete beams with a span of 1.5 m, a width b = 400 mm and a total depth h = 200 mm (fig. 1). The effective depth d equals 165 mm and the tensile reinforcement of the beams consists of deformed TEMPCORE bars Ø 14 mm. The beam designation (table 1) consists of the capitals P (preliminary), R (reference) and L (low temperature) followed by the longitudinal reinforcement ratio $\rho_s = A_s/bd$ in % and the web reinforcement ratio $\rho_{sw} = A_{sw}/bs$ also in % (s denoting stirrup spacing). The stirrups consist of 4 legged closed stirrups, 6 or 8 mm in diameter. By way of example, the dimensions and the reinforcement of beams R/1.86/0.20 and L/1.86/0.20 are shown in fig. 1.

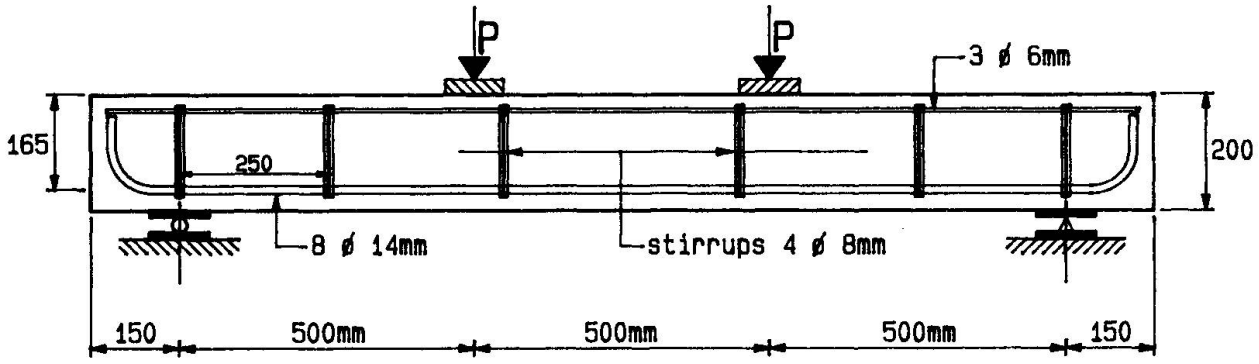


Fig. 1 Dimensions and reinforcement of beams R/1.86/0.20 and L/1.86/0.20

The beams designated P and R were tested at room temperature (20°C) at an age of respectively 28 days and 3 months. The upper face of the beams designated L, was cooled with liquid nitrogen (-196°C) until, at the level of the tensile reinforcement, a temperature of about -165°C was reached. This latter value corresponds to the temperature of liquefied natural gas. Cooling took about 6 hours. Subsequently the loads were gradually increased up to failure. Vertical copper strips, partially embedded in the beams' upper surface, served to retain the liquid nitrogen. Insulating pannels were glued at the side faces, in order to obtain a uniform temperature distribution over the width of the beams.

| Beam designation | $\rho_s$ (%) | $\rho_{sw}$ (%) | s (mm) | $P_u$ (kN) | $\tau_u$ (N/mm$^2$) | Type of failure |
|---|---|---|---|---|---|---|
| P/0.93/0.00 | 0.93 | 0 | - | 105 | 1.59 | shear |
| P/1.86/0.00 | 1.86 | 0 | - | 122 | 1.85 | shear |
| R/0.93/0.00 | 0.93 | 0 | - | 107 | 1.62 | bending |
| R/0.93/0.19 | 0.93 | 0.19 | 150 | 108 | 1.64 | bending |
| R/1.40/0.00 | 1.40 | 0 | - | 120 | 1.82 | shear |
| R/1.86/0.00 | 1.86 | 0 | - | 136 | 2.06 | shear |
| R/1.86/0.20 | 1.86 | 0.20 | 250 | 201 | 3.05 | shear |
| R/1.86/0.34 | 1.86 | 0.34 | 150 | 195 | 2.95 | bending |
| L/0.93/0.00 | 0.93 | 0 | - | 150 | 2.27 | shear |
| L/0.93/0.19 | 0.93 | 0.19 | 150 | 189 | 2.86 | bending |
| L/1.40/0.00 | 1.40 | 0 | - | 194 | 2.94 | shear |
| L/1.86/0.00 | 1.86 | 0 | - | 278 | 4.21 | shear |
| L/1.86/0.20 | 1.86 | 0.20 | 250 | 315 | 4.77 | shear |
| L/1.86/0.34 | 1.86 | 0.34 | 150 | 275 | 4.17 | shear |

Table 1 Survey of beam characteristics

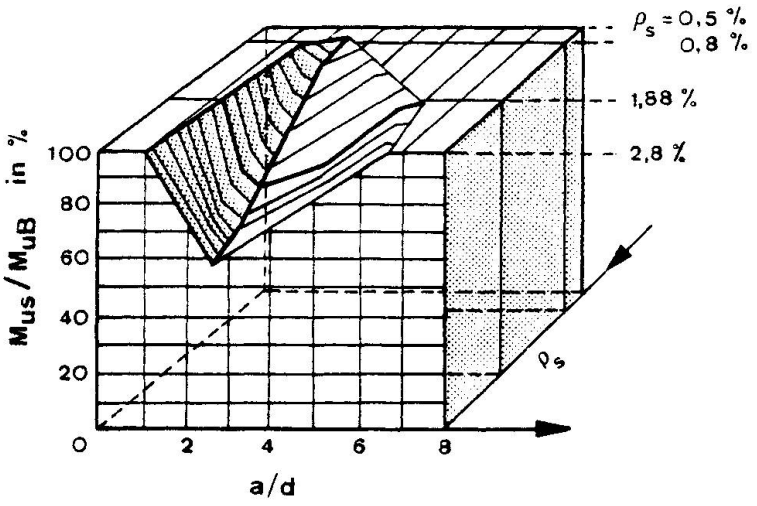


The beams were submitted to two point loads at a third of the span. Hence the shear span "a" equals 500 mm and a/d = 3. This latter value is known to be the most critical for shear strength [3]. In fig. 2 Kani's "shear failure valley" for beams without shear reinforcement is shown [3]. The diagram depicts the influence of a/d and $\rho_s$ on the ratio of the ultimate moment corresponding to shear failure ($M_{uS}$) to the ultimate moment for bending failure ($M_{uB}$).

Fig. 2 Kani's shear failure valley [3]

Stirrup spacing s = 150 mm corresponds to z/s = 1, where z = 0.9 d equals the depth in the equivalent truss model. In the case of s = 250 mm, the ratio z/s equals 150/250 = 3/5 which is the lower value of the crack inclination $\theta$ allowed in the "accurate" shear design method according to the CEB-FIP Model Code for Concrete Structures (1978 Edition).

## 3. MATERIAL PROPERTIES

The beams and the accompanying test specimens were cured in a moist room at 20°C until 24 hr before testing. Mean concrete strength characteristics are given in table 2. Due to the low temperature effect, compressive strength $f_{c,cub}$ increased by a factor 1.78 and flexural tensile strength $f_{ctb}$ by a factor 1.49.

| Beam type | 28 days | 3 months | | | | | |
|---|---|---|---|---|---|---|---|
| | $f_{c,cub}$ | $f_{c,cub}$ | | $f_c$ | $f_{ct}$ | $f_{ctb}$ | |
| | 20°C | 20°C | -165°C | 20°C | 20°C | 20°C | -165°C |
| P | 63.4 | 70.7 | - | - | - | - | - |
| R | 62.2 | 70.8 | - | 62.8 | 3.53 | 8.53 | - |
| L | - | 72.0 | 128.0 | 61.9 | 4.50 | 8.75 | 13.08 |

Table 2 Concrete strength characteristics in N/mm$^2$

For the longitudinal tensile reinforcement $f_y$ = 504 N/mm$^2$ and $f_{st}$ = 588 N/mm$^2$ were obtained as mean values at 20°C. For the type of reinforcing steel used it was found in previous research programs that the yield stress at -165°C increased by about 50 % compared to the value at 20°C [4]. However, calculated ultimate moments for the beams considered indicate that in this case the increase might be about 70 %. The ratio $f_{st}/f_y$ approaches 1 under cryogenic conditions.

## 4. TEST RESULTS

The ultimate loads $P_u$ and the type of failure are mentioned in table 1. Shear failures occured due to flexure shear cracking in the shear spans. For all beams, included those failing in bending, the nominal shear stress $\tau_u = V_u/bd$ is indicated in table 1.

## 5. DISCUSSION OF TEST RESULTS

### 5.1. General analysis

Comparison of the $\tau_u$-values for similar beams failing in shear both at 20°C and -165°C, yields ratios varying between 1.43 and 2.04. This increase in shear resistance must mainly be attributed to the increase in tensile strength of the concrete due to the low temperatures (see also section 5.2).

The observation that for two identical beams, P/0.93/0.00 and R/0.93/0.00, the first fails in shear and the latter in bending can be explained by the fact that the value of $\rho_s$ corresponds to the onset of Kani's shear failure valley (fig. 2). Hence, due to the scatter inherent to this type of test, either failure mode is equally likely to occur. However, at low temperatures, the shear failure mode is clearly predominant. The presence of stirrups in beam L/0.93/0.19 is not apparent form the failure load since beam L/0.93/0.00 failed already in bending.

Beam R/1.86/0.20, failing in shear, was probably already very near to the transition from shear to bending failure as beam R/1.86/0.34 fails at a slightly lower load in bending. At low temperatures shear failure is predominant for $\rho_s$ = 1.86 %. The difference in web reinforcement ratio for the three beams L/1.86 is not reflected in the failure loads. Probably the onset of yielding of the tensile reinforcement initiated shear failure.

According to [3], the stirrups become active from a value $\tau_{oD} = 0.24\sqrt{f_{c,cub}}$ on. For beam R/1.86/0.20 this corresponds to a shear force $0.24\sqrt{70.9} \times 0.9 \times 165 \times 400$ = 120 kN. This value is in very good agreement with the experimental

strain measurements. These also indicate yielding of the stirrups at ultimate and hence the corresponding force equals $F_{sw} = f_y \times A_{sw} = 472 \times 201 = 95$ kN. Summation of both contributions yields 215 kN as estimate of the experimental value of 201 kN.

## 5.2. Influence of tensile strength on shear resistance

The influence of tensile strength on shear resistance is accounted for by a factor $\sqrt{f_c}$ in the formulas for the ultimate nominal shear stress. According to [3] the nominal shear stress for beams without stirrups is given by

$$\tau_{u,1} = 0.18 \sqrt{f_{c,cub}} \sqrt[3]{100\ \rho_s} \qquad (1)$$

for the particular values of the scale factor and a/d applicable to the beams considered. In [5], the following modification of the ACI 318 Building Code formula (11-6) was proposed

$$\tau_{u,2} = 0.15 \sqrt{f_c} + 62.6\ \rho_s \frac{d}{a} \qquad (2)$$

The calculated values are mentioned in table 3 and compared with the experimental values $\tau_u$. For the cooled beams, the material properties at -165°C have been considered. Formulas (1) and (2) underestimate the experimental values by about 10 % and 25 % respectively, at least for the beams tested at 20°C and beam L/0.93/0.00. A better fit can be obtained for (1) by increasing the first factor up to 0.20 and for (2) by doubling the second term.

| Beam | $\tau_u$ (N/mm$^2$) | $\tau_{u,1}$ (N/mm$^2$) | $\frac{\tau_u}{\tau_{u,1}}$ | $\tau_{u,2}$ (N/mm$^2$) | $\frac{\tau_u}{\tau_{u,2}}$ |
|---|---|---|---|---|---|
| P/0.93/0.00 | 1.59 | 1.41 | 1.13 | 1.33 | 1.20 |
| P/1.86/0.00 | 1.85 | 1.75 | 1.06 | 1.51 | 1.23 |
| R/1.40/0.00 | 1.82 | 1.67 | 1.09 | 1.49 | 1.22 |
| R/1.86/0.00 | 2.06 | 1.79 | 1.15 | 1.56 | 1.32 |
| L/0.93/0.00 | 2.27 | 1.99 | 1.14 | 1.78 | 1.27 |
| L/1.40/0.00 | 2.94 | 2.28 | 1.29 | 1.88 | 1.56 |
| L/1.86/0.00 | 4.21 | 2.55 | 1.65 | 1.97 | 2.14 |

Table 3 Experimental and calculated nominal shear stresses.

From table 3 it follows that for the lower temperatures and the higher $\rho_s$ values the underestimation becomes very important which indicates that phenomena other than those accounted for by (1) and (2) must have a beneficial contribution to shear resistance.

## 5.3. Other phenomena affecting shear resistance at low temperatures

Under cryogenic conditions, the coefficient of thermal expansion of steel is only slightly reduced whereas that of concrete significantly decreases, depending on the moisture content. As pointed out in [4], the restrained differential shortening in a reinforced concrete section causes a kind of artificial prestressing. Considering a symmetrical section subjected to a uniform temperature drop $\Delta T$, the compressive stress in the concrete can be calculated by the following formula

$$\sigma_c = \frac{E_s.\rho.(\alpha_{ts} - \alpha_{tc}).\Delta T}{1 + (\alpha - 1)\ \rho} \qquad (3)$$

where $\alpha_{ts}$ and $\alpha_{tc}$ are the coefficients of thermal epansion of steel and concrete and $\rho$ is calculated as $(A_s + A_{sc})/bh$. In the case of a non-symmetric reinforcement arrangement, this formula still holds for the stress at the centroid of the equivalent section $A_c + \alpha A_s$. Introducing $\Delta T = 190°C$, $E_c = 35000$ N/mm$^2$, $\alpha_{ts} - \alpha_{tc} = 3.10^{-6}/°C$ and the appropriate values of $\rho$, one finds $\sigma_c = 0.96$ N/mm$^2$ ($\rho_s = 0.93$ %), $\sigma_c = 1.36$ N/mm$^2$ ($\rho_s = 1.40$ %) and $\sigma_c = 1.74$ N/mm$^2$ ($\rho_s = 1.86$ %). The induced compressive stress $\sigma_c$ has a beneficial influence on the principal tensile stress $\sigma_I = \sqrt{\sigma_c^2/4 + \tau_c^2} - \sigma_c/2$.

This effect is merely related to the first contributing term in (2) and does not fully account for the observed higher $\tau_u$ values at low temperatures and highest $\rho_s$ values. The second term in (2), which reflects the influence of $A_s$, must also increase because of higher bond strength, and smaller crack widths and deflections at the same load level. These phenomena, confirmed by experimental observations, hamper propagation and opening of the inclined cracks.

## 6. CONCLUSIONS

From loading tests on reinforced concrete beams both at reference temperature (+20°C) and under cryogenic conditions (-165°C), it can be concluded that the beneficial effect of very low temperatures on shear strength has to be attributed to the following phenomena (in descending order of importance)

- increased tensile strength of concrete
- restrained thermal shortening of the steel, creating a kind of prestressing
- higher bond strength and smaller crack widths, causing a higher contribution of the shear strength term proportional to $\rho_s$.

## ACKNOWLEDGMENT

The authors gratefully acknowledge research grant no. 2.9002.85 from the Belgian Fund for Joint Basic Research.

## REFERENCES

1. BREEN J., Why structural concrete. Introductory Report, IABSE Colloquium "Structural Concrete", 1991, Stuttgart.

2. HILLERBORG A., Reliance upon concrete tensile strength. Introductory Report for Theme 2.5, IABSE Colloquium "Structural Concrete", 1991, Stuttgart.

3. LEONHARDT F., Schub bei Stahlbeton und Spannbeton - Grundlagen der neueren Schubbemessung. Beton- und Stahlbetonbau 11/1977, pp. 270-277, 12/1977, pp. 295-302.

4. LAMBOTTE H., TAERWE L., DE SAINT MOULIN I., Shear resistance at low temperatures of deep hyperstatic reinforced concrete beams. Proceedings "Symposium on Transport and Storage of LPG & LNG", Brugge, 1984, Royal Flemish Society of Civil Engineers (K.VIV), pp. 357-364.

5. SMITH K., VANTSIOTIS A., Deep Beam Test Results Compared with Present Building Code Models. ACI Journal, July-August, 1982, pp. 280-287.

# Shear Strength of Beams without Shear Reinforcement

## Cisaillement des poutres en béton précontraint dépourvues d'étriers

## Schubtragfähigkeit von Spannbetonbalken ohne Schubbewehrung

**Tamon UEDA**
Assoc. Prof.
Univ. of Tokyo
Tokyo, Japan

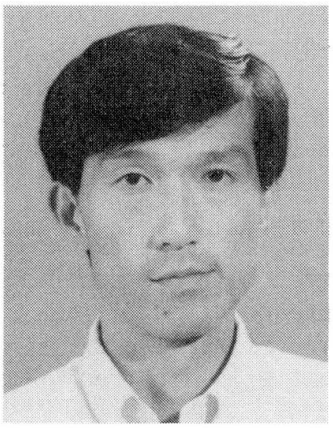

Tamon Ueda, born in 1954, obtained his Doctor of Engineering degree from University of Tokyo in 1982. He served as Assistant and Associate Professor at Asian Institute of Technology. His research interests relate to the deformation mechanism of concrete.

**Heru Darjudi Eko PUTRO**
Civil Eng.
Asian Inst. of Technol.
Bangkok, Thailand

Heru Darjudi Eko Putro obtained his Master of Engineering degree from Asian Institute of Technology in 1990. Currently he is in a consulting firm in Jakarta.

### SUMMARY

Strengths of shear compression failure in prestressed concrete beams can be predicted by the finite elements method analysis, in which a main shear crack is modelled as a discrete crack. Compression failure of concrete in the maximum moment region causes shear failure of the beams. A narrower compression zone is considered to make the shear strength less than the flexural strength. Force transferred along the main shear crack does not affect the shear strength of the beam too much.

### RÉSUMÉ

La résistance ultime au cisaillement des poutres en béton précontraint peut être prévue à l'aide d'une analyse non-linéaire par la méthode des éléments finis, où chaque fissure de cisaillement est modélisée comme une fissure discrète. La rupture en compression du béton dans la zone de moment maximum est responsable dans les poutres de la ruine par cisaillement. Une zone comprimée plus étroite rend la résistance au cisaillement plus faible que la résistance flexionnelle. La force transmise le long de la fissure principale d'effort tranchant n'a qu'un faible effet sur la résistance au cisaillement de la poutre.

### ZUSAMMENFASSUNG

Die Tragfähigkeit von Spannbetonbalken mit Schubdruckbrüchen kann mit einer Finite Element Berechnung ermittelt werden, bei der ein Hauptschubriss diskret modelliert wird. Betondruckversagen im Bereich des grössten Biegemoments verursacht den Schubbruch. Kleinere Druckzonenhöhen vermindern die Schubtragfähigkeit stärker als die Biegetragfähigkeit. Die Kraftübertragung längs des Hauptschubrisses beeinflusst die Schubtragfähigkeit nur gering.

## 1. INTRODUCTION

Shear strength of reinforced concrete beams has been clarified by many studies, most of which were of experimental approach. Studies on shear strength of beams subjected to axial force, such as prestressed concrete, however, have not been conducted sufficiently yet. Since the accuracy in the shear strength prediction is poor in the case with axial force, a rational prediction method is urgently required. In this study, therefore, prediction of shear strength of prestressed concrete beams without shear reinforcement was done by a nonlinear finite element method ( FEM ). In the FEM constitutive laws, which have been greatly developed in recent years, were implemented. As results of the FEM analysis, several intersting and useful points were newly found on the shear strength prediction.

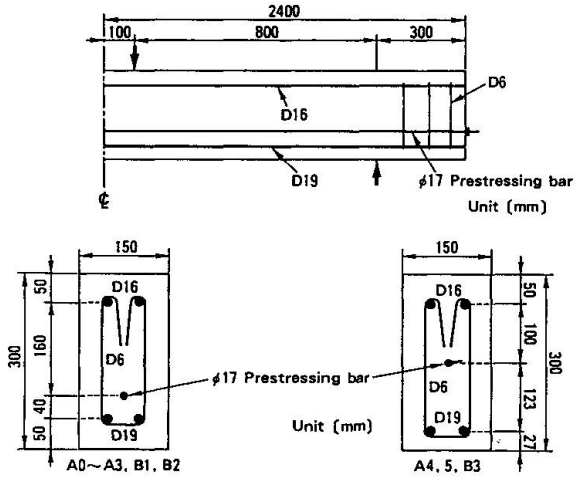


Fig.1 Specimen

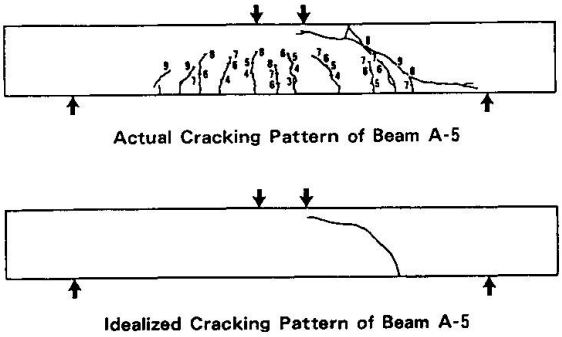


(a) Observed and analyzed cracks

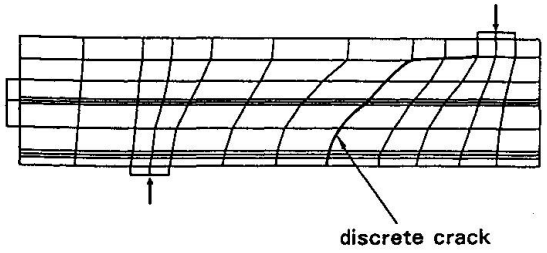


(b) Meshing and discrete crack

Fig.2 Observed and modeled cracks

## 2. OUTLINE OF FEM ANALYSIS

The program used for the FEM analysis was "COMM2"[1] in which Maekawa model is applied for concrete element. The bond link elements which are available in COMM2 were used for force transfer along shear crack and for bond force between concrete and steel. The force transferred along shear crack was calculated by Li & Maekawa model[2] for the case that slip occurred ( $\delta$>0.001mm ), and Reinhardt et al's model[3] was used for the case of no slip ( $\delta$<0.001mm ). The model for the bond force was Shima et al's model[4]. The main shear crack was modeled as a discrete crack whose location and configuration were determined according to the observed shear crack in the previous study[5]. The details of nine specimens[5] which were analysed are shown in Fig.1 and Table 1. An example of observed cracking pattern and the corresponding meshing pattern were given in Fig.2. All the concrete elements adjacent to the discrete crack were assumed not to crack, while the other concrete elements were ordinary one in which crack was modeled as smeared crack. The prestressing force was applied by imposing the force at a node of a steel element for the anchor plate in the actual beam[5]. The magnitude of the imposed force was equal to the observed effective prestressing force[5].

## 3. ANALYTICAL RESULTS

### 3.1 Effect of Prestressing Force on Shear Strength

| Specimen | $f_c'$ | $P_{eff}$ | $x_1$ | $x_2$ | $x_3$ | $V_{su,exp}$ | $V_{su,FEM}$ | $V_{su,cal}$ | (7) | (7) | $V_{fu,cal}$ | $V_{su,cal2}$ | $V_{su,cal3}$ |
|---|---|---|---|---|---|---|---|---|---|---|---|---|---|
| | MPa | kN | mm | mm | mm | kN | kN | kN | — | — | kN | kN | kN |
| (1) | (2) | (3) | (4) | (5) | (6) | (7) | (8) | (9) | (8) | (9) | (10) | (11) | (12) |
| A-0 | 26.6 | 0 | 28 | 55 | 119 | 44.1 | 40.5 | 40.4 | 1.08 | 1.09 | 75.8 | 42.7 | 28.1 |
| A-1 | 24.6 | 48 | 43 | 85 | 136 | 51.5 | 53.9 | 54.7 | 0.96 | 0.94 | 76.5 | 59.1 | 42.5 |
| A-2 | 26.6 | 112 | 57 | 90 | 145 | 59.3 | 54.1 | 61.9 | 1.10 | 0.96 | 84.8 | 62.8 | 52.3 |
| A-3 | 24.6 | 152 | 66 | 115 | 162 | 72.6 | 62.6 | 69.6 | 1.14 | 1.04 | 83.7 | 76.8 | 65.1 |
| A-4 | 36.5 | 99 | 62 | 65 | 102 | 63.3 | 63.2 | 64.4 | 1.00 | 0.98 | 83.3 | 75.6 | 57.8 |
| A-5 | 36.5 | 0 | 34 | 55 | 86 | 46.6 | 63.5 | 55.5 | 0.73 | 0.84 | 77.7 | 64.3 | 38.5 |
| B-1 | 57.5 | 148 | 38 | 55 | 84 | 89.2 | 101.4 | 87.5 | 0.88 | 1.02 | 118.6 | 110.1 | 77.9 |
| B-2 | 57.5 | 41 | - | 40 | 83 | 67.7 | 70.9 | 65.4 | 0.96 | 1.03 | 117.7 | 73.9 | 42.2 |
| B-3 | 57.5 | 152 | 37 | 60 | 83 | 78.5 | 79.3 | 94.6 | 0.99 | 0.83 | 102.5 | 96.3 | 70.1 |

Note (2) Cylinder strength at test
(3) Effective prestressing force
(4) Observed depth to shear crack at loading point
(5) Calculated depth to neutral axis at maximum moment region when flexural failure
(6) Depth to neutral axis obtained by FEM at maximum moment region when shear failure
(7) Measured ultimate shear strength
(8) Ultimate shear strength obtained by FEM
(9) Calculated ultimate shear strength using $x_2$
(10) Calculated ultimate flexural strength
(11) Shear strength calculated by the method in the previous study[6]
(12) Shear strength calculated by the method in the previous study[7]

Table 1 Shear strengths

Comparing the analytical strengths, $V_{su,FEM}$ with the experimental strengths, $V_{su,exp}$, shown in Table 1 and Fig.3, it can be said that the shear strengths of all the specimens are predicted well by the FEM except specimen A-5. It was found in the FEM analysis that the ultimate shear strengths were controlled by compression failure ( strain softening ) of concrete element in compression zone of the maximum moment region. Although the concrete compression failure looked the same as in flexural failure of the beams, the ultimate strengths are much less than the calculated flexural strengths as shown in Table 1. The reason for this fact can be found in concrete strain distribution at a cross-section in the maximum moment region. As shown in Table 1 and Fig.4, depths to the neutral axis, $x_2$, obtained from the concrete strain distribution calculated by the FEM, are much less than depths, $x_3$, calculated by a conventional method for ultimate flexural strength using an equivalent stress block. This narrow compression zone leads

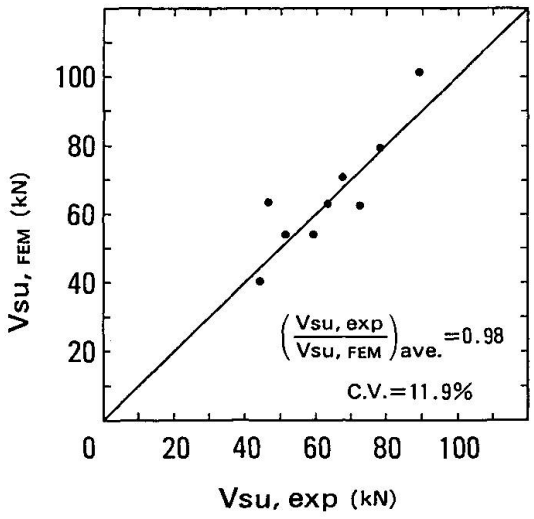


Fig.3 Test and FEM predictions

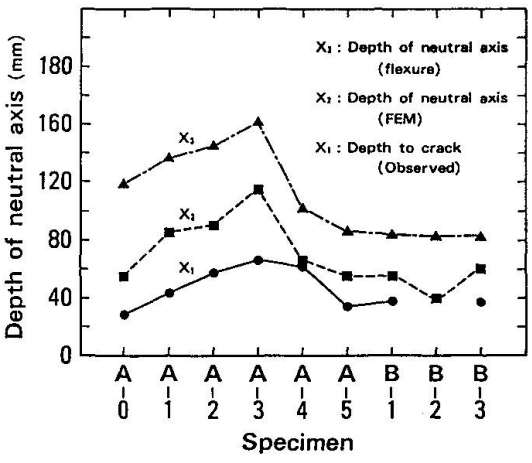


Fig.4 Depths of compression zone

earlier concrete failure in compression zone, which means that the shear strength is less than the flexural strength. It is also seen in Fig.4 and Table 1 the depth to the neutral axis at shear compression failure is significantly greater than the depth to shear crack, $x_1$. Shear cracks penetrated in the compression zone.

The FEM analysis predicts adequately increase in the shear strength with increase of prestressing force as observed in the experiment[5]. Table 1 and Fig.4 indicate that among specimens A-0 to A-3 the computed depth of compression zone, $x_2$, increases with increase of prestressing force. This increase of compression zone depth causes increase of the shear strength.

An observed depth to shear crack tip, $x_1$, was greater in a beam with a greater prestressing force. Location of shear cracking in compression zone varies as prestressing force varies. In order to see the effect of depth to shear crack tip on the shear strength, the shear strengths were calculated by the FEM for two cases of the depths, 20mm and 70mm. The calculated strengths, however, were not so different. It seems that the difference in the depth to shear crack tip hardly causes the difference in the shear strength.

The FEM analysis indicates that the depth of compression zone just outside the maximum moment region is greater than that in the maximum moment region. Therefore, despite combination of flexural moment and shear force, the principal compressive stress is much less than that in the maximum moment region. This is considered to be the reason why the failure of concrete did not occur outside the maximum moment region. The concrete compression failure in compression zone of the maximum moment region is failure criterion for the case of shear compression failure of a beam. To calculate the shear strength, therefore, the depth to the neutral axis should be evaluated by some means. The shear strengths, $V_{su,cal}$, in Table 1 and Fig.5 were calculated by a conventional method for ultimate flexural strength with an equivalent stress block and neutral axis depth given by the FEM analysis. Similar ways for calculation of the shear strength were proposed by the previous studies[6][7]. Although simplified assumptions were adopted, the predicted shear strengths, $V_{su,cal}$, have a good agreement with the experimental ons, $V_{su,exp}$, as shown in Fig.5 and Table 1, while the values predicted by the previous studies[6][7] have less agreements. Figure 5 implies that the ultimate strength for shear compression failure may be estimated easily if estimation of the neutral axis depth is possible.

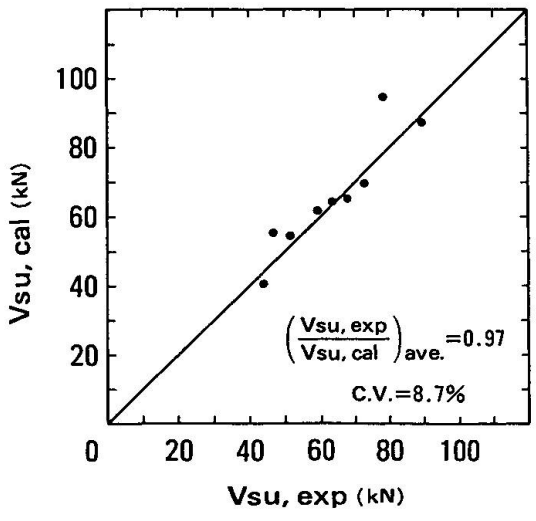


Fig.5 Test and simplified predictions

## 3.2 Effect of Force Transferred along Shear Crack

The force transfer model along a discrete shear crack was varied to see its effect on the shear strength. There were four cases in which the stiffness of the model was varied in such a way that it was 100%, 10%, 1% or 0% of the original model's stiffness. The shear strengths for the four cases were 100%, 91%, 89% and 23% of that with the original model. With 0% of the stiffness the shear strength was greatly

reduced, but with 1% of the stiffness reduction in the strength was only 11%. Length of the shear crack in the analysis was shorter than the observed one for every case. For another case, 0% of the stiffness was implemented only along the shear cracked part in the case of 100% stiffness, while in the vicinity of tip of the discrete shear crack 100% of the stiffness was implemented. In this case the shear strength was 95% of that with 100% of the stiffness at all the part of the discrete shear crack.

From the FEM analysis it was observed that slip ( $\delta$>0.001mm ) takes place at most of the part along the shear crack. In the analysis, therefore, Li & Maekawa's model was used for most of the part along the shear crack. Considering this fact, Reinhardt's model was assumed under any amount of slip to see the effect of type of force transfer model on the shear strength. The predicted shear strength in this case was 97% of that of the original case.

From comparison of the predicted shear strengths of the beams with a various force transfer model along the discrete shear crack, it can be said that effect of the force transferred along a main shear crack on the shear strength is negligibly small. Only the force transferred near the tip of the shear crack which is close to the loading point and in the compression zone affects the shear strength. Estimated transferred stresses along the shear crack were considerably smaller than the stresses in concrete near the shear crack. This fact seems to support the little effect of the force transfer model on the shear strength.

### 3.3 Effect of Crack Model Type

In this study type of shear failure is "shear compression failure", for which shear cracking does not mean ultimate state. In this sense tensile strength of concrete has less significant than in shear tension failure. Furthermore, model for post-cracking is rather little significant for the ultimate shear strength as discussed in the previous subsection It was found, however, that whether discrete crack or smeared crack was assumed for a main shear crack did affect the shear strength of the beam. In the original FEM analysis a discrete crack was assumed, and concrete elements next the discrete crack were assumed to be non-cracking elements. In another case smeared cracking was assumed for all the concrete elements. The predicted strength in this case was 78% of the original case. It seemed that more cracking elements in compression zone at the maximum moment region caused early failure.

## 4. CONCLUSIONS

(1) The FEM analysis, in which concrete is modeled as nonlinear material subjected to bi-axial stress state and a main shear crack is modeled as a discrete crack, can predict the strengths for shear compression failure in reinforced concrete beams subjected to axial force.
(2) Shear compression failure is caused by compression failure of concrete in compression zone at the maximum moment region. The depth of the compression zone is less than that in flexural failure, so that the shear strength is less than the flexural strength.
(3) Using the depth of compression zone obtained by the FEM analysis, the strength for shear compression failure can be estimated by the conventional method of flexural strength.
(4) Cracking and post-cracking models, which is force transfer model along the

discrete shear crack, affect little the predicted shear strength. Whether discrete crack or smeared crack is assumed for the main shear crack, however, influences the prediction of the shear strength.

ACKNOWLEDGEMENT

This study was supported in part by Saito Memorial Research Foundation of Prestressed Concrete Technology.

REFERENCES

1. MAEKAWA K., NIWA J. and OKAMURA H., Computer Program "COMM2" for Analysing Reinforced Concrete. Proceedings of JCI 2nd Colloquium on Shear Analysis of RC Structures, October 1982, pp.79-86 ( in Japanese ).
2. LI B., MAEKAWA K. and OKAMURA H., Contact Density Model for Stress Transfer across Cracks in Concrete. Journal of the Faculty of Engineering, the University of Tokyo(B), Vol.XL, No.1, March 1989, pp.9-52.
3. REINHARDT H., CORNELISSEN H. A. W. and HORDIJK D. A., Tensile Tests and Failure Analysis of Concrete, Journal of Structural Engineering, ASCE, Vol.112, 1986, pp.2462-2477.
4. SHIMA H., CHOU L. L. and OKAMURA H., Micro and Macro Models for Bond in Reinforced Concrete. Journal of the Faculty of Engineering, the University of Tokyo(B), Vol.XXXIX, No.2, September 1987, pp.133-194.
5. HORIBE K. and UEDA T., Influence of Axial Force on Shear Behavior of Reinforced Concrete Beams. Proceedings of 40th Annual Convention of JSCE, Div.5, September 1985, pp.319-320 ( in Japanese ).
6. ZOWYER E. M., Shear Strength of Simply-Supported Prestressed Concrete Beams. Structural Research Series No.53, Civil Engineering Studies, University of Illinois, Urbana, Illinois, June 1953.
7. EVANS R. H. and SCHMACHER E. G., Shear Strength of Prestressed Beams Without Web Reinforcement. Journal of ACI, Vol.60, November 1963, pp.1621-1643.

# Precast Reinforced Concrete Planks as Structural Members

## Plaques en béton armé préfabriquées utilisées comme éléments de construction d'une structure

## Vorgefertigte Stahlbetonplatten als tragende Bauteile

**John T. BLADES**
Structural Engineer
Rankine & Hill Pty Ltd
Sydney, Australia

John Blades, born in Sydney, 1959, received an Honours degree in Civil Engineering from the University of Sydney and a Master of Engineering Science degree from the University of New South Wales. He has been involved in the structural design of reinforced concrete and structural steelwork for industrial and commercial structures and prestressed concrete bridges.

**Leon A. GRILL**
Civil Engineer
Private Consultant
Sydney, Australia

Born in Vienna, Austria. Graduated «Cum Laude» from 1948 Politechnicum School of Bucharest. Twenty-two years of experience in the design of civil and structural projects in Uruguay, Argentina and Brazil. From 1971 to 1986, Head of the structural checking section of Rankine & Hill in Australia. Presently contracted as a Private Consultant to the same company.

**Neil C. MICKLEBOROUGH**
Sen. Lecturer
Univ. of New South Wales
Sydney, Australia

Neil Mickleborough studied at both Carleton University, Ottawa, Canada and the University of Tasmania, Australia, where he received his Ph.D. in Structural Engineering in 1979. He worked as a structural design engineer until 1983 when he took up his present appointment. Dr. Mickleborough has published in the areas of reinforced and prestressed concrete, as well as structural dynamics. Recently he has had a book published on prestressed concrete design.

**SUMMARY**
This paper investigates the differences in behaviour of «thin» precast reinforced simply supported concrete when subjected to static and impact loads. Many such planks have failed dramatically in practice. The causes and modes of failure are presented. The importance of detailing and the tensile strength of the concrete are discussed and practical guidelines are given for the design and detailing of such elements.

**RÉSUMÉ**
Cet article examine les différences de comportement des plaques minces en béton armé simplement appuyées, soumises à des charges statiques et à des chocs. Dans la pratique, nombreuses ont été les plaques qui se sont dramatiquement effondrées; ainsi, causes et modes de ruine sont présentés. Les détails constructifs, ainsi que la prise en compte de la résistance en traction du béton sont discutés; des directives pratiques sont données pour la conception et le détail de tels éléments.

**ZUSAMMENFASSUNG**
Dieser Artikel untersucht das unterschiedliche Verhalten von dünnen vorgefertigten Einfachplatten statischer und dynamischer Belastung. Viele von diesen Platten haben in der Praxis dramatisch versagt und die Ursachen des Versagens werden erläutert. Es wird die Bedeutung der Berechnungsführung und der Betonzugfestigkeit diskutiert und praktische Richtlinien für Entwurf und Detaillierung von solchen Bauteilen werden gegeben.

## 1. INTRODUCTION

This paper is based on work carried out for a thesis at the University of New South Wales in 1988 [1].

Precast reinforced concrete planks are used, in Australia, as structural members in three main areas:

a) Treads in steel stringer stairs. This is particularly common in stairs where the use of steel sections to frame the stair and "thin" concrete planks as treads reduces the imposed dead load on the whole structure and makes for ease of construction. Fig. 1 shows such a stair in a major hotel in Sydney, planks being of dimensions 2,200 x 280 x 70mm thick, spanning 1,350mm.

b) Planks in steel framed pedestrian footbridges.

c) Footway slabs which span over electrical services on roadbridges.

In each of these applications, the loading can be applied statically or dynamically as an impact load.

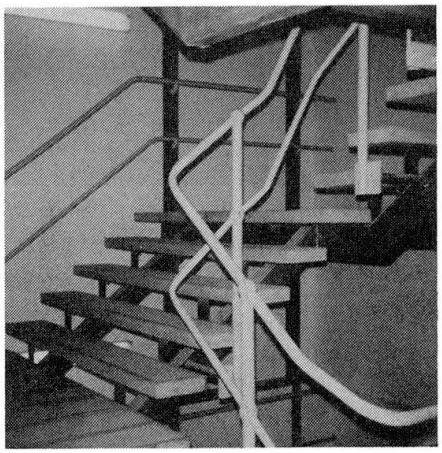

Fig. 1 Treads in a Hotel Fire Stair

Such planks are in common use and over the years many have failed dramatically in flexure due to incorrect analysis, design and/or detailing. With respect to analysis, much of the problem seems to have been, as stated by Breen [3], that designers have focused on "local section behaviour rather than the overall action."

The aim of the project was to study the behaviour in detail and produce practical recommendations for the design and detailing of such planks.

## 2. THE MODEL

### 2.1 General

The planks tested in the laboratory are shown in Fig. 2. These test planks were designed using ultimate strength theory to the Australian Standard AS 3600 (Concrete Structures Code) [5]. The live load of 1.4 kN is for stair treads and is from AS 1170, Part 1 [5]. The dimensions and span are typical for such planks in practice.

The test plank thickness was varied to establish the importance of this dimension.

The position of the reinforcement in the cross-section was varied because it was considered that these planks fail in practice primarily due to the fact that "the dimensions of the precast treads are such that the reinforcement provided is near or at the neutral axis of the section and is therefore unutilised when the first loading occurs" [2].

The steel reinforcement used was welded wire fabric, which is common practice within Australia, and has a yield strength of 450 MPa. The concrete was of approximately 20 MPa compressive strength with 10mm aggregate and 80mm slump. No admixtures were used. The curing procedure adopted was typical of that used in practice by precast concrete manufacturers in Sydney.

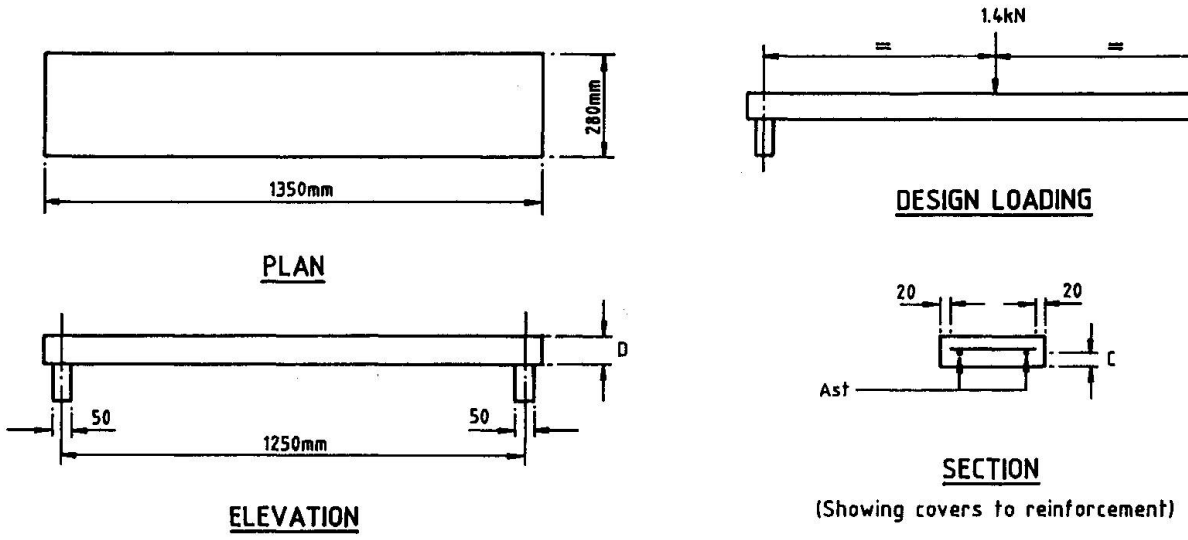


| Depth D (mm) | Cover c (mm) | Area of Tensile Reinforcement Ast ($mm^2$) |
|---|---|---|
| 70 | 15 | 62.3 |
| | 25 | 62.3 |
| 60 | 15 | 62.3 |
| | 25 | 79.2 |
| 50 | 15 | 79.2 |
| | 20 | 100.5 |

Fig. 2 Plank Design Details

Two sets of planks were made, one for testing under static loads, the other under impact loads.

2.2 Static Loading

The main aim of the static loading was to study, under controlled laboratory conditions, the pre-cracking, cracking and post-cracking behaviour of the precast reinforced concrete planks. The applied load and the displacement under the load were measured and the resultant cracking patterns were observed and recorded (photographically) at various load stages throughout the testing procedure.

2.3 Impact Loading

For impact loading the same aim applied as for the static loading. The applied impact load, the maximum impact force absorbed by the plank and the displacement under the impact load were measured. The resultant cracking patterns were observed and recorded (photographically) at various loading stages throughout the testing procedure.

The type of loading used was repeated impact with increments of increasing mass. A load was 'dropped' onto the plank then raised to the required drop height with a further mass increment then being added before dropping the load again on to the plank. This modelled very realistically the type of repeated impact load such elements would undergo in practice (see Section 1).

The drop mass was increased in approximately 12.5kg increments with the masses being clamped together. The load was applied to the planks through a steel ring (120mm OD x 25mm) welded to the underside of the load carrier. This, it was believed, would model the load application through the sole or heel of a foot on a plank in service. The drop height was set at 300mm based on the real in service drop height when a person runs down a flight of stairs.

The two parameters of greatest importance in studying the impact behaviour of the planks were found to be:

Mass ratio: $\alpha = \frac{\text{mass of plank}}{\text{mass of striker}} = \frac{m_p}{m_s}$

and

Dynamic Load Factor (DLF) $= \frac{y_i}{y_s}$

Where $y_i$ = impact displacement due to load P
Where $y_s$ = static displacement due to load P

## 3. EXPERIMENTAL RESULTS

### 3.1 Static Loading

The Load/Displacement plots for the 60mm thick planks are shown in Fig. 3. In the case of the plank with 15mm cover the plot resembled that of the stress/strain curve for the steel wire fabric, as expected for under-reinforced sections such as these where the behaviour of the tensile steel dominates behaviour of the cross-section. The behaviour of the plank with 25mm cover was entirely different. Here the reinforcement was near the centroid of the gross cross-section and due to the steel having very low stress, its behaviour did not dominate the behaviour of the cross section. The plot shows less ductility (than for 15mm cover) with a shorter linear relationship followed by sudden failure.

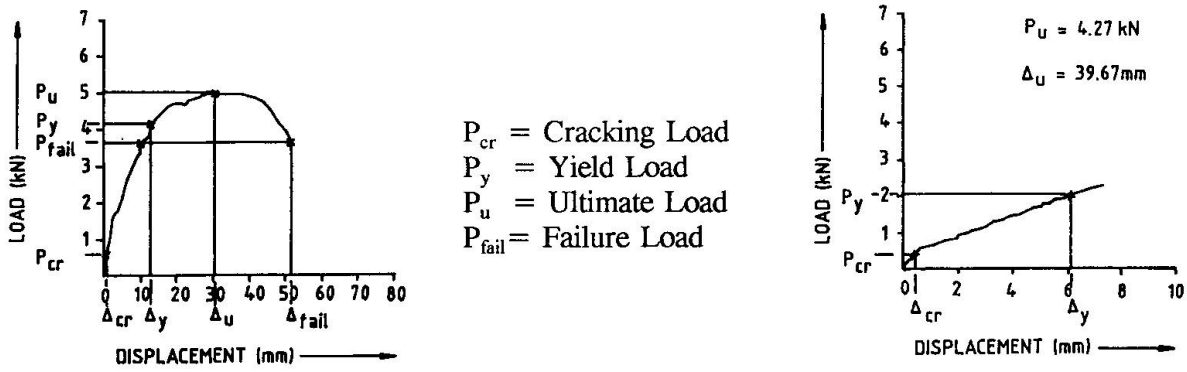


Cover = 15mm Cover = 25mm

$f_c$ = 18 MPa, Thickness = 60mm

Fig. 3 Load/Displacement Plots - Static Loading

The cracking patterns for the 60mm thick planks are shown in Fig. 4. In the case of the plank with 15mm cover, the cracking was finer and more uniform, the cracks coincided with the positions of cross wires in the reinforcing fabric which caused crack initiation. In the case of the plank with 25mm cover, cracks occurred at mid-span with one or two major cracks which opened to as much as 6mm wide, causing the mid-span displacement and rotation of the plank.

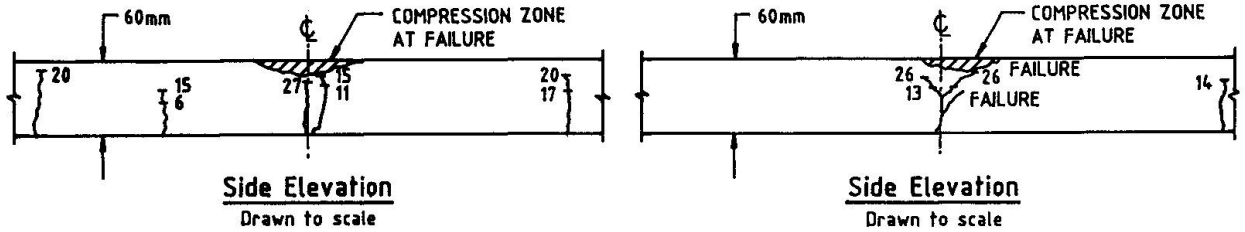


15mm Cover 25mm Cover

(numbers indicate loading stages)

Fig. 4 Cracking Patterns - Static Loading 60mm Thick Planks

3.2 Impact Loading

Generally, the behaviour of the planks with 15mm cover was similar to that for the planks with 25mm cover. The planks failed under the impact loading in a brittle manner. The failure was generally due to crushing of the concrete in the compression zone, which occurred more suddenly in the case of the more brittle planks with the reinforcement at mid-depth.

The cracking patterns for the 60mm thick planks are shown in Fig 5. The maximum crack widths which developed for the planks with reinforcement at mid-depth (25mm cover) were generally greater than for those with 15mm cover, the maximum being approximately 6mm as for the static loading. The planks with 25mm cover exhibited faster crack propagation and deeper crack penetration at an earlier load stage than did those with 15mm cover. This is because in the latter the tensile reinforcement had high stresses and was effective in controlling the formation and propagation of flexural cracks, being closer to the extreme tensile fibre of the concrete.

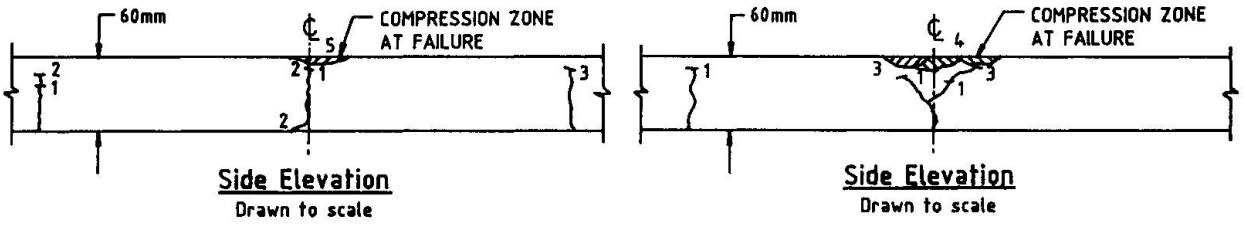


15mm Cover 25mm Cover

(numbers indicate loading stages)

Fig. 5 Cracking Patterns - Impact Loading 60mm Thick Planks

The Dynamic Load Factors (DLF) for the planks varied between 2.94 (50mm thick) and 8.40 (70mm thick). For each plank thickness, the value was higher for that with 25mm cover than 15mm cover.

## 4. CONCLUSION

4.1 Comparison Between Static and Impact Loadings

The loads required to cause cracking and failure under static loading were up to eight times higher than the cracking and failure loads observed under impact loading where the planks behaved in a very brittle manner. Generally, the planks with reinforcement at mid-depth exhibited more extensive cracking at the first load stage of the impact testing than did those with 15mm cover. This is due to the former being similar to a mass concrete element and therefore more brittle, with a faster rate of crack propagation.

For both the static and impact loadings, the ultimate load for the planks with reinforcement near mid-depth was approximately 85% of that for the planks with only 15mm cover.

In both types of loading, the displacements were generally reduced by placing the reinforcement at 15mm cover rather than at mid-depth.

As the mass ratio of the planks ($\alpha$) decreases, the deformation or "lost" energy increases leading to more permanent deformation of the plank, less recovery (or restitution) and larger displacements. Thus, to reduce the energy loss and permanent deformation during impact, the plank mass should be kept as high as possible, as suggested by Grill [2]. The 50mm thick planks (the lowest mass ratio), generally behaved in an unstable manner and should be avoided in practice.

In relation to cracking, the cracks formed later and were better controlled by placing the reinforcement at only 15mm cover rather than at mid-depth, where the behaviour is similar to that

for mass concrete where the tensile strength of the concrete is very important. As Hillerborg says, "...a crack may form which has a tendency to propagate, as cracks in their turn give rise to stress concentrations. If the crack propagation is not prevented the structure (or plank) will crack" [5].

4.2 Review of Current Design Loading Requirements

The precast reinforced concrete planks for this project were designed using the recommended loadings of the current Australian Standard for Dead and Live Loads (AS 1170, Part 1, 1989) [5]. However, under impact loading they failed at less than half of the service design load of 1.4kN.

Such planks undergo impact loads in practice (e.g., persons running down a flight of stairs or across a footbridge). The Authors recommend that loading codes recognise this by giving a range of impact factors (say 1.5 to 4.0) by which one would multiply the static load depending on whether the structure were a major or minor pedestrian facility (e.g., major entrance/escape stair in a large hotel or maintenance stair/footway).

4.3 Design Recommendations

1. Plank Thickness $\geq$ 60mm (irrespective of span).
2. Design Live Load at least twice the current value of 1.4kN concentrated (or 2.2kN/m) to take account of impact.
3. Reinforcement - diameter $\leq$ 0.1 x plank thickness.
   - pitch of main longitudinal wires and cross wires = 100mm.
4. Cover to Main Longitudinal Tensile Reinforcement $\leq$15mm; $\neq$ 10mm.
5. For planks in locations exposed to the weather; specify hot-dipped galvanised reinforcement.
6. Minimum 28 day Compressive Strength of Concrete = 25MPa - all locations.

REFERENCES

1. BLADES J.T., Precast Reinforced Concrete Planks as Structural Members. Master of Engineering Science Thesis, School of Civil Engineering, The University of New South Wales, Australia, February 1988.

2. GRILL L.A., Building Failures: The Use of Experience for Diagnosis and Repair. Proceedings of the 12th Biennial Conference of the Concrete Institute of Australia, 1985.

3. BREEN J.E., Why Structural Concrete? Introductory Report: IABSE Colloquium on Structural Concrete, Stuttgart, April 1991.

4. HILLERBORG A., Reliance Upon Concrete Tensile Strength. IABSE Colloquium on Structural Concrete, Stuttgart, April 1991.

5. Standards Association of Australia, Concrete Structures Code, AS 3600-1988, Loading Code, Part 1 - Dead and Live Loads, AS1170, Part 1 - 1989.

# Design and Detailing of Cellular Concrete Structures

## Conception et détails des structures cellulaires en béton

## Entwurf und Ausführung von Beton-Zellenkonstruktionen

**Mohamed I. SOLIMAN**
Professor
Ain Shams Univ.
Cairo, Egypt

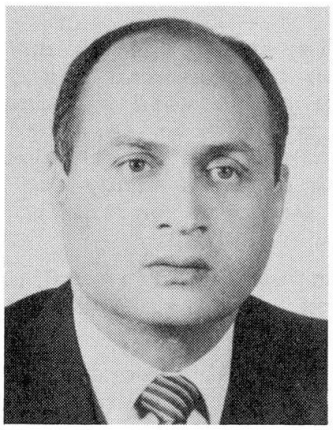

M.I. Soliman, born in 1946, obtained his B.Sc. degree in civil engineering from Ain Shams Univ., Cairo in 1969, his M.Sc. degree from the same Univ. in 1972, and an M.Eng. degree from McGill Univ., Canada in 1975 and his Ph.D. in 1979 from the same University. Dr. Soliman is the Liaison officer for Canada, CSCE.

**SUMMARY**

An experimental-theoretical study was conducted to investigate the general deformational behaviour of reinforced concrete cellular structures. Six reinforced concrete voided slabs, and six reinforced concrete box section girders were tested. The varying parameters of the voided slabs were the void's diameters and the percentage of reinforcement, while for the box section girders, the varying parameters were the percentage of reinforcement and the end conditions, (warping restrained or unrestrained). The finite element method was used in the analysis of these cellular structures. General conclusions are summarized.

**RÉSUMÉ**

Une étude expérimentale ainsi que théorique a été conduite afin d'examiner le processus de déformation des structures cellulaires en béton armé. Six dalles et six caissons ont été testés, en tenant compte des paramètres suivants: diamètre des vides et pourcentage d'armature pour les dalles, pourcentage d'armature et conditions aux limites (torsion libre ou empêchée) pour les caissons. La méthode des éléments finis a été utilisée dans l'analyse de ces structures cellulaires. Les conclusions sont résumées.

**ZUSAMMENFASSUNG**

Eine experimentelle und theoretische Studie wurde durchgeführt, um die allgemeine Verhaltensweise von Stahlbeton-Zellenkonstruktionen zu ermitteln. Sechs Stahlbeton-Hohlplatten mit verschiedenen kreisförmigen Aussparungen oder unterschiedlicher Bewehrung und sechs Stahlbeton-Kastenträger mit unterschiedlicher Bewehrung und verschiedenem Endzustand (Krümmung, eingespannt oder nicht eingespannt) wurden getestet. Die Methode der Finite Elemente wurde benutzt, um diese Strukturen zu analysieren. Die allgemeinen Schlussfolgerungen sind zusammengefasst.

## 1. INTRODUCTION

Reinforced concrete is particularly well suited for use in bridges, because of its durability , rigidity and economy, as well as the comparative ease, with which a pleasing appearance can be achieved. In the recent years, there has been a general tendency to adopt cellular construction for reiforced concrete small & medium-span bridges. This has been a result of functional structural and aesthetic requirements coupled with economic considerations.

In the present work an experimental and theoretical study was conducted to define and explain the general deformational behaviour of reinforced concrete cellular structures under symmetrical and unsymmetrical cases of loading within the serviceability and uultimate states and up to the failure of this type of structures.

The specified aims of this study was to define a simplified method for the design of R.C. voided slab bridges and box girders. Also, this study aims to study the effect of changing the void's diameter, the location and percentage of the longitudinal and transverse reinforcement on the characteristics of load distribution betweenthe webs of the voided slsbs from zero up to the failure load. Also the aim of this study was to investigate the effect of the warping restraint at the supports on the torsional and warping behaviour of R.C. box girder bridges.

The finite element method was used in this study for the analysis of the voided slabs, and the box girders. The adaptability and validity of this method is discussed.

The results of this experimental-theoretical study were combined with other available information and the code provisions to formulate some recommendations to simplify the analysis, design and detailing of this type of structures.

## 2. ANALYSIS

In the analysis and design of voided slabs or box girders, the commonly used approach is to assume the concrete to be uncracked and linearly elastic, and thus ignoring the reinforcement. This approach has the advantage of simplicity and closely modeling the bahaviour of the structure within the service load level. However, this approach lags accuracy, and may lead to unnecessary overestimating the dimensions of these structures. In addition, it cannot predict the nonlinear behaviour of the reinforced concrete cellular structure up to failure.

### 2.1 Finite Element Analysis

#### 2.1.1 Element used

In this study a layered rectangular element was used with 7 degrees of freedom per node for the voided slabs, and 6 degrees of freedom per node for the box girder.

The rigidity matrix of the rectangular element was developed using the concept of layered plates, (i.e. the integration involving the material properties is being done layer by layer [7,12]). The structures were divided into a number of layers of different elastic properties as follows;

i- The voids were replaced with an orthotropic solid core layer of equivalent properties as the actual voids.

ii- The steel reinforcement was replaced with a smeared orthotropic layer which resists only normal stresses, and Poisson's ratio is considered to be equal to zero.

iii- The solid concrete layers were considered as isotropic solid layers in the elastic stage, and orthotropic in the inelastic stages.

2.1.2 Material Nonlinearity

The analytical model for concrete which was used in the present analysis was originally developed by Darwin and Pecknold [4 ]. In Darwin's model, concrete was assumed to be an orthotropic material in the two principal stress directions. In this model the concrete was treated as an incrementally linear elastic material. At the end of each increment, (or iteration), material stiffness were crrected to reflect the latest changes in deflection and strain. Also in this study the smeared cracking model was adopted in the solution(1,7). The advantages of this model was that it offers an automatic generation of cracks without the redefinition of the finite element topology,and second, it offers a complete generality in possible crack direction. The failure criteria used in this model was that proposed by Kupfer and Gerstle (8).

The steel is considred as an approximately elastic plastic material with yield stresses fy and elastic modulus Es. After the yielding of the steel its tangent modulus of elasticity was reduced. It was further assumed that the reinforcement carry only axial stresses in its direction, hence, the principal stress directions was always taken in the global x-y directions, the same as the reinforcement arrangement. Perfect bond was assumed between the steel and concrete layers.

Finally the nonlinear finite element analysis was performed in an incremental manner using an iterative scheme within each load increment. The Newton-Raphson, or the modified Newton-Raphson scheme were used for stiffness updating.

3. EXPERIMENTAL WORK

3.1 The voided slabs

Six reinforced concrete voided slabs with 10 voids were tested. The dimensions of these slabs are 1.04 x 1.80 m. and thickness 12 cm. These slabs were tested, as simply supported on spsn of 1..60 m., twice. Once with a single concentrated load acting at center of gravity of the slab within the elastic range, and the second time, with an eccentric concentrated load, of eccentricity 0.3 m. from the center of the mid section. The six slabs were divided into two groups, each group consisted of three slabs as follows;

Group (1) : The three slabs had a bottom reinforcement of 10 $\phi$ 6 mm/m' in the longitudinal direction and 10 $\phi$ 6 mm/1.5 m' in the transverse direction. The varying parameter was the void's size (For slab S1/6 the void diameter was 63 mm., slab S2/6 the void diameter was 50 mm. and for slab S3/6 the void diameter was 40 mm ). The spacing of center line of voids was 0.1 m.

Group (2) : The three slabs had the same void sizes as used in group (1) but the reinforcement used was $\phi$ 8 mm instead of $\phi$ 6 mm. The slabs were named S1/8, S2/8 and S3/8, respectively.

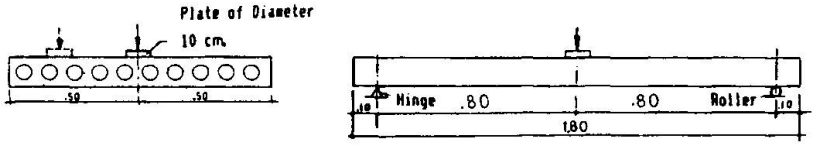


Fig. 1 Test setup for the voided slabs

3.2 The box girders

Six Medium size direct model of R.C.box section girders were tested. The six models had the same length, (2.30 m), and cross-sectional dimensions, (the outer and inner dimensions were 400x260 mm and 260x120 mm. respectively), but they had a different end conditions, (warping restrained or unrestrained).

Also, they had a different percent of reinforcement in both the longitudinal and the transverse directions. These girders were divided into the following two groups;

Group (3) : [G1,G2,G3], consisted of three models which had no transverse diaphragms at the supports, (warping unrestrained condition). Within this group, three girders had a different percent of reinforcement in both the longitudinal and transverse directions.

Group (4) : [G4,G5,G6], consisted of three models which had two end diaphragms of length 400 mm. at both ends to simulate the warping restraint condition at the supports. Also within this group, these girders had a different percent of reinforcement in both directions similar to those of group (3).

All these girders were tested on a fixed end condition of clear span 1.50 m. and were loaded with an eccentric cocentrated load at the midspan section to provide a combined torsion, bending and shear condition.

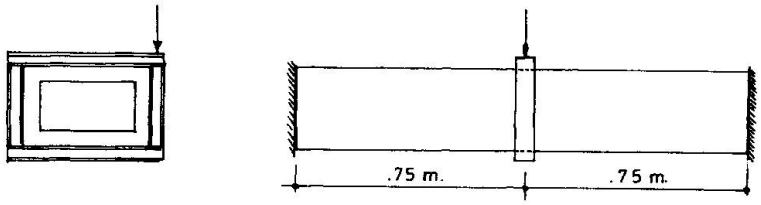


Fig. 2 Test setup for the box girders

## 4.BEHAVIOUR OF THE TESTED SPECIMENS

### 4.1 The voided slabs

The behaviour of the tested slabs can be summarized in the following points;

i) The first crack appeared at a load level of about one quarter of the ultimate load for all slabs.

ii) Increasing the transverse reinforcement, or decreasing the void depth ratio, leads to a more uniform load distribution between the webs of the voided slabs. This was observed by;
   a) Increase in the cracking load.
   b) Decrease in deflections and longitudinal strains of the loaded web and an increase in the transverse strains.

iii) Cracking due to longitudinal moments leads to a more uniform load distribution between the webs. This is due to the decrease in the longitudinal flexural stiffness of the slabs while the transverse flexural and torsional were approximately constant.

iv) As the void depth ratio increases, the ratio between the transverse and the longitudinal increases, while the ratio between the transverse and the longitudinal moment decrease. This was explained by the existence of shear deformations due to the cell distortions.

v) The effect of the torsional moment was obvious on the crack pattern of the slabs. This can be observed from the direction of cracking on the opposite sides of the slabs.

### 4.2 The box girders

The behaviour of the tested box girders can be summarized in the following points;

i) The end diaphragms had a slight effect on the cracking load but it increases the failure load.

ii) The end diaphragms reduce the vertical and lateral deformations of the loaded and unloaded webs.

iii) The longitudinal and transverse steel stresses at both the midspan and

support sections of the unrestrained condition were higher than those of the warping restraint condition at the supports. however, the box girders of group (3) reached the yield earlier than those of group (4).

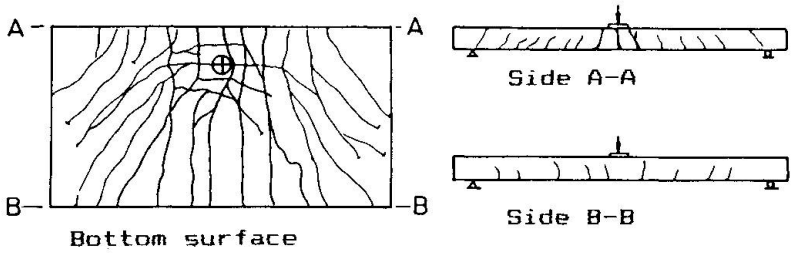


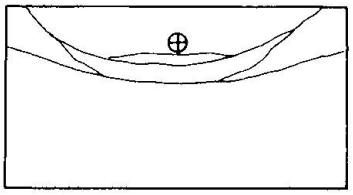


Fig. 3 Crack pattern of the tested voided slabs.

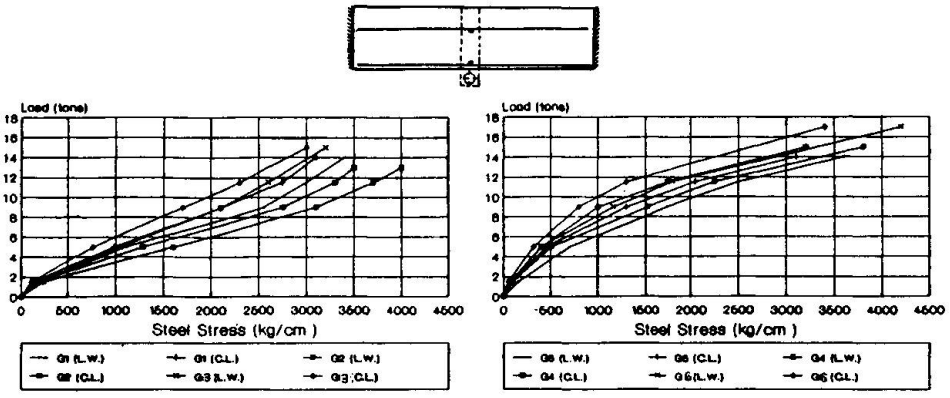


(Warping Unrestrained Group) (Warping Restrained Group)

Fig. 4 Load-Longitudinal steel stress in bottom slab of midspan section for all box girders.

## 5. CONCLUSIONS

1) The proposed finite element model, which considers the nonlinear behaviour of concrete and steel, is a powerful tool in the analysis of reinforced concrete cellular structures, especially after cracking of concrete.
2) The transverse stresses should be taken into consideration, and hence care should be given for the detailing of the transverse reinforcement of this type of structures.
3) Shear deformations have a significant effect on the behaviour of cellular structures and its effect should not be neglected, and hence, special web reinforcement, and detailing should be considered.
4) The values of the transverse moments should be calculated individually taking into cosideration the ratio between the longitudinal and transverse reinforcement, and shoud not be related to the longitudinal moment by Poisson's Ratio.
5) The effect of torsional and the effect of warping restraint should be considered in the analysis and design of box girders structures and accordingly the detailing of the longitudinal and trasverse reinforcement at the support region is very important.

## 6. REFERENCES


1. ASCE Committee on Concrete and Masonary structures, Finite Element Analysis of reinforced Concrete, State-of-the-Art Report, ASCE, USA, 1982.
2. Bakht, B.; Jaeger, L.G. and cheung, M.S., Cellular and Voided Slab bridges, Journal of the Structural Division, Proceedings of the American Society of Civil Engineers. ASCE, Vol. 107. No. ST9, Sept. 1981. pp.1797-1813.
3. Clark, L.A., Comparisons of Various Methods of Calculation the Torsional Inertia of Right Voided Slab Bridges. Technical Report 42.508,Cement and Concrete Association, London, June 1975. pp 34.
4. Darwin, D. and Pecknold, D.A., Nonlinear Biaxial Stress-Strain Law For concrete, Journal of the Engineering Mechanics Division, ASCE, Vol. 103, No. EM4, Aug. 1977. PP. 229-241.
5. Elliot, G. and CLARK, L.A., Circular Voided Concrete Slab Stiffnesses, Jounal of the Structural Division, Proceedings of the American Society of Civil Engineers.ASCE, Vol. 108. ST11, Nov.1982. pp. 2379-2393.
6. Rehiem, F.A. Analysis and Behaviour of Box Girder Bridges, M.Sc. Thesis, Civil Eng. Dept., Ain Shams University, Cairo, Egypt, Oct. 1990.
7. Fouad, N.A. Analysis of Reinforced concrete Voided Slabs, M.Sc. Thesis Civil Eng. Dept., Ain Shams University Cairo, Egypt, Sept. 1989.
8. Kupfer, H.B. and Gerstle, K.H., Behaviour of Concrete Under Biaxial stresses, Journal of the Engineering Mechanics Division, ASCE, V01. 99, No EM4, Aug. 1973, PP. 853-866.
9. ROWE, R.E.,Concrete Bridge Design, London, OR Books Ltd, 1962. pp. 336.
10. El Behairy, S.A, Soliman, M.I., and Fouad , N.A., Behaviour of Voided Reinforced concrete slabs, 3rd Arab Conference for structural Enginnering, Al-Ain, Emirates, March 1989.
11. El Behairy, S.A., Soliman, M.I., and Fouad, N.A., Beraviour and Analysis of Voided Concrete Slabs, IABSE Symposium Lisbon, September 1989.
12 El Behairy, S.A., Soliman, M.I., and Fouad, N.A., Nonlinear Finite Element Analysis of Voided Reinforced Concrete Slabs, 1990 Annual Conference of the Canadian Society for Civil Eng., Hamilton, Ontario, Canada, May 1990.
13 El Behairy, S.A., Soliman, M.I., and Fouad, N.A., Nonlinear Behaviour of Reinforced Concrete Voided Slab Bridges. Third International Conference on Short and Medium Span Bridges, Toronto, Canada, August1990.
14. Soliman, M.I., Behaviour and Analysis of a Reinforced Concrete Box Girder Bridge, Ph. D. Thesis, Department of Civil Engineering and applied Mechanics, McGill University, Montereal, March 1979.

# Cracking and Shear Capacity of Prestressed Hollow Core Slabs

## Résistance à la fissuration et à l'effort tranchant des dalles alvéolées précontraintes

## Kapazität der vorgespannten Hohlplatten

**Matti PAJARI**
Senior Research Scientist
Techn. Res. Centre of Finland
Espoo, Finland

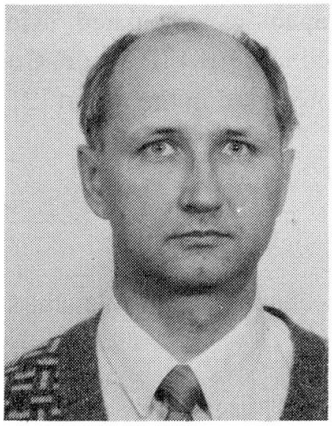

Matti Pajari, born 1948, received his Lic Tech at Helsinki University of Technology and has, since 1979, been involved in research and development projects concerning concrete structures.

**SUMMARY**

Predicted and observed cracking and shear capacities of prestressed hollow core slabs are compared. The flexural tensile strength of the concrete seems to be independent of the thickness of the slab. The shear compression failure is not needed to predict the observed shear capacities. A reliable criterion for the shear tension failure is obtained by setting the maximum principal stress in the web equal to the direct tensile strength of the concrete.

**RÉSUMÉ**

On compare ici les valeurs prévues et observées de la résistance à la fissuration et à l'effort tranchant de dalles alvéolées précontraintes. La résistance à la traction du béton fléchi semble être indépendante de l'épaisseur de la dalle. La connaissance de la rupture par cisaillement de la dalle comprimée n'est pas nécessaire pour prévoir la capacité de résistance à l'effort tranchant observées. Un critère fiable pour évaluer la ruine par effort tranchant de la dalle en traction peut être obtenu en introduisant dans la section une contrainte principale maximale égale à la résistance à la traction du béton.

**ZUSAMMENFASSUNG**

Berechnete und gemessene Rissmomente- und Schubtragfähigkeiten von vorgespannten Hohlplatten werden verglichen. Die Biegezugfestigkeit des Betons scheint unabhängig von der Dicke der Hohlplatte zu sein. Es ist nicht nötig, den Schubdruckbruch bei der Berechnung der Schubtragfähigkeit zu berücksichtigen. Ein zuverlässiges Kriterium für den Schubzugbruch ist es, die grösste Hauptspannung im Steg gleich der Zugfestigkeit des Betons zu setzen.

## 1. INTRODUCTION

The production method of extruded prestressed hollow core slabs does not allow the use of crosswise reinforcement. For this reason, the shear stresses and the local tensile stresses due to the transfer of the prestressing force must be carried by the concrete itself. The same is true also for the positive bending stresses due to the prestressing moment. In the following, discussion is limited to slabs that can be modelled by a simply supported beam without torsion. Possible failure or cracking at the release of the prestressing force or during transportation or installation are also excluded. The purpose is to show the correspondence between results of full scale tests and theoretical load-bearing capacities calculated using basic structural mechanics and the material properties closely related to CEB-FIP Model Code [1]. The theory and the results of the loading tests are discussed in more detail in the report [2].

## 2. CRITICAL LIMIT STATES

Fig. 1 shows possible failure mechanisms and relevant serviceability limit states for prestressed hollow core slabs.

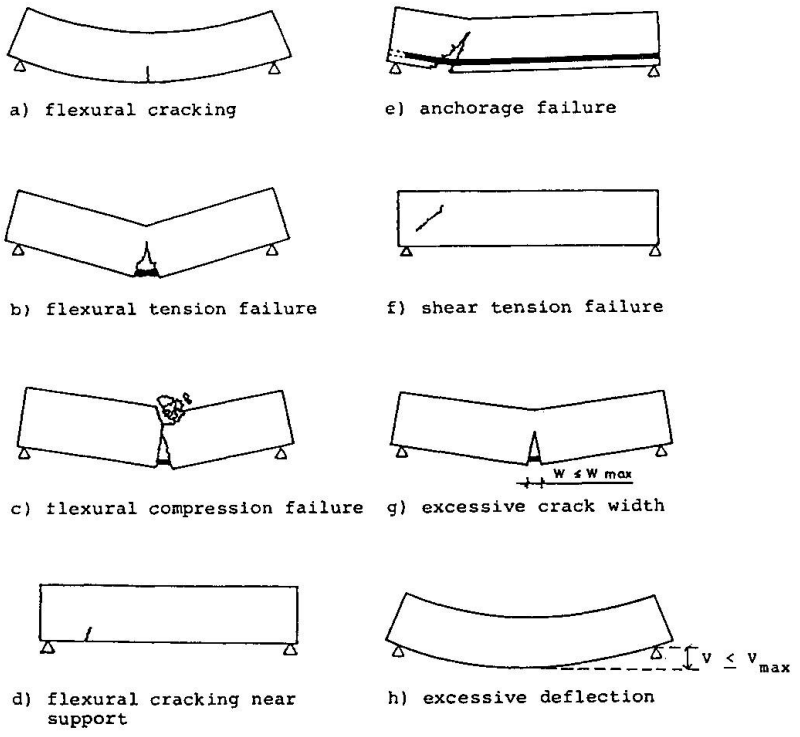


Fig. 1 Relevant limit states.

The limit states where the tensile strength of concrete is of minor importance are not discussed here. To these belong flexural tension failure, flexural compression failure, excessive crack width and excessive deflection.

## 2.1 Flexural cracking

The horizontal bending stress $\sigma$ is obtained from

$$\sigma = \frac{-P}{A_r} + \frac{-Pe + M_g + M_q}{I_r / y} \qquad (1)$$

where P is the prestressing force of strands with due regard to the losses of prestressing, $A_r$ the reduced area of cross-section (steel reduced to concrete), y the vertical coordinate with origin at the centroid of the reduced cross-section and positive direction downwards, $I_r$ the reduced second moment of area of the cross-section, e is y coordinate of the strands, $M_g$ the bending moment due to the self-weight of the slab and $M_p$ bending moment due to the imposed load. By setting $\sigma$ equal to the flexural tensile strength of concrete $f_{ctf}$ and y equal to the y coordinate of the bottom fibre of the slab, cracking moment capacity can be solved from Eq. 1.

## 2.2 Anchorage failure and shear compression failure

If the strands are anchored firmly enough, the presence of an inclined crack does not cause the structure to fail. Instead, the crack width increases with increasing load until the strands yield or break (flexural tension failure, Fig. 1b), slip (anchorage failure, Fig. 1e) or the concrete is crushed at the top of the slab (shear compression failure). For concrete to be crushed at the top surface, the crack width and strand slip at the bottom surface must be so great that a test which seems to end in compression failure, might equally well be regarded as having ended in anchorage failure. It was assumed that shear compression failure need not be examined separately. The anchorage capacity was checked according to the free body diagram shown in Fig. 2. Only cross-sections cracked in flexure were considered.

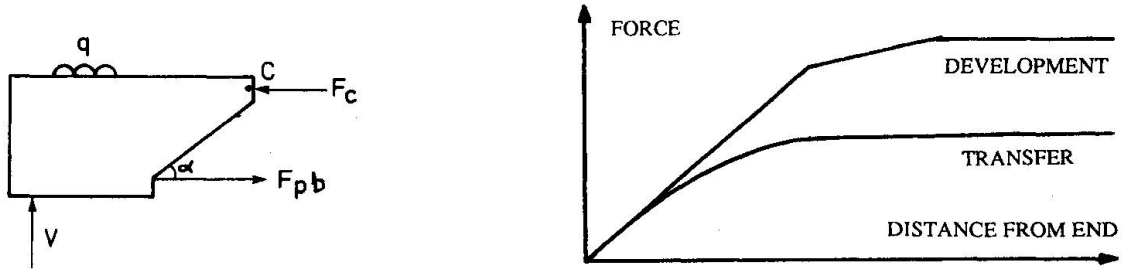


Fig. 2 (a) Free body diagram for anchorage failure.
(b) Development of anchorage force and transfer of prestress.

## 2.3 Shear tension failure

Shear tension failure refers to cracking that starts in the web and leads to a brittle failure (Fig. 1f). If diagonal cracking takes place near the support, the development length of the

strands is too short to prevent collapse. The simplest way of assessing such a failure is to compare the greatest principal stress in the web with the tensile strength of concrete. Finite element calculations have shown that in hollow core slabs with circular voids the most critical cross-section for shear tension failure is about at distance H/2 from the support where H is the thickness of the slab [3]. The most critical point at this cross-section is close to the point where the cross-section is narrowest. As a first approximation, it was supposed that this point is critical for all slabs irrespective of the shape of the hollow cores. The greatest principal stress $\sigma_{p1}$ was calculated by combining the horizontal stress $\sigma$ obtained from Eq. 1 with the shear stress $\tau$. $\tau$ was obtained from $\tau = VS/(I_r b)$ where V is the shear force, S the first moment of area and b the width of the concrete cross-section, width of the voids excluded. $I_r$ is the same as in Eq. 1.

### 3. MATERIAL PROPERTIES USED WHEN SIMULATING LOADING TESTS

The modulus of elasticity $E_c$ and the characteristic tensile strength of concrete $f_{ctk}$ were obtained from

$$E_c = 4800\, f_{ck}^{1/2} \tag{2}$$

$$f_{ctk} = 0.20\, f_{ck}^{2/3} \tag{3}$$

where $f_{ck}$ is the characteristic cube strength of concrete (150 mm cubes). The strength of steel used in calculations was 1600 MPa and the modulus of elasticity 195 000 MPa. The parabolic curve used for the transfer of the prestressing force and the trilinear curve used for the development of anchorage force are shown schematically in Fig. 2b.

### 4. LOADING TESTS

Finnish quality control tests and shear tests carried out by Jonsson [2,3], cf. Fig. 3., were used to verify the proposed calculation method. In both test series, both the geometry of the slab and the strength of the concrete were measured. These were used in the calculations. The prestress was not measured but taken from the documents of the slab producers.

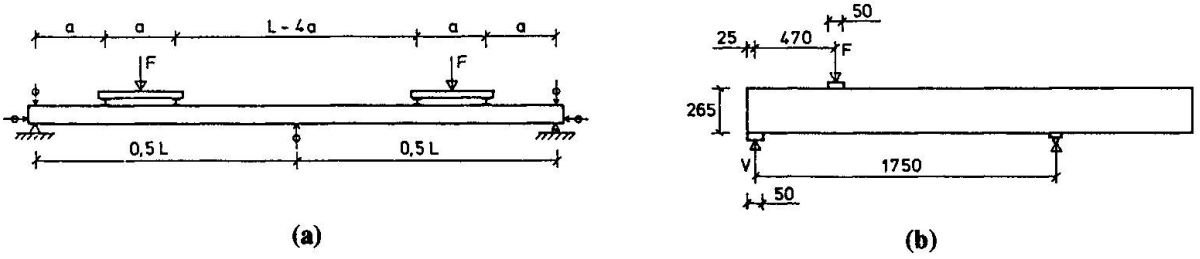


Fig. 3 Test layout. (a) quality control tests, (b) Jonsson's tests.

### 4.1 Cracking capacity

The ratio $\alpha_{cr} = M_{pre}/M_{obs}$, i.e. ratio predicted/observed cracking moment was calculated for each slab by using two different values for the flexural tensile strength $f_{ctf}$. The results are shown in Table 1. When $f_{ctf}$ was chosen according to Mayer [4], the share of slabs for which $\alpha_{cr}$ was greater than 1.0 was far too big. Furthermore, this share increased with increasing flexural tensile strength. When $f_{ctf}$ was chosen equal to $1.1*f_{ctk}$, the probability for $M_{pre} > M_{obs}$ was of the order 20% for all slab thicknesses. This is still greater that one should expect if $1.1*f_{ctk}$ is regarded as the 5% fractile of the flexural tensile strength. Obviously $f_{ctf}$ should still have been reduced.

| Thickness of slab mm | Number of slabs | $f_{ctf}/f_{ct}$ (Mayer) | Share of slabs with $M_{pre} > M_{obs}$ | $f_{ctf}/f_{ct}$ | m | s | Probability for $\alpha_{cr} > 1$ % |
|---|---|---|---|---|---|---|---|
| 150 | 46 | 1.5 | 43 | 1.1 | 0.875 | 0.130 | 17 |
| 200 | 92 | 1.4 | 35 | 1.1 | 0.893 | 0.119 | 18 |
| 265 | 90 | 1.3 | 31 | 1.1 | 0.905 | 0.125 | 22 |
| 400 | 25 | 1.2 | 28 | 1.1 | 0.947 | 0.057 | 18 |

Table 1 Comparison of predicted and observed cracking capacities for two choices of $f_{ctf}$. m is the mean and s the standard deviation for the ratio $\alpha_{cr} = M_{pre}/M_{obs}$.

### 4.2 Shear capacity

The ratio $\alpha_v = V_{pre}/V_{obs}$, i.e. ratio of predicted/observed shear capacity, was calculated for each slab. Here are discussed only slabs that were subject to an experimental or predicted shear failure. When compared to the observed capacities, the predicted capacities were acceptable for others but for the 400 mm slabs far too high. In fact, the assumption of the most critical point

| Thickness of slab mm | Number of slabs | $f_{ctf}/f_{ct}$ | m | s | Probability for $\alpha_v > 1$ % |
|---|---|---|---|---|---|
| 150(F) | 3 | 1.1 | 0.898 | 0.045 | 1.2 |
| 200(F) | 24 | 1.1 | 0.881 | 0.140 | 19.0 |
| 265(F) | 25 | 1.1 | 0.817 | 0.118 | 6.2 |
| 265(J) | 42 | 1.1 | 0.767 | 0.130 | 3.6 |
| 400(F) | 27 | 1.1 | 0.848 | 0.112 | 8.6 |

Table 2 Comparison of predicted and observed shear capacities for Finnish (F) and Jonsson's tests. m is the mean and s the standard deviation for the ratio $\alpha_v = V_{pre}/V_{obs}$.

stated in paragraph 2.3 is not correct. Finite element calculations show that the assumed stress distribution for the end of the 400 mm slabs with non-circular voids is not correct. The greatest principal stress may be even 40 - 50% higher than that obtained according to 2.3, and it is found lower and closer to the support. Based on this, the greatest principal stress calculated according to 2.3 for 400 mm slabs was multiplied by 1.4. The great value of p for the 200 mm slabs is mainly due to one questionable test result. The results are shown in Table 2.

## 5. CONCLUSIONS

In prestressed hollow core slabs, the flexural tensile strength of the concrete seems to be independent of the thickness of the slab. This is not in accordance with Hillerborg [5] and König & Duda [6]. The reason for the discrepancy may be due to the large hollow cores, which do not allow exploitation of the strain-softening behaviour of the concrete. It is recommended that the same value is used both for the flexural tensile strength and for the direct tensile strength.

The shear capacity can be predicted accurately enough using the characteristic tensile strength of the concrete and realistic methods to calculate the tensile stresses. A reliable criterion for the shear tension failure is obtained by setting the greatest principal stress in the web equal to the direct tensile strength of the concrete. For slabs with non-circular cross-section, the greatest principal stress in the web cannot be predicted adequately by using the elementary beam theory. The shear compression failure need not be considered.

## REFERENCES

[1] CEB-FIP Model Code for concrete structures. Bulletin d'information CEB No. 124-125/ 1978.

[2] PAJARI, M., Design of prestressed hollow core slabs. Technical Research Centre of Finland, Research Reports 657 / 1978. 88 pp. + App.

[3] WALRAVEN, J. C. & MERCX, W.P.M., The bearing capacity of prestressed hollow core slabs. Heron 28(1983) 3, 46 pp.

[4] MAYER, H., Die Berechnung der Durchbiegung von Stahlbetonbauteilen. Deutscher Ausschuss für Stahlbeton, Heft 194 / 1967. 73 pp.

[5] HILLERBORG, A., Reliance upon concrete tensile strength. IABSE Colloqium "Structural Concrete, Stuttgart 1991.

[6] KÖNIG, G. & DUDA, H., Basic concept for using concrete tensile strength. IABSE Colloqium "Structural Concrete", Stuttgart 1991.